

НАЦІОНАЛЬНА АКАДЕМІЯ НАУК УКРАЇНИ  
ІНСТИТУТ ОРГАНІЧНОЇ ХІМІЇ НАН УКРАЇНИ  
НАЦІОНАЛЬНИЙ ФАРМАЦЕВТИЧНИЙ УНІВЕРСИТЕТ

---

Рік заснування – 1966

ЖУРНАЛ  
ОРГАНІЧНОЇ ТА  
ФАРМАЦЕВТИЧНОЇ  
ХІМІЇ

JOURNAL OF  
ORGANIC AND  
PHARMACEUTICAL  
CHEMISTRY

2023 — том 21, випуск 1 (81)

Харків  
НФаУ

Головні редактори І. М. Владимірова (Харків)  
М. В. Вовк (Київ)  
Заступники головного редактора С. В. Власов (Харків)  
Ю. В. Рассукана (Київ)  
Відповідальні секретарі Д. О. Лега (Харків)  
Т. А. Васільєва (Київ)

Редакційна колегія:

Н. А. Бісько (Київ), М. К. Братенко (Чернівці), В. С. Броварець (Київ),  
Ю. В. Буйдін (Київ), Ж. Ф. Буйон (Руан, Франція), А. Варнек (Страсбург, Франція),  
З. В. Войтенко (Київ), Д. М. Волочнюк (Київ), В. А. Георгіянець (Харків),  
І. С. Гриценко (Харків), З. Гуджинскас (Вільнюс, Литва), М. М. Доля (Київ),  
І. О. Журавель (Харків), Л. Запруго (Познань, Польща),  
Л. Іванаускас (Каунас, Литва), М. М. Івашура (Харків), О. А. Коваленко (Миколаїв),  
С. І. Коваленко (Запоріжжя), С. М. Коваленко (Харків), С. Козачок (Пулави, Польща),  
М. І. Короткіх (Київ), А. Ж. Костич (Белград, Сербія), О. М. Костюк (Київ),  
С. М. Крамарьов (Дніпро), Р. Б. Лесик (Львів), В. В. Ліпсон (Харків),  
В. Манос (Нікозія, Кіпр), О. О. Михайленко (Харків), М. Д. Обушак (Львів),  
П. П. Онисько (Київ), Л. О. Рябовол (Умань), А. В. Семеніхін (Ніжин),  
О. Б. Смолій (Київ), М. В. Стасевич (Львів), О. О. Стасик (Київ),  
Г. Федорова (Чеські Будейовиці, Чехія), Л. А. Шемчук (Харків)

Редакційна рада:

**С. А. Андронаті** (Одеса), О. М. Біловол (Харків), А. І. Вовк (Київ),  
Б. С. Зіменковський (Львів), В. І. Кальченко (Київ), Г. Л. Камалов (Одеса),  
В. А. Чебанов (Харків), В. П. Черних (Харків), Ю. Г. Шермолівич (Київ),  
Ю. Л. Ягупольський (Київ)

**У журналі розглянуто проблеми синтезу й аналізу органічних та елементо-органічних сполук, аналогів природних сполук і лікарських субстанцій, наведено результати фізико-хімічних досліджень у вищезазначених напрямках. Також з погляду (біо)органічної, фармацевтичної, аналітичної та фізичної хімії проаналізовано питання з різних аспектів рослинництва, ґрунтознавства й дослідження навколишнього середовища.**

**Для працівників науково-дослідних установ, вищих навчальних закладів та фахівців хімічного, фармацевтичного, біологічного, медичного і сільськогосподарського профілів.**

«Журнал органічної та фармацевтичної хімії» внесено до затвердженого МОН України Переліку наукових фахових видань України (категорія «Б») для опублікування результатів дисертаційних робіт за спеціальністю 102 – Хімія та 226 – Фармація, промислова фармація (наказ МОН України від 28.12.2019 р. № 1643); індексовано в наукометричних базах даних: Chemical Abstracts (CAS), Index Copernicus; внесено до каталогів та пошукових систем: Directory of Open Access Journals (DOAJ), Bielefeld Academic Search Engine (BASE), Directory of Open Access scholarly Resources (ROAD), PKP Index, Ulrich's periodicals, Worldcat, НБУ ім. В. І. Вернадського і УРЖ «Джерело».

Затверджено до друку вченою радою Інституту органічної хімії НАН України, протокол № 5 від 12.04.2023 р.

Затверджено до друку вченою радою Національного фармацевтичного університету, протокол № 4 від 28.04.2023 р.

Адреса для листування: 61002, м. Харків, вул. Пушкінська, 53, Національний фармацевтичний університет, редакція «Журналу органічної та фармацевтичної хімії», тел./факс (572) 68-09-60. E-mail: [press@nuph.edu.ua](mailto:press@nuph.edu.ua), [orgpharm-journal@nuph.edu.ua](mailto:orgpharm-journal@nuph.edu.ua). Сайт: <http://ophcj.nuph.edu.ua>

Передплатні індекси: для індивідуальних передплатників — 08383, для підприємств — 08384

Свідчення про державну реєстрацію серії КВ № 23086-12926ПР від 05.01.2018 р.

Підписано до друку 05.05.2023 р. Формат 60 × 84 1/8.

Папір офсетний. Друк ризо. Умовн. друк. арк. 9,3. Обліков.-вид. арк. 10,76. Тираж 50 прим.

Редактори — О. Ю. Гурко, Л. І. Дубовик. Комп'ютерне верстання — О. М. Білінська

«Журнал органічної та фармацевтичної хімії». Том 21, випуск 1 (81), 2023

ISSN 2308-8303 (Print)

ISSN 2518-1548 (Online)

UDC 615: 54.057:547.833:577.113

O. V. Oksiuta<sup>1,2</sup>, A. E. Pashenko<sup>1,3,4</sup>, R. V. Smalii<sup>3</sup>, D. M. Volochnyuk<sup>1,3,4</sup>,  
S. V. Ryabukhin<sup>1,3,4</sup><sup>1</sup> Institute of Organic Chemistry of the National Academy of Sciences of Ukraine,  
5 Academician Kukhar str., 02660 Kyiv, Ukraine<sup>2</sup> Chemspace Ltd., 85 Winston Churchill str., 02094 Kyiv, Ukraine<sup>3</sup> Enamine Ltd., 78 Winston Churchill str., 02094 Kyiv, Ukraine<sup>4</sup> Taras Shevchenko National University of Kyiv, 60 Volodymyrska str., 01033 Kyiv, Ukraine

## Heterocyclization vs Coupling Reactions: A DNA-Encoded Libraries Case

### Abstract

**Aim.** DNA-encoded libraries technologies (DEL) are gradually becoming an important part of standard drug discovery toolbox. DELT is looking to find its place between classic low-molecular-weight drug candidates on the one hand, and high-molecular-weight antibodies and peptides on the other hand. On its natural path to overcoming the “childhood diseases” typical for every novel technology, DELT has reached a point where the chemical diversity of DNA-encoded libraries (DELs) becomes an important factor to look out for. In this paper, we aim to take a closer look at the chemical diversity of DELs in their present state and find the ways to improve it.

**Results and discussion.** We have identified the DEL-viable building blocks from the Enamine Ltd. stock collection, as well as from Chemspace Ltd. virtual collection, using the SMARTS set, which takes into account all the necessary structural restrictions. Using modern cheminformatics tools, such as Synt-On, we have analyzed the scaffold diversity of both stock and virtual core bi- and tri-functional building blocks (BBs) suitable for DNA-tolerant reactions. The identification of scaffolds from the most recently published on-DNA heterocyclization reactions and analysis of their inclusion into the existing BBs space have shown that novel DNA-tolerant heterocyclizations are extremely useful for expanding chemical diversity in DEL technologies.

**Conclusions.** The analysis performed allowed us to recognize which functional groups should be prioritized as the most impactful when the new BBs are designed. It is also made clear that the development of new DNA-tolerant reactions, including heterocyclizations, have a significant potential to further expand DEL molecular diversity.

**Keywords:** DNA-encoded libraries technology; orthogonal functional groups; coupling reactions; polyfunctional building blocks; heterocyclizations; cheminformatics; scaffold diversity

O. V. Оксютя<sup>1,2</sup>, А. Е. Пащенко<sup>1,3,4</sup>, Р. В. Смалій<sup>3</sup>, Д. М. Волочнюк<sup>1,3,4</sup>, С. В. Рябухін<sup>1,3,4</sup>

<sup>1</sup> Інститут органічної хімії Національної академії наук України,  
вул. Академіка Кухаря, 5, м. Київ, 02660, Україна

<sup>2</sup> ТОВ «Кемспейс», вул. Вінстона Черчилля, 85, м. Київ, 02094, Україна

<sup>3</sup> НВП «Енамін», вул. Вінстона Черчилля, 78, м. Київ, 02094, Україна

<sup>4</sup> Київський національний університет імені Тараса Шевченка,  
вул. Володимирська, 60, м. Київ, 01033, Україна

### Гетероциклізація або реакції каплінгу: випадок ДНК-кодованих бібліотек

#### Анотація

**Мета.** Технології ДНК-кодованих бібліотек (DEL) поступово стають важливою частиною стандартного набору інструментів для пошуку нових лікарських субстанцій. Наразі DELT прагне знайти своє місце у просторі між класичними низькомолекулярними кандидатами у ліки з одного боку та високомолекулярними антитілами й пептидами з іншого. На своєму шляху до подолання «дитячих хвороб», характерних для кожної нової технології, DELT досягли того моменту, коли хімічна різноманітність ДНК-кодованих бібліотек (DEL) стає важливим фактором, на який варто звернути увагу. У цій статті ми прагнемо ближче розглянути хімічне різноманіття ДНК-кодованих бібліотек у їхньому поточному стані та знайти можливості для його покращення.

**Результати та їх обговорення.** Ми визначили DEL-життєздатні будівельні блоки з наявної колекції Enamine Ltd., а також із віртуальної колекції Chemspace Ltd., використовуючи набір SMARTS, який враховує всі необхідні структурні обмеження.

За допомогою таких сучасних інструментів хемоінформатики, як Synt-On, ми проаналізували різноманітність каркасів як уже синтезованих, так і віртуальних бі- та трифункціональних білдинг-блоків (BB), придатних для реакцій, у яких ДНК залишається інтактною. Ідентифікація молекулярних скафолдів, використовуваних у нещодавно опублікованих «on-DNA» реакціях гетероциклізації, та аналіз їх внесення до простору BB, який існує, засвідчили, що нові толерантні до ДНК гетероциклізації є надзвичайно корисними для розширення хімічної різноманітності в технологіях DEL.

**Висновки.** Виконаний аналіз дозволив нам визначити, яким функціональним групам варто віддати пріоритет як найбільш впливовим у процесі дизайну нових BB. Також стало зрозуміло, що розвиток нових толерантних до ДНК реакцій, зокрема й гетероциклізації, має значний потенціал для подальшого розширення молекулярного різноманіття DEL.

**Ключові слова:** технологія ДНК-кодованих бібліотек; ортогональні функціональні групи; реакції каплінгу; поліфункціональні білдинг-блоки; гетероциклізації; хемоінформатика; різноманітність молекулярних каркасів

**Citation:** Oksiuta, O. V.; Pashenko, A. E.; Smalii, R. V.; Volochnyuk, D. M.; Ryabukhin, S. V. Heterocyclization vs Coupling Reactions: A DNA-Encoded Libraries Case. *Journal of Organic and Pharmaceutical Chemistry* 2023, 21 (1), 3–19.

<https://doi.org/10.24959/ophcj.23.275133>

**Supporting information:** The links to source databases: Enamine Ltd. DEL-viable stock bi- and tri-functional core building blocks (freely available at <https://cloud.chem-space.com/s/zk7QraSYsrcn7c4>); ChemSpace tangible virtual DEL-viable bi- and tri-functional core building blocks (freely available at <https://cloud.chem-space.com/s/ePmFyzNYj6bQbci>). The set of SMARTS used for separating the abovementioned sub-sets is available free of charge at <https://cloud.chem-space.com/s/3DbC7KZeKGK4ZaW>.

**Received:** 14 January 2023; **Revised:** 23 February 2023; **Accepted:** 5 March 2023

**Copyright** © 2023, O. V. Oksiuta, A. E. Pashenko, R. V. Smalii, D. M. Volochnyuk, S. V. Ryabukhin. This is an open access article under the CC BY license (<http://creativecommons.org/licenses/by/4.0>).

**Funding:** The authors received no specific funding for this work.

**Conflict of interests:** The authors have no conflict of interests to declare.

## ■ Introduction

DNA-Encoded Libraries Technology (DEL) was first proposed as an idea by *Brenner* and *Lerner* back in 1992 [1]. Since then it has become an actively developing tool for Drug Discovery, which allows to generate the multi-billion screening molecules collection in a single vial [2] and identify the hit molecules by decoding their unique DNA tags. The synthesis of DNA-encoded chemical libraries (DECLs) [3] is based on the split-and-pool strategy [4, 5], which is a common combinatorial chemistry approach topped with DNA fragments as chipping tags. The most general sequence for a DNA-encoded library synthesis is schematically presented in Figure 1. Building-blocks and the corresponding DNA tags are repeatedly connected to DNA primers from the opposing end (Figure 1).

The most common approach to screening the DNA-encoded libraries [6, 7] demands placing the protein target of interest (POI) on the solid support bed and exposing it to the action of the set of DNA-tagged molecules from the library (Figure 2). The binders remain connected to the protein, and the non-binding molecules are washed away (Figure 2). Then the binders (potential hits) are eluted, their chemical structures are disclosed using PCR sequencing of the coding DNA-tags, and the data obtained is analyzed. At the current stage of the DELT development, it is gradually beginning to expand into more complex biological assays, for instance cell-based assays

[8–11], which is a positive sign indicating the flexibility and translation potential of DELT-based platforms.

It is notable that the size of libraries created using the DEL technology nowadays exceeds the size of the conventional high-throughput screening (HTS) combinatorial libraries by several orders of magnitude. The HTS libraries almost never exceed one million individual compounds, while 3- and 4-cycle DNA-encoded libraries with the input size of 1000 molecules on each cycle generate a billion and a trillion molecules, respectively.

The typical sequence for the four-cycle assemblies is given in Figure 3. It is worth mentioning that there are also several approaches to DNA-tagging, likewise double-strand [4, 12] and single-strand [13] technologies. However, this technical aspect is non-important for the current discussion. Although traditionally viewed as the major advantage, the gigantic size of the DELs also introduces several risks and drawbacks. First of all, chemical diversity of such libraries relies heavily on the pool of reactions available for the DNA-friendly environment [7, 14], as well as on the sufficient number of suitable and available bi- and tri-functional core building blocks (BBs) with orthogonal functional groups (FGs), and diverse monofunctional molecules (capping agents) [15–19]. Another important factor influencing the success of DEL-derived screening campaigns is the development of the readout methods [4, 20, 21] and statistical analysis of the hits [21–23].

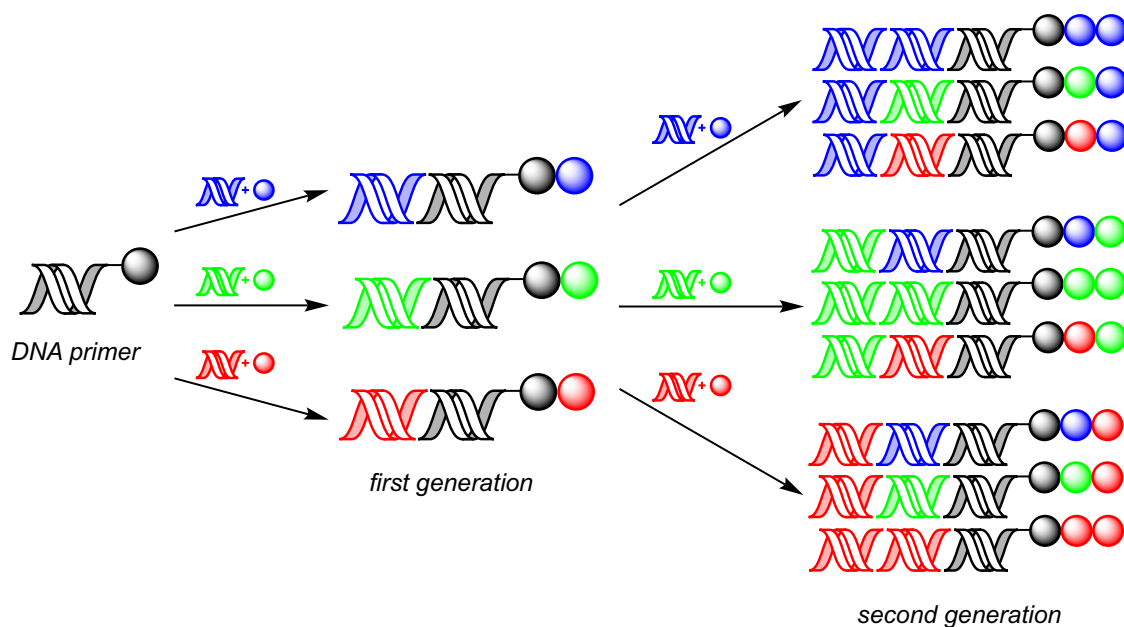


**Figure 1.** Schematic representation of the split-and-pool process for the DNA-encoded library synthesis

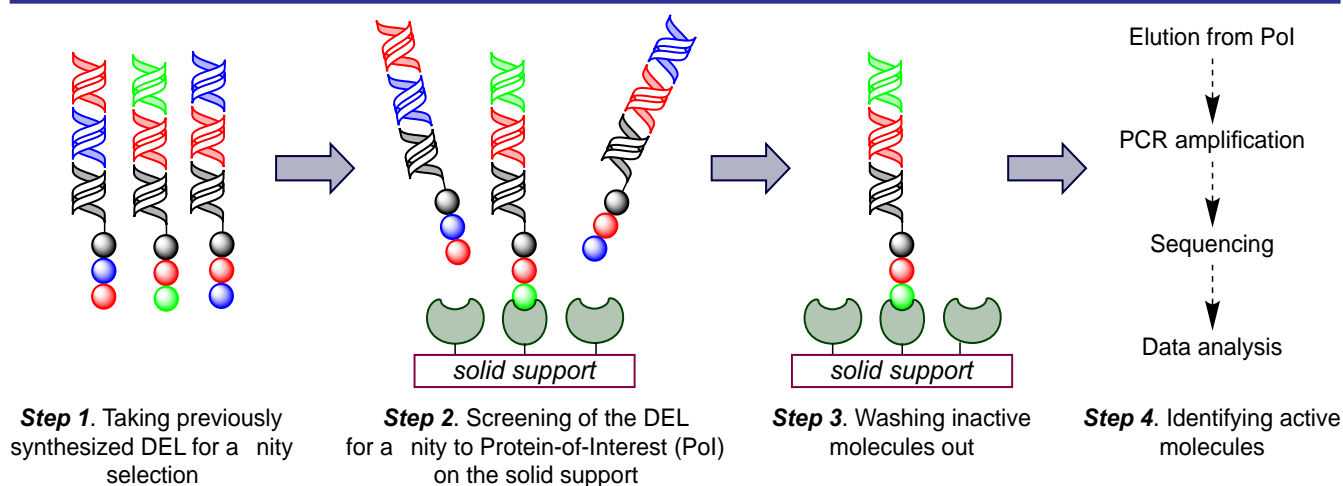


**Figure 2.** Workflow for identifying an active molecule from DEL

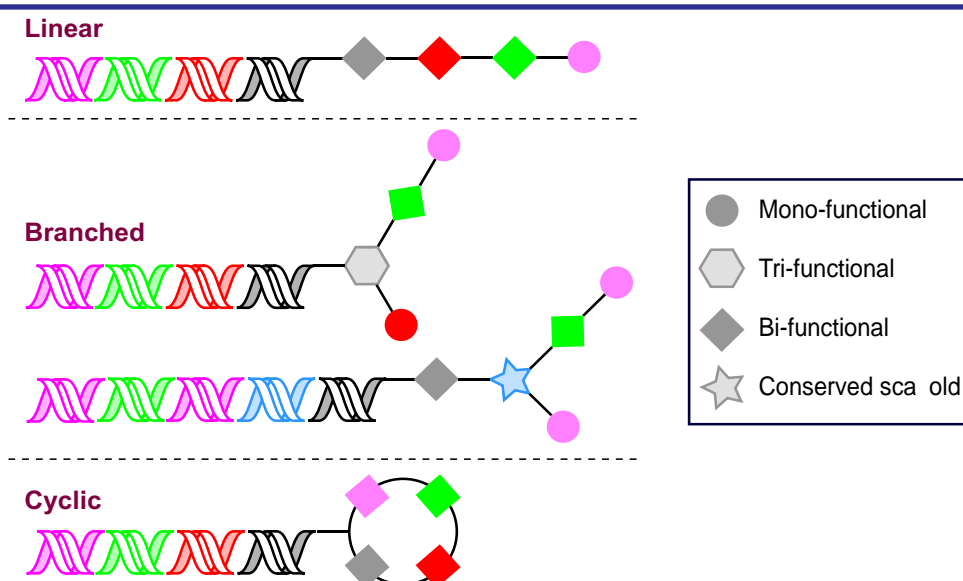


**Figure 3.** Typical DEL sequence for a 4-step cycle with examples of mono-, bi-, tri-functional BBs

As it is mentioned above, the main limitation for DELT is the demand to use only such chemical transformations, which leave DNA fragments intact. At the early stages of development, DELT was used as a platform for amide couplings only [24]; however, the overall advances in organic synthesis techniques enabled the application of a broad spectrum of chemical transformations in DNA-tolerant conditions, including classical C-C and C-N cross-couplings [25], metathesis [26, 27], click reactions [17, 28–33], photoredox reactions [34], and many others. Now that the vast majority of common transformations used in the cross-couplings has been successfully translated into on-DNA chemistry, and DELT is approaching the moment when the search for new chemotypes again becomes a limiting factor. In this connection, the cheminformatic algorithms, such as eDESIGNER [35], which helps to design libraries accounting both diversity and reaction applicability factors, have been developed and reported recently. Eventually, in the “maturation” [36] process DELT replicates the evolutionary route of traditional HTS-derived combinatorial chemistry [37, 38] and is on a track from amide coupling to more complex cross-coupling reactions [39] and, finally, to the on-DNA heterocycles formation. One can find a comprehensive review on DNA-tolerant couplings described in multiple review articles [3, 14, 39, 40], however, the works focused on the on-DNA heterocycles formation started to show up in the periodical press on a regular basis only recently. In this paper, we aim to give an overview on the diversity of DELT-suitable BBs for “traditional” cross-coupling reactions based on the catalogue of stock molecules provided by Enamine Ltd., and virtual set provided by Chemspace Ltd., and evaluate the potential contribution of the chemotypes emerging from the most recent discoveries in the field of on-DNA heterocyclizations.

## ■ Results and discussion

For the decomposition of the pool of stock (Enamine) building blocks we used the SMARTS set (see the experimental part for details) specially designed to account orthogonality of FGs in the multifunctional compounds, the absence of undesired functions (alkylators, moisture-sensitive groups, etc.), and find compatible mono-functional molecules or “capping agents” [19]. We distributed the molecules obtained according to the combination of functional and protective groups.

In case of stock polyfunctional cores, 11 classes of bi-functional and 8 classes of tri-functional molecules were identified. We decided not to include capping agents to our analysis. This is the most widespread group having a decent overlap with “traditional” monofunctional BBs commonly used for combinatorial chemistry, and it hardly contributes much to the chemical diversity, in contrast with rather scarce suitable multifunctional core molecules. In case of stock BBs (Enamine), 26816 bi- and 1438 tri-functional “core” compounds were obtained (Figures 4 and 5, respectively).

We performed the same type of extraction using SMARTS and further analysis in Chemspace (virtual) database. Additionally, the Synt-On software package was used for this analysis [41, 42]. Using Synt-On, 43 848 442 molecules in 33 sub-classes of bi- and 3 119 488 molecules in 25 sub-classes of tri-functional BBs were identified. Low-reactive BBs and those with non-orthogonal functional groups were removed. The molecules obtained were combined into broader classes as we did previously for stock compounds. This approach allows to evaluate which FGs and, consequently, which reactions contribute the most to the DEL-derived chemical space. Despite the insignificant shuffle in the “lower bracket” of the histogram for bi-functional molecules (Figure 6), the proportion between the most widespread chemotypes in virtual space remains close to the stock case (Figure 4). However, in case of tri-functional cores, the fraction of acids, which fulfill the selection criteria on the virtual side (Figure 7), is significantly smaller than in the stock (Figure 5). In all the remaining classes, the general trend for virtual structures correlates with the stock. This observation led to the conclusion that despite many reactions were optimized for DNA-friendly conditions, the chemical diversity of DELs remains to the most part to be limited to either amide- or ArX-amine cross-couplings.

Introducing heterocycle formation reactions is a beneficial way to expand the chemical space of combinatorial chemistry-derived molecules, which have proven itself in the HTS development [43, 44]. It is also true that with the development of organic synthesis many heterocyclic cores became readily available as scaffolds for classical combinatorial chemistry, as well as DEL-chemistry. Considering the growing number of publications focused on the on-DNA cycle formation we assumed that DELT is about to cross the same frontier as traditional combinatorial

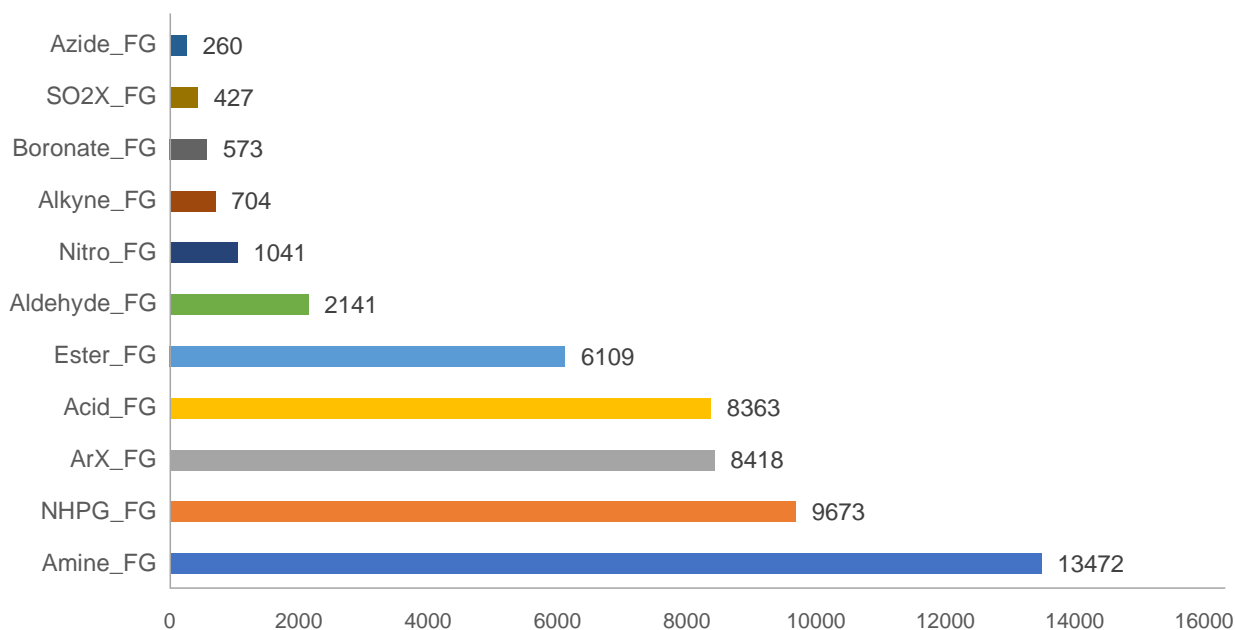


Figure 4. Enamine stock bifunctional DEL-viable BBs, 26816 molecules in 11 classes

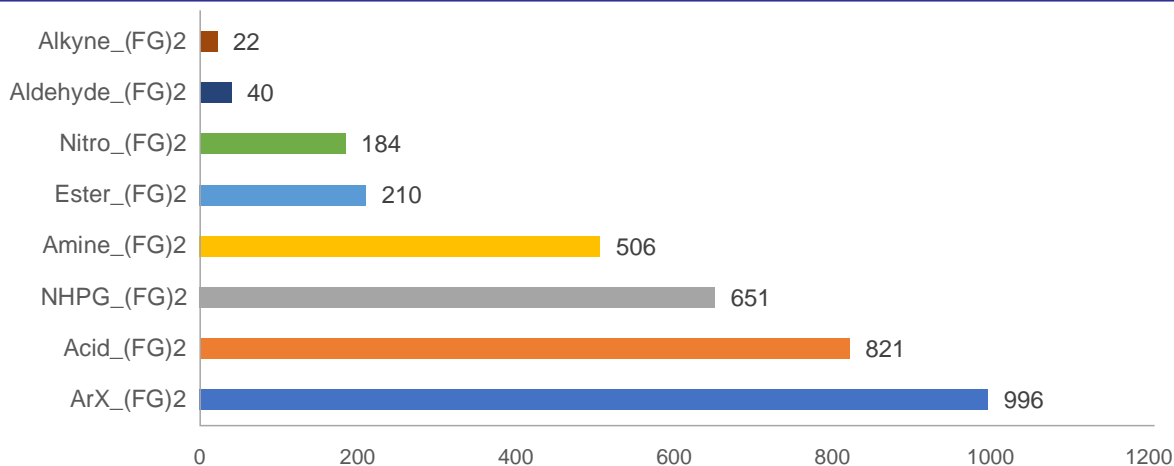


Figure 5. Enamine stock trifunctional DEL-viable BBs, 1438 molecules in 8 classes

chemistry did at the time when heterocyclizations became noticeable part of the combinatorial reaction toolkit. In order to have a closer look at this tendency, we studied the literature sources over the period from 2016 to 2020. We observed the growing number of such publications over time: a single one in 2015, and 14 in 2020. We also identified 26 distinct types of the on-DNA heterocycle formation reactions. They are summarized in Table 1.

With this in mind, we wanted to study in more detail if scaffolds from on-DNA heterocyclizations occur as scaffolds in cross-coupling based DEL builds. In other words, we wanted to look at the population of heterocyclization-derived scaffolds in the bi- and tri-functional core BBs subsets, and evaluate the potential contribution of heterocyclizations to the DELT-relevant chemical

space diversity. We used Synt-On to identify scaffolds in both stock and virtual bi- and trifunctional BBs sets, as well as in heterocyclization reactions products in Table 1. The latter provided 30 separate heterocyclic scaffolds. The scaffold-inclusion analysis for the scaffolds from Table 1 relative to bifunctional cores subclasses (Table 2) and trifunctional core subclasses (Table 3) was performed. The structure of Tables 2 and 3 is as follows: entry (subclass) number in the first column; subclass abbreviation and an overall number of compounds in the subclass; “scaffolds in ref” shows how many times scaffolds from Table 1 are included “as is” or as substructures to the BBs subclass scaffolds; in the “molecules in ref” the number of molecules with “sub-class” scaffolds, which contain the exact structure of scaffolds from the heterocyclic set,

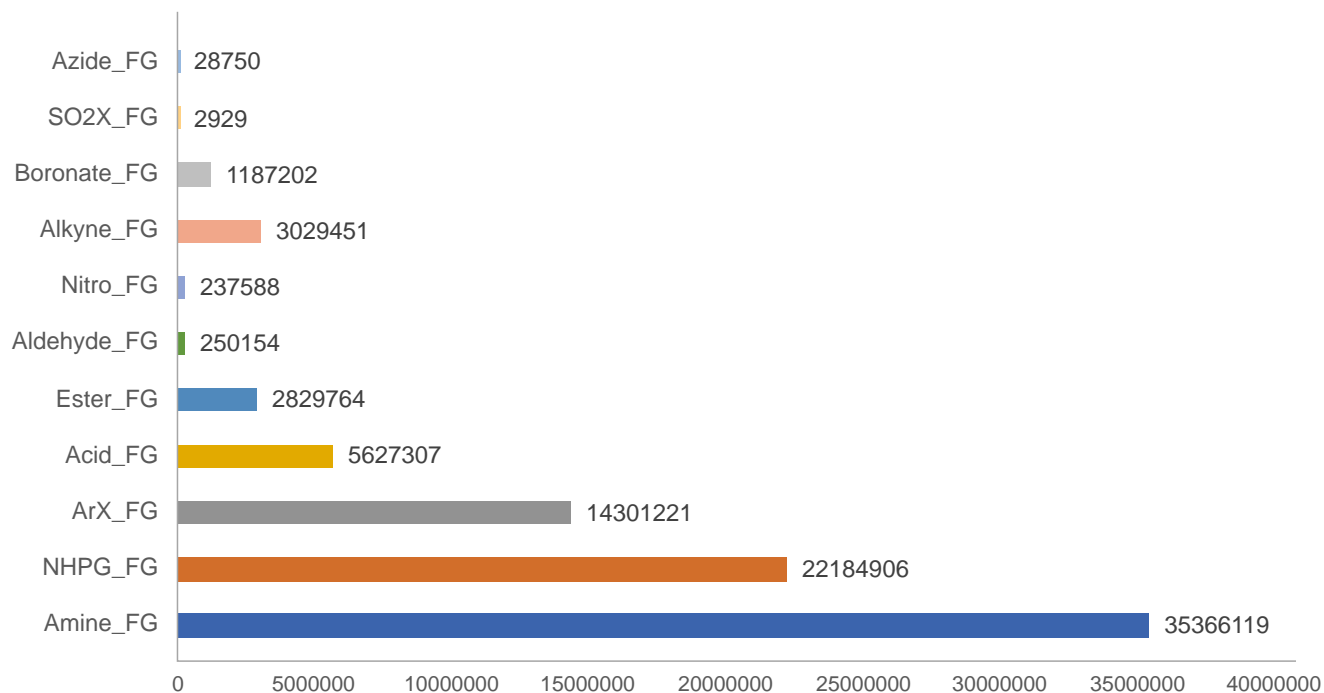


Figure 6. Chemspace “tangible” virtual bifunctional DEL-viable BBs, 43 848 442 molecules in 11 classes

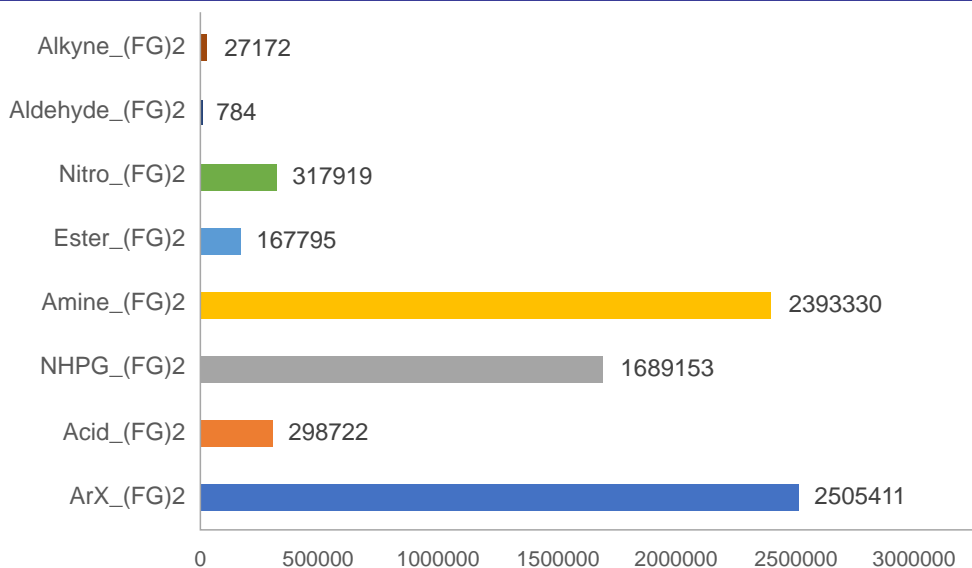


Figure 7. Chemspace “tangible” virtual trifunctional DEL-viable BBs, 3 119 488 molecules in 8 classes

or contain those as substructures, is given; the “unique scaffolds” column contains data on how many scaffolds are represented in the subclass; the “unique molecules” shows exactly how many molecules contain “unique scaffolds”.

To summarize the data obtained, we combined the results of our calculations into a single table (Table 4). The latter shows the inclusion of heterocyclization-derived scaffolds into the overall pool of bi- and tri-functional BBs, the stock (Enamine), as well as the virtual ones (Chemspace). The results of this analysis are not entirely expected: despite the fact that over the half of the core BBs chemotypes used in the

heterocyclizations described in Table 1 remain in DEL-chemistry for a long time (functional aldehydes, amines, etc.), their use in the reaction types outside “traditional” cross-couplings immediately provide more than 30% of the scaffold diversity in the entire DELT chemical extra-space.

For better visualizing the outline from Table 4, we constructed diagrams showing the contribution of the heterocyclic scaffolds to bifunctional BBs space, both stock (Figure 8A) and virtual (Figure 8B). We did the same for stock and virtual trifunctional blocks (Figure 9A and 9B, respectively).

**Table 1.** Heterocyclization reactions on DNA from the first case study to 2020

#	Reaction	Scaffold/Code
1	2	3
<b>Reaction type: 5-membered Aromatic Rings formation</b>		
1. [31]		Scaf_01
2. [45]		Scaf_02
3. [45]		Scaf_03
4. [46]		Scaf_04
5. [47]		Scaf_05
<b>Reaction type: 6-membered Aromatic Rings formation</b>		
6. [32]		Scaf_06
7. [32]		Scaf_07
8. [32]		Scaf_08
<b>Reaction type: Fused Aromatic Rings formation</b>		
9. [48]		Scaf_09

1	2	3
10. [49]	<p>1. <math>R^1-NH_2</math> 2. Reduction 3. <math>R^2-CHO</math></p>	<p>Scaf_10</p>
Reaction type: Carbocyclic, 5 and 6-membered Non-Aromatic Rings formation		
11. [50]	<p>[Ir] blue LED array</p>	<p>Scaf_11</p>
12. [51]	<p>1. <math>R-CHO</math> 2. <math>R^1-CH=CH-CO-R^2</math></p>	<p>Scaf_12</p>
13. [27]	<p>[Ru]</p>	<p>Scaf_13</p>
14. [49]		<p>Scaf_14</p>
15. [49]	<p>1. <math>R^1-CHO</math> 2. <math>R^2-CHO</math></p>	<p>Scaf_15</p>
16. [52]	<p>1. <math>Ph-CH_2-NH_2</math> 2. <math>O_2N-CH_2-CH=CH-CO-Cl</math> <math>Zr(DS)_4, ACN/H_2O</math></p>	<p>Scaf_16</p>
17. [52]	<p>1. <math>Ph-CH_2-NH_2</math> 2. <math>Cl-CH_2-CH=CH-CO-Cl</math> <math>Zr(DS)_4, ACN/H_2O</math></p>	<p>Scaf_17</p>
18. [27]	<p>[Ru]</p>	<p>Scaf_18</p> <p>Scaf_19</p> <p>Scaf_20</p>

1	2	3
Reaction type: Polycyclic Non-Aromatic Rings formation		
19. [53]		 Scaf_21
20. [54]		 Scaf_22  Scaf_23
21. [55]		 Scaf_24
22. [56]		 Scaf_25
23. [51]		 Scaf_26
24. [57]		 Scaf_27
25. [58]		 Scaf_28  Scaf_29
26. [49]		 Scaf_30

## Notes:

- DNA fragment (double-stranded), ds-DNA
- DNA fragment (single-stranded), ss-DNA
- ss-DNA fragment on a solid support

**Table 2.** The impact of heterocyclization-derived scaffolds to the bifunctional BBs chemical space

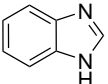
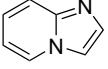
#	Sub-class	Scaffolds in ref	Molecules in ref	Unique scaffolds	Unique molecules
1	Acid_Aldehyde	6	12	55	331
2	Acid_Alkyne	6	10	25	141
3	Acid_ArX	79	234	311	2440
4	Acid_Azide	13	24	21	71
5	Acid_Ester	23	71	95	521
6	Acid_Nboc	257	806	349	1919
7	Acid_Ncbz	10	28	23	84
8	Acid_NCS	0	0	2	7
9	Acid_Nfmoc	179	437	247	1509
10	Acid_Nitro	29	46	119	781
11	Aldehyde_ArX	20	54	92	820
12	Aldehyde_Azide	0	0	6	8
13	Aldehyde_Ester	11	37	68	368
14	Aldehyde_Nboc	53	115	86	262
15	Aldehyde_Nitro	7	11	46	222
16	Aldehyde_SO2X	0	0	4	12
17	Amino_Alkyne	23	63	59	430
18	Amino_ArX	177	422	577	3352
19	Amino_Azide	7	16	21	54
20	Amino_Ester	267	878	523	4047
21	ArX_AlkyneCH	2	4	18	108
22	ArX_ArX	57	168	232	1227
23	Azide_ArX	4	8	11	80
24	Azide_SO2X	0	0	3	17
25	Diamines_Nbn	67	131	75	205
26	Diamines_Nboc	302	807	469	1761
27	Diamines_Ncbz	11	18	19	46
28	Diamines_Nfmoc	3	7	9	11
29	Ester_Isocyanates	1	2	6	31
30	Ester_SO2X	9	29	43	372
31	Functional tetrazine	0	0	2	8
32	Functional_Boronates	21	40	90	562
33	Functional_BF3K	8	12	18	51

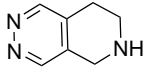
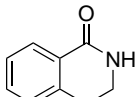
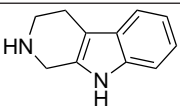
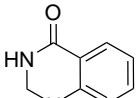
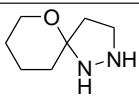
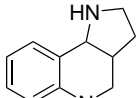
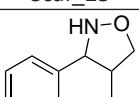
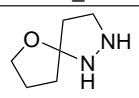
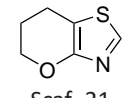
**Table 3.** The impact of heterocyclization-derived scaffolds to the trifunctional BBs chemical space

#	Sub-class	Scaffolds in ref	Molecules in ref	Unique scaffolds	Unique molecules
1	2	3	4	5	6
1	1,3,5-Trisubstituted_benzenes	12	15	20	257
2	Acid_Aldehyde_AlkyneCH	0	0	1	1
3	Acid_Aldehyde_ArX	1	3	6	23
4	Acid_Aldehyde_Nitro	0	0	1	4
5	Acid_ArX_Ester	0	0	5	16
6	Acid_ArX_Nitro	0	0	9	71
7	Acid_Ester_Nitro	0	0	2	5
8	Amino_ArX_ArX	3	10	35	172
9	Amino_ArX_Nitro	0	0	13	102
10	ArX_ArX_ArX	3	4	27	93
11	ArX_ArX_Carboxy	9	27	27	201
12	Azide_ArX_Carboxy	0	0	0	0
13	NbocAA_AlkyneCH	1	2	4	16
14	NbocAA_ArX	4	6	18	69
15	NbocAA_Ester	4	10	4	30
16	NbocAA_Nitro	0	0	1	4

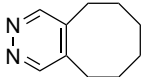
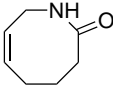
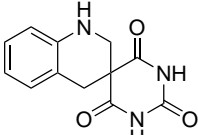
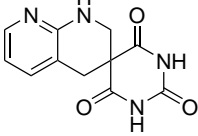
1	2	3	4	5	6
17	NbocArX_Amino	10	11	29	40
18	NbocEsterAA_Aldehyde	3	3	7	10
19	NbocEsterAA_Amino	23	41	24	57
20	NbocNCbzAA	2	2	4	8
21	NbocNfmocAA	21	34	23	75
22	NfmocAA_alkyneCH	1	1	3	7
23	NfmocAA_ArX	17	20	15	54
24	NfmocAA_Ester	1	4	5	27
25	NfmocAA_Nitro	0	0	1	3

**Table 4.** The overall quantity of bi- and tri-functional molecules containing the generated scaffolds (stock and virtual)

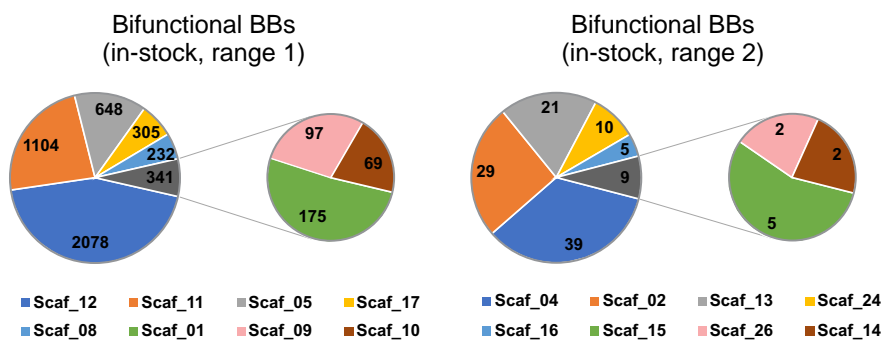
#	Scaffold (SMILES)	Scaffold Structure/Code	Bifunctional BBs		Trifunctional BBs	
			Stock	Virtual	Stock	Virtual
1	2	3	4	5	6	7
1	C1CCNC1	 Scaf_12	2078	7871461	109	485045
2	C1CCC1	 Scaf_11	1104	5941890	27	312303
3	S1C=CN=C1	 Scaf_05	648	1533087	15	75218
4	C1COCCN1	 Scaf_17	305	939622	3	51623
5	N1C=CN=N1	 Scaf_01	175	660222	2	53908
6	C1=CC=NN=C1	 Scaf_08	232	573015	33	52826
7	N1C=NC2=CC=CC=C12	 Scaf_10	69	175965	0	3524
8	O1C=NC=N1	 Scaf_04	39	156634	0	5888
9	N1C=NN=N1	 Scaf_02	29	103910	3	5056
10	C1NCC=C1	 Scaf_13	21	57571	0	4304
11	C1=CN2C=CC=CC2=N1	 Scaf_09	97	50346	5	1530

1	2	3	4	5	6	7
12	<chem>O=C1NCCO1</chem>	 Scaf_16	5	15795	0	756
13	<chem>O=C1CNCN1</chem>	 Scaf_15	5	4651	0	133
14	<chem>C1CC2=C(CN1)C=NN=C2</chem>	 Scaf_07	0	2694	0	16
15	<chem>O=C1NCCCC2=CC=CC=C12</chem>	 Scaf_26	2	274	0	5
16	<chem>O=C1NCC=C1</chem>	 Scaf_14	2	253	0	11
17	<chem>C1CC2=C(CN1)NC1=C(C=CC21)</chem>	 Scaf_24	10	220	0	2
18	<chem>O=C1CC=CCN1</chem>	 Scaf_18	0	96	0	12
19	<chem>O=C1NCNC2=CC=CC=C12</chem>	 Scaf_30	0	11	0	0
20	<chem>C1CC2(CCCC2)NN1</chem>	 Scaf_29	0	0	0	0
21	<chem>C1CC2CNC3=CC=CC=C3C2N1</chem>	 Scaf_25	0	0	0	0
22	<chem>C1ONC2C1COC1=CC=CC=C21</chem>	 Scaf_27	0	0	0	0
23	<chem>C1COC2(C1)CCNN2</chem>	 Scaf_28	0	0	0	0
24	<chem>C1COC2=C(C1)SC=N2</chem>	 Scaf_21	0	0	0	0

Continuation of Table 4

1	2	3	4	5	6	7
25	<chem>C1CCCC2=C(CC1)C=NN=C2</chem>	 Scaf_06	0	0	0	0
26	<chem>O1C=NN=C1</chem>	 Scaf_03	0	0	0	0
27	<chem>O=C1CCC=CCN1</chem>	 Scaf_19	0	0	0	0
28	<chem>O=C1CCCC=CCN1</chem>	 Scaf_20	0	0	0	0
29	<chem>O=C1NC(=O)C2(CNC3=CC=CC=C3C2)C(=O)N1</chem>	 Scaf_22	0	0	0	0
30	<chem>O=C1NC(=O)C2(CNC3=NC=CC=C3C2)C(=O)N1</chem>	 Scaf_23	0	0	0	0

A



B

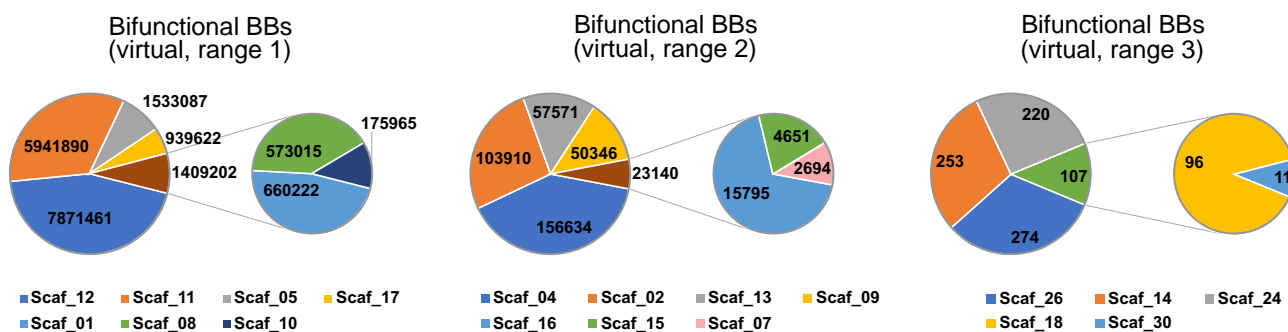


**Figure 8.** The visualized impact of the on-DNA heterocyclization reactions-derived scaffold to the existing chemical space of stock (A) and tangible virtual (B) bifunctional DEL-viable BBs

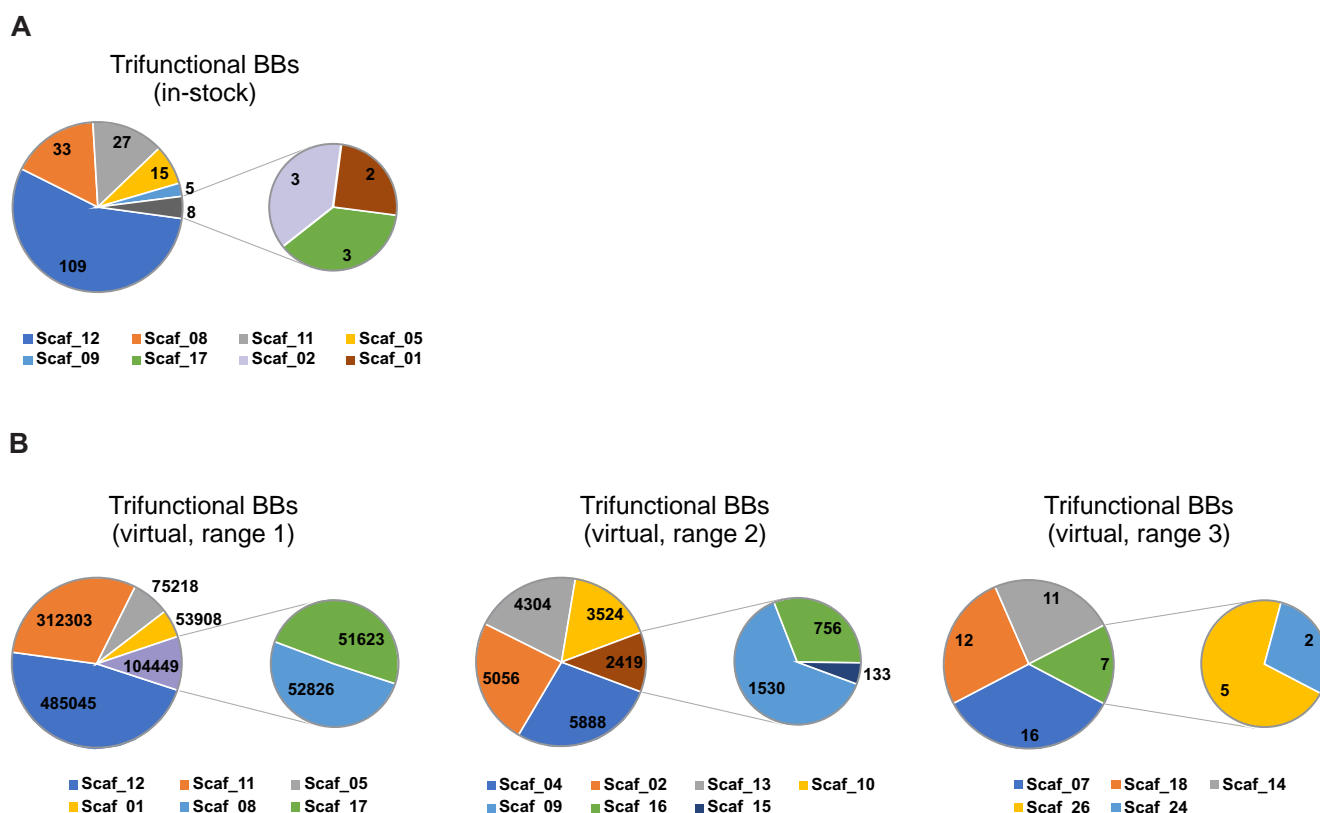


**Figure 9.** The visualized impact of the on-DNA heterocyclization reactions-derived scaffold to the existing chemical space of stock (A) and tangible virtual (B) trifunctional DEL-viable BBs

## Conclusions

We have analyzed both stock and virtual chemical spaces of bi- and tri-functional DELT-viable building blocks using Enamine Ltd. stock collection (*ca.* 30000 molecules) and Chemspace Ltd. tangible set (over 43 million structures) as case studies. Despite seeming variability within both groups (bi- and tri-functional BBs), the compounds with functions suitable for classic cross-coupling reactions, such as amide couplings or ArX – NHR<sub>2</sub> couplings, namely acids, amines, protected amines and aryl halides, vastly outnumber other functional classes. The latter significantly limits both current and nearest-time potential chemical diversity of the DNA-encoded libraries composed on the basis of these types of BBs, especially on the background of the huge size of such libraries: literally what we get is massive numbers of chemically homogeneous molecules, and it extremely complicates readout at the stages of the biological testing. Considering the fact that in case of the cross-coupling approach to the DEL synthesis, the overwhelming majority of potentially useful transformations were already adapted for DNA-friendly conditions, one promising way to

approach better diversity of DEL chemical space is to facilitate the synthesis of less common classes of bi- and tri-functional cores like those with sulfonyl halide, boronate, nitro- or aldehyde FGs. However, recent advances in on-DNA heterocyclizations introduced some new chemotypes to the field. Surprisingly, adding 30 scaffolds derived from 26 types of heterocyclizations, even with many of these scaffolds already being a part of the multifunctional cores space, has allowed to expand the general scaffold diversity of the chemical space observed by more than 30%. This finding clearly indicates that adapting the existing and/or finding new heterocyclizations suitable for DNA-friendly conditions, which first and foremost could feed on the existing pool of BBs, is another very potent way to expand the scaffold diversity in DELs.

## Acknowledgments

The authors express their gratitude to Enamine Ltd. and Chemspace Ltd. for granting access to their data sets, and personally to Prof. Andrey A. Tolmachev for encouragement and comprehensive support in preparing the manuscript.

## References

- Brenner, S.; Lerner, R. A. Encoded combinatorial chemistry. *Proceedings of the National Academy of Sciences* **1992**, *89* (12), 5381–5383. <https://doi.org/10.1073/pnas.89.12.5381>.
- Goodnow, R. A., Jr.; Dumelin, C. E.; Keefe, A. D. DNA-encoded chemistry: enabling the deeper sampling of chemical space. *Nat. Rev. Drug Discov.* **2017**, *16* (2), 131–147. <https://doi.org/10.1038/nrd.2016.213>.
- Satz, A. L.; Brunschweiler, A.; Flanagan, M. E.; Gloger, A.; Hansen, N. J. V.; Kuai, L.; Kunig, V. B. K.; Lu, X.; Madsen, D.; Marcaurelle, L. A.; Mulrooney, C.; O'Donovan, G.; Sakata, S.; Scheuermann, J. DNA-encoded chemical libraries. *Nature Reviews Methods Primers* **2022**, *2* (1). <https://doi.org/10.1038/s43586-021-00084-5>.
- Mannocci, L.; Zhang, Y.; Scheuermann, J.; Leimbacher, M.; De Bellis, G.; Rizzi, E.; Dumelin, C.; Melkko, S.; Neri, D. High-throughput sequencing allows the identification of binding molecules isolated from DNA-encoded chemical libraries. *Proc. Natl. Acad. Sci. U. S. A.* **2008**, *105* (46), 17670–5. <https://doi.org/10.1073/pnas.0805130105>.
- Liu, R.; Li, X.; Lam, K. S. Combinatorial chemistry in drug discovery. *Curr. Opin. Chem. Biol.* **2017**, *38*, 117–126. <https://doi.org/10.1016/j.cbpa.2017.03.017>.
- Deng, H.; O'Keefe, H.; Davie, C. P.; Lind, K. E.; Acharya, R. A.; Franklin, G. J.; Larkin, J.; Matico, R.; Neeb, M.; Thompson, M. M.; Lohr, T.; Gross, J. W.; Centrella, P. A.; O'Donovan, G. K.; Bedard, K. L.; van Vloten, K.; Mataruse, S.; Skinner, S. R.; Belyanskaya, S. L.; Carpenter, T. Y.; Shearer, T. W.; Clark, M. A.; Cuzzo, J. W.; Arico-Muendel, C. C.; Morgan, B. A. Discovery of highly potent and selective small molecule ADAMTS-5 inhibitors that inhibit human cartilage degradation via encoded library technology (ELT). *J. Med. Chem.* **2012**, *55* (16), 7061–79. <https://doi.org/10.1021/jm300449x>.
- Madsen, D.; Azevedo, C.; Micco, I.; Petersen, L. K.; Hansen, N. J. V. An overview of DNA-encoded libraries: A versatile tool for drug discovery. *Prog. Med. Chem.* **2020**, *59*, 181–249. <https://doi.org/10.1016/bs.pmch.2020.03.001>.
- Petersen, L. K.; Christensen, A. B.; Andersen, J.; Folkesson, C. G.; Kristensen, O.; Andersen, C.; Alzu, A.; Slok, F. A.; Blakskjaer, P.; Madsen, D.; Azevedo, C.; Micco, I.; Hansen, N. J. V. Screening of DNA-Encoded Small Molecule Libraries inside a Living Cell. *J. Am. Chem. Soc.* **2021**, *143* (7), 2751–2756. <https://doi.org/10.1021/jacs.0c09213>.
- Satz, A. L.; Kuai, L.; Peng, X. Selections and screenings of DNA-encoded chemical libraries against enzyme and cellular targets. *Bioorg. Med. Chem. Lett.* **2021**, *39*, 127851. <https://doi.org/10.1016/j.bmcl.2021.127851>.
- Huang, Y.; Li, Y.; Li, X. Strategies for developing DNA-encoded libraries beyond binding assays. *Nat. Chem.* **2022**, *14* (2), 129–140. <https://doi.org/10.1038/s41557-021-00877-x>.
- Roy, A.; Kodadek, T. DELs Inside Cells. *Trends in Pharmacological Sciences* **2020**, *41* (4), 225–227. <https://doi.org/10.1016/j.tips.2020.01.007>.
- Bassi, G.; Favalli, N.; Oehler, S.; Martinelli, A.; Catalano, M.; Scheuermann, J.; Neri, D. Comparative evaluation of DNA-encoded chemical selections performed using DNA in single-stranded or double-stranded format. *Biochem. Biophys. Res. Commun.* **2020**, *533* (2), 223–229. <https://doi.org/10.1016/j.bbrc.2020.04.035>.
- Li, X.; Liu, D. R. DNA-templated organic synthesis: nature's strategy for controlling chemical reactivity applied to synthetic molecules. *Angew. Chem. Int. Ed. Engl.* **2004**, *43* (37), 4848–70. <https://doi.org/10.1002/anie.200400656>.
- Fair, R. J.; Walsh, R. T.; Hupp, C. D. The expanding reaction toolkit for DNA-encoded libraries. *Bioorg. Med. Chem. Lett.* **2021**, *51*, 128339. <https://doi.org/10.1016/j.bmcl.2021.128339>.
- Clark, M. A.; Acharya, R. A.; Arico-Muendel, C. C.; Belyanskaya, S. L.; Benjamin, D. R.; Carlson, N. R.; Centrella, P. A.; Chiu, C. H.; Creaser, S. P.; Cuzzo, J. W.; Davie, C. P.; Ding, Y.; Franklin, G. J.; Franzen, K. D.; Geftner, M. L.; Hale, S. P.; Hansen, N. J.; Israel, D. I.; Jiang, J.; Kavaran, M. J.; Kelley, M. S.; Kollmann, C. S.; Li, F.; Lind, K.; Mataruse, S.; Medeiros, P. F.; Messer, J. A.; Myers, P.; O'Keefe, H.; Oliff, M. C.; Rise, C. E.; Satz, A. L.; Skinner, S. R.; Svendsen, J. L.; Tang, L.; van Vloten, K.; Wagner, R. W.; Yao, G.; Zhao, B.; Morgan, B. A. Design, synthesis and selection of DNA-encoded small-molecule libraries. *Nat. Chem. Biol.* **2009**, *5* (9), 647–54. <https://doi.org/10.1038/nchembio.211>.
- Gerry, C. J.; Wawer, M. J.; Clemons, P. A.; Schreiber, S. L. DNA Barcoding a Complete Matrix of Stereoisomeric Small Molecules. *J. Am. Chem. Soc.* **2019**, *141* (26), 10225–10235. <https://doi.org/10.1021/jacs.9b01203>.
- Fitzgerald, P. R.; Paegel, B. M. DNA-Encoded Chemistry: Drug Discovery from a Few Good Reactions. *Chem. Rev.* **2021**, *121* (12), 7155–7177. <https://doi.org/10.1021/acs.chemrev.0c00789>.
- Song, M.; Hwang, G. T. DNA-Encoded Library Screening as Core Platform Technology in Drug Discovery: Its Synthetic Method Development and Applications in DEL Synthesis. *J. Med. Chem.* **2020**, *63* (13), 6578–6599. <https://doi.org/10.1021/acs.jmedchem.9b01782>.
- Pikalyova, R.; Zabolotna, Y.; Volochnyuk, D. M.; Horvath, D.; Marcou, G.; Varnek, A. Exploration of the Chemical Space of DNA-encoded Libraries. *Molecular Informatics* **2022**, *41* (6). <https://doi.org/10.1002/minf.202100289>.
- Shi, B.; Zhou, Y.; Huang, Y.; Zhang, J.; Li, X. Recent advances on the encoding and selection methods of DNA-encoded chemical library. *Bioorg. Med. Chem. Lett.* **2017**, *27* (3), 361–369. <https://doi.org/10.1016/j.bmcl.2016.12.025>.
- Salamon, H.; Klika Skopic, M.; Jung, K.; Bugain, O.; Brunschweiler, A. Chemical Biology Probes from Advanced DNA-encoded Libraries. *ACS Chem. Biol.* **2016**, *11* (2), 296–307. <https://doi.org/10.1021/acschembio.5b00981>.
- Zhu, H.; Foley, T. L.; Montgomery, J. I.; Stanton, R. V. Understanding Data Noise and Uncertainty through Analysis of Replicate Samples in DNA-Encoded Library Selection. *J. Chem. Inf. Model.* **2022**, *62* (9), 2239–2247. <https://doi.org/10.1021/acs.jcim.1c00986>.
- Foley, T. L.; Burchett, W.; Chen, Q.; Flanagan, M. E.; Kapinos, B.; Li, X.; Montgomery, J. I.; Ratnayake, A. S.; Zhu, H.; Peakman, M. C. Selecting Approaches for Hit Identification and Increasing Options by Building the Efficient Discovery of Actionable Chemical Matter from DNA-Encoded Libraries. *SLAS Discov.* **2021**, *26* (2), 263–280. <https://doi.org/10.1177/2472555220979589>.
- Needels, M. C.; Jones, D. G.; Tate, E. H.; Heinkel, G. L.; Kochersperger, L. M.; Dower, W. J.; Barrett, R. W.; Gallop, M. A. Generation and screening of an oligonucleotide-encoded synthetic peptide library. *Proc. Natl. Acad. Sci. U. S. A.* **1993**, *90* (22), 10700–4. <https://doi.org/10.1073/pnas.90.22.10700>.
- de Pedro Beato, E.; Priego, J.; Gironda-Martinez, A.; Gonzalez, F.; Benavides, J.; Blas, J.; Martin-Ortega, M. D.; Toledo, M. A.; Ezquerria, J.; Torrado, A. Mild and Efficient Palladium-Mediated C-N Cross-Coupling Reaction between DNA-Conjugated Aryl Bromides and Aromatic Amines. *ACS Comb. Sci.* **2019**, *21* (2), 69–74. <https://doi.org/10.1021/acscmbosci.8b00142>.
- Monty, O. B. C.; Nyshadham, P.; Bohren, K. M.; Palaniappan, M.; Matzuk, M. M.; Young, D. W.; Simmons, N. Homogeneous and Functional Group Tolerant Ring-Closing Metathesis for DNA-Encoded Chemical Libraries. *ACS Comb. Sci.* **2020**, *22* (2), 80–88. <https://doi.org/10.1021/acscmbosci.9b00199>.

27. Lu, X.; Fan, L.; Phelps, C. B.; Davie, C. P.; Donahue, C. P. Ruthenium Promoted On-DNA Ring-Closing Metathesis and Cross-Metathesis. *Bioconjug. Chem.* **2017**, *28* (6), 1625–1629. <https://doi.org/10.1021/acs.bioconjchem.7b00292>.
28. Devaraj, N. K.; Finn, M. G. Introduction: Click Chemistry. *Chem. Rev.* **2021**, *121* (12), 6697–6698. <https://doi.org/10.1021/acs.chemrev.1c00469>.
29. Reddavid, F. V.; Lin, W.; Lehnert, S.; Zhang, Y. DNA-Encoded Dynamic Combinatorial Chemical Libraries. *Angew. Chem. Int. Ed. Engl.* **2015**, *54* (27), 7924–8. <https://doi.org/10.1002/anie.201501775>.
30. An, Y.; Yan, H.; Dong, Z.; Satz, A. L. DNA-Compatible Click Reaction Employing In Situ Generated Azides from Boronic Acids. *Curr. Protoc.* **2021**, *1* (5), e125. <https://doi.org/10.1002/cpz1.125>.
31. Qu, Y.; Wen, H.; Ge, R.; Xu, Y.; Gao, H.; Shi, X.; Wang, J.; Cui, W.; Su, W.; Yang, H.; Kuai, L.; Satz, A. L.; Peng, X. Copper-Mediated DNA-Compatible One-Pot Click Reactions of Alkynes with Aryl Borates and TMS-N(3). *Org. Lett.* **2020**, *22* (11), 4146–4150. <https://doi.org/10.1021/acs.orglett.0c01219>.
32. Li, H.; Sun, Z.; Wu, W.; Wang, X.; Zhang, M.; Lu, X.; Zhong, W.; Dai, D. Inverse-Electron-Demand Diels-Alder Reactions for the Synthesis of Pyridazines on DNA. *Org. Lett.* **2018**, *20* (22), 7186–7191. <https://doi.org/10.1021/acs.orglett.8b03114>.
33. Sun, H.; Xue, Q.; Zhang, C.; Wu, H.; Feng, P. Derivatization based on tetrazine scaffolds: synthesis of tetrazine derivatives and their biomedical applications. *Organic Chemistry Frontiers* **2022**, *9* (2), 481–498. <https://doi.org/10.1039/d1qo01324f>.
34. Matsuo, B.; Granados, A.; Levitre, G.; Molander, G. A. Photochemical Methods Applied to DNA Encoded Library (DEL) Synthesis. *Acc. Chem. Res.* **2023**, *56* (3), 385–401. <https://doi.org/10.1021/acs.accounts.2c00778>.
35. Martín, A.; Nicolaou, C. A.; Toledo, M. A. Navigating the DNA encoded libraries chemical space. *Communications Chemistry* **2020**, *3* (1). <https://doi.org/10.1038/s42004-020-00374-1>.
36. Conole, D.; Hunter, J. H.; Waring, M. J. The maturation of DNA encoded libraries: opportunities for new users. *Future Med. Chem.* **2021**, *13* (2), 173–191. <https://doi.org/10.4155/fmc-2020-0285>.
37. Pereira, D. A.; Williams, J. A. Origin and evolution of high throughput screening. *Br. J. Pharmacol.* **2007**, *152* (1), 53–61. <https://doi.org/10.1038/sj.bjp.0707373>.
38. Volochnyuk, D. M.; Ryabukhin, S. V.; Moroz, Y. S.; Savych, O.; Chuprina, A.; Horvath, D.; Zabolotna, Y.; Varnek, A.; Judd, D. B. Evolution of commercially available compounds for HTS. *Drug Discov. Today* **2019**, *24* (2), 390–402. <https://doi.org/10.1016/j.drudis.2018.10.016>.
39. Buskes, M. J.; Blanco, M. J. Impact of Cross-Coupling Reactions in Drug Discovery and Development. *Molecules* **2020**, *25* (15). <https://doi.org/10.3390/molecules25153493>.
40. Shi, Y.; Wu, Y. R.; Yu, J. Q.; Zhang, W. N.; Zhuang, C. L. DNA-encoded libraries (DELs): a review of on-DNA chemistries and their output. *RSC Adv.* **2021**, *11* (4), 2359–2376. <https://doi.org/10.1039/d0ra09889b>.
41. Zabolotna, Y.; Volochnyuk, D. M.; Ryabukhin, S. V.; Gavrylenko, K.; Horvath, D.; Klimchuk, O.; Oksiuta, O.; Marcou, G.; Varnek, A. Synthli: A New Open-Source Tool for Synthon-Based Library Design. *J. Chem. Inf. Model.* **2022**, *62* (9), 2151–2163. <https://doi.org/10.1021/acs.jcim.1c00754>.
42. Zabolotna, Y.; Volochnyuk, D. M.; Ryabukhin, S. V.; Horvath, D.; Gavrylenko, K. S.; Marcou, G.; Moroz, Y. S.; Oksiuta, O.; Varnek, A. A Close-up Look at the Chemical Space of Commercially Available Building Blocks for Medicinal Chemistry. *J. Chem. Inf. Model.* **2022**, *62* (9), 2171–2185. <https://doi.org/10.1021/acs.jcim.1c00811>.
43. Verma, A.; Ram Yadav, M.; Giridhar, R.; Prajapati, N.; C. Tripathi, A.; K. Saraf, S. Nitrogen Containing Privileged Structures and their Solid Phase Combinatorial Synthesis. *Combinatorial Chemistry & High Throughput Screening* **2013**, *16* (5), 345–393.
44. Mishra, B. B.; Kumar, D.; Mishra, A.; Mohapatra, P. P.; Tiwari, V. K., Chapter 2 - Cyclo-Release Strategy in Solid-Phase Combinatorial Synthesis of Heterocyclic Skeletons. In *Advances in Heterocyclic Chemistry*, Katritzky, A. R., Ed. Academic Press: 2012; Vol. 107, pp 41–99.
45. Kunig, V. B. K.; Ehrt, C.; Domling, A.; Brunschweiler, A. Isocyanide Multicomponent Reactions on Solid-Phase-Coupled DNA Oligonucleotides for Encoded Library Synthesis. *Org. Lett.* **2019**, *21* (18), 7238–7243. <https://doi.org/10.1021/acs.orglett.9b02448>.
46. Du, H. C.; Bangs, M. C.; Simmons, N.; Matzuk, M. M. Multistep Synthesis of 1,2,4-Oxadiazoles via DNA-Conjugated Aryl Nitrile Substrates. *Bioconjug. Chem.* **2019**, *30* (5), 1304–1308. <https://doi.org/10.1021/acs.bioconjchem.9b00188>.
47. Potewar, T. M.; Ingale, S. A.; Srinivasan, K. V. Catalyst-free efficient synthesis of 2-aminothiazoles in water at ambient temperature. *Tetrahedron* **2008**, *64* (22), 5019–5022. <https://doi.org/10.1016/j.tet.2008.03.082>.
48. Shaaban, S.; Abdel-Wahab, B. F. Groebke-Blackburn-Bienayme multicomponent reaction: emerging chemistry for drug discovery. *Mol. Divers.* **2016**, *20* (1), 233–54. <https://doi.org/10.1007/s11030-015-9602-6>.
49. Satz, A. L.; Cai, J.; Chen, Y.; Goodnow, R.; Gruber, F.; Kowalczyk, A.; Petersen, A.; Naderi-Oboodi, G.; Orzechowski, L.; Strebel, Q. DNA Compatible Multistep Synthesis and Applications to DNA Encoded Libraries. *Bioconjug. Chem.* **2015**, *26* (8), 1623–32. <https://doi.org/10.1021/acs.bioconjchem.5b00239>.
50. Kolmel, D. K.; Ratnayake, A. S.; Flanagan, M. E.; Tsai, M. H.; Duan, C.; Song, C. Photocatalytic [2+2] Cycloaddition in DNA-Encoded Chemistry. *Org. Lett.* **2020**, *22* (8), 2908–2913. <https://doi.org/10.1021/acs.orglett.0c00574>.
51. Potowski, M.; Kunig, V. B. K.; Losch, F.; Brunschweiler, A. Synthesis of DNA-coupled isoquinolones and pyrrolidines by solid phase ytterbium- and silver-mediated imine chemistry. *MedChemComm* **2019**, *10* (7), 1082–1093. <https://doi.org/10.1039/c9md00042a>.
52. Fan, L.; Davie, C. P. Zirconium(IV)-Catalyzed Ring Opening of on-DNA Epoxides in Water. *ChemBiochem* **2017**, *18* (9), 843–847. <https://doi.org/10.1002/cbic.201600563>.
53. Wu, W.; Sun, Z.; Wang, X.; Lu, X.; Dai, D. Construction of Thiazole-Fused Dihydropyrans via Formal [4+2] Cycloaddition Reaction on DNA. *Org. Lett.* **2020**, *22* (8), 3239–3244. <https://doi.org/10.1021/acs.orglett.0c01016>.
54. Tian, X.; Basarab, G. S.; Selmi, N.; Kogej, T.; Zhang, Y.; Clark, M.; Goodnow Jr, R. A. Development and design of the tertiary amino effect reaction for DNA-encoded library synthesis. *MedChemComm* **2016**, *7* (7), 1316–1322. <https://doi.org/10.1039/c6md00088f>.
55. Li, K.; Liu, X.; Liu, S.; An, Y.; Shen, Y.; Sun, Q.; Shi, X.; Su, W.; Cui, W.; Duan, Z.; Kuai, L.; Yang, H.; Satz, A. L.; Chen, K.; Jiang, H.; Zheng, M.; Peng, X.; Lu, X. Solution-Phase DNA-Compatible Pictet-Spengler Reaction Aided by Machine Learning Building Block Filtering. *iScience* **2020**, *23* (6), 101142. <https://doi.org/10.1016/j.isci.2020.101142>.
56. Skopic, M. K.; Gotte, K.; Gramse, C.; Dieter, M.; Pospich, S.; Raunser, S.; Weberskirch, R.; Brunschweiler, A. Micellar Bronsted Acid Mediated Synthesis of DNA-Tagged Heterocycles. *J. Am. Chem. Soc.* **2019**, *141* (26), 10546–10555. <https://doi.org/10.1021/jacs.9b05696>.
57. Gerry, C. J.; Yang, Z.; Stasi, M.; Schreiber, S. L. DNA-Compatible [3+2] Nitron-Olefin Cycloaddition Suitable for DEL Syntheses. *Org. Lett.* **2019**, *21* (5), 1325–1330. <https://doi.org/10.1021/acs.orglett.9b00017>.

58. Klika Skopic, M.; Willems, S.; Wagner, B.; Schieven, J.; Krause, N.; Brunschweiger, A. Exploration of a Au(I)-mediated three-component reaction for the synthesis of DNA-tagged highly substituted spiroheterocycles. *Org. Biomol. Chem.* **2017**, *15* (40), 8648–8654. <https://doi.org/10.1039/c7ob02347b>.

---

*Information about the authors:*

**Oleksandr V. Oksiuta**, Ph.D. Student of the Biologically Active Compounds Department, Institute of Organic Chemistry of the National Academy of Sciences of Ukraine; Data Scientist at Chemspace Ltd.; <https://orcid.org/0000-0003-3049-0373>.

**Alexander E. Pashenko**, Ph.D. in Chemistry, Junior Researcher of the Department of Physicochemical Investigations, Institute of Organic Chemistry of the National Academy of Sciences of Ukraine; <https://orcid.org/0000-0001-6157-0785>.

**Radomyr V. Smalii**, Ph.D. in Chemistry, Project Manager at Enamine Ltd.; <https://orcid.org/0000-0003-0379-1138>.

**Dmitriy M. Volochnyuk** (*corresponding author*), Dr.Sci. in Chemistry, Professor of the Supramolecular Chemistry Department, Institute of High Technologies, Taras Shevchenko National University of Kyiv; Head of the Biologically Active Compounds Department, Institute of Organic Chemistry of the National Academy of Sciences of Ukraine; Senior Scientific Advisor, Enamine Ltd.; <https://orcid.org/0000-0001-6519-1467>; e-mail for correspondence: [d.volochnyuk@gmail.com](mailto:d.volochnyuk@gmail.com).

**Sergey V. Ryabukhin** (*corresponding author*), Dr.Sci. in Chemistry, Professor, Head of the Supramolecular Chemistry Department, Institute of High Technologies, Taras Shevchenko National University of Kyiv; Senior Scientific Advisor, Enamine Ltd.; Senior Researcher of the Department of Physicochemical Investigations, Institute of Organic Chemistry of the National Academy of Sciences of Ukraine; <https://orcid.org/0000-0003-4281-8268>; e-mail for correspondence: [s.v.ryabukhin@gmail.com](mailto:s.v.ryabukhin@gmail.com).

UDC 54.057:547.833:615.2

M. A. Jordaan, O. Ebenezer

Department of Chemistry, Faculty of Natural Sciences, Mangosuthu University of Technology,  
511 Griffiths Mxenge Highway, 4031 Umlazi, South Africa

## Biological Activities of Tetrahydroisoquinolines Derivatives

### Abstract

1,2,3,4-Tetrahydroisoquinoline (THIQ) is a common scaffold of many alkaloids isolated from several plants and mammalian species. THIQ derivatives possess a broad spectrum of biological activities, including antitumor, antitubercular, antitrypanosomal, antibacterial, anti-HIV, anti-inflammatory, anti-Alzheimer, and anticonvulsant ones.

**Aim.** To cover updated studies on the biological properties of THIQ derivatives, as well as their structure-activity relationship (SAR), in order to highlight the effect of diverse functional groups responsible for the manifestation of the desired activity.

**Results and discussion.** We have presented the review on biological activities of THIQ. The SAR studies show that the electron-donating, electron-withdrawing and some heterocyclic functional groups on the backbone plays a vital role in modulating the biological potential of the compounds synthesized.

**Conclusions.** This review will help pharmaceutical researchers to synthesize novel and potent compounds containing THIQ scaffold.

**Keyword:** tetrahydroisoquinoline; assessment of biological activity; structure-activity relationship; molecular docking

**М. А. Джордаан, О. Ебенезер**

Кафедра хімії, Факультет природничих наук, Технологічний університет Мангосуту,  
Шосе Гріффітс Мксенге, 511, Умлазі, 4031, Південно-Африканська Республіка

### Біологічна активність похідних тетрагідроізохіноліну

#### Анотація

1,2,3,4-Тетрагідроізохінолін (ТГІХ) є розповсюдженим каркасом багатьох алкалоїдів, виділених з кількох видів рослин і ссавців. Похідні ТГІХ мають широкий спектр біологічних активностей, зокрема протипухлинну, протитуберкульозну, протитрипаносомну, антибактеріальну, анти-ВІЛ, протизапальну, протисудомну дію, а також є перспективними агентами для лікування хвороби Альцгеймера.

**Мета.** Цей огляд охоплює оновлені дослідження з біологічних властивостей похідних ТГІХ, а також взаємозв'язок між їхньою структурою та активністю (SAR), щоб підкреслити вплив різноманітних функціональних груп, відповідальних за прояв бажаної активності.

**Результати та їх обговорення.** У роботі наведено огляд біологічної активності ТГІХ. SAR дослідження свідчать, що електронодонорні, електроноакцепторні та деякі гетероциклічні функціональні групи, зв'язані з каркасом ТГІХ, відіграють дуже важливу роль у модулюванні біологічного потенціалу синтезованих сполук.

**Висновки.** Цей огляд допоможе дослідникам у галузі фармацевтики синтезувати нові та ефективні сполуки, що містять базову структуру ТГІХ.

**Ключові слова:** тетрагідроізохінолін; оцінка біологічної активності; зв'язок структура-активність; молекулярний докінг

**Citation:** Jordaan, M. A.; Ebenezer, O. Biological Activities of Tetrahydroisoquinolines Derivatives. *Journal of Organic and Pharmaceutical Chemistry* **2023**, 21 (1), 20–38.

<https://doi.org/10.24959/ophcj.23.268358>

**Received:** 5 December 2022; **Revised:** 26 February 2023; **Accepted:** 26 March 2023

**Copyright** © 2023, M. A. Jordaan, O. Ebenezer. This is an open access article under the CC BY license (<http://creativecommons.org/licenses/by/4.0>).

**Funding:** The authors received no specific funding for this work.

**Conflict of interests:** The authors have no conflict of interests to declare.

## ■ Introduction

1,2,3,4-Tetrahydroisoquinoline (THIQ) is a common scaffold of many alkaloids isolated from several plants and mammalian species. Several synthetic routes for the synthesis of substances that could be incorporated as privileged structural motifs into therapeutic compounds have been reported, and this has led to outstanding advances in drug discovery. Although most of the general methods for the synthesis of THIQ involve with the metal-catalyzed hydrogenation of isoquinolines [1], THIQ possesses a broad spectrum of biological activities, including antitumor, antitubercular, antitrypanosomal, antibacterial, anti-HIV, anti-inflammatory, anti-Alzheimer, and anticonvulsant ones [2–9]. Some of the naturally occurring THIQ-based compounds and clinically available THIQ drugs, such as quinapril, nospapine, tubocurarine (one of the quaternary ammonium muscle relaxants), and apomorphine, are shown in Figure 1. Examples of clinical drugs containing 4-substituted THIQ include nomifensine and diclofensine. Nomifensine is a bicyclic antidepressant, and its powerful inhibitory effect on the dopamine uptake makes the drug have a distinct pharmacological profile different from that of tricyclic drugs [10]. The drug was withdrawn from the market due to the large number of reported cases of acute hemolytic anemia with intravascular hemolysis. The continued use of the drug required a new strategy to reduce the dose and increase its effectiveness. *Kang and coworkers* reported that nomifensine optimized by ionizing radiation (IR)-NF could enhance the therapeutic effectiveness in obstructing breast cancer proliferation by inducing cell death [11]. Diclofensine (Ro-8-4650) is an effective monoamine reuptake inhibitor, blocking the uptake of dopamine, noradrenaline, and serotonin by rat brain synaptosomes with  $IC_{50}$  values of 0.74, 2.3, and 3.7 nM, respectively. In addition, diclofensine binds to adrenergic, dopamine, serotonin, and trace amine-associated receptors [12]. This review, therefore, aims to present an updated information on the biological properties of THIQ derivatives and their structure-activity relationship (SAR) in order to highlight the effect of diverse functional groups responsible for the manifestation of the desired activity.

## ■ Results and discussion

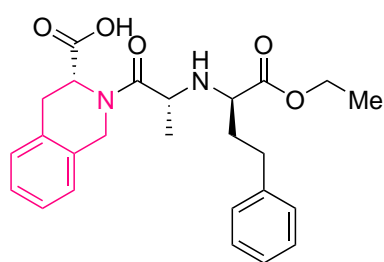
### Orexin receptor antagonists

Orexins (hypocretins) have been reported in the literature as endogenous compounds for two

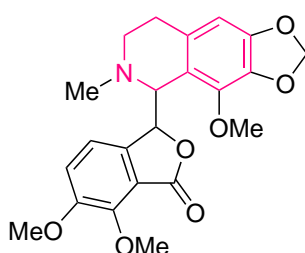
orphan G-protein-coupled receptors in the lateral hypothalamic area. Orexins can initiate orexin neurons, monoaminergic and cholinergic neurons to conserve an extensive, consolidated awake period in the hypothalamus/brainstem regions, [13, 14]. The orexin receptor stimulus is primarily excitatory and releases various neurotransmitters responsible for maintaining arousal, wakefulness, and appetite. Currently, three orexin receptor antagonists, namely, suvorexant, lemborexant, and daridorexant, are FDA approved for the treatment of insomnia. Several THIQ derivatives have been reported as orexin antagonists. ACT-335827, a phenylglycine-amide-substituted THIQ derivative, was reported by *Actelion and coworkers* as potent and  $OX_1$  selective (**1**,  $IC_{50}$   $OX_1 = 6$  nM and  $OX_2 = 417$  nM) [15]. RTIOX-276, **2** blocked the development of the locomotor sensitization to cocaine in rats and thereby reduced cravings for cocaine [16, 17] (Figure 2).

*Watanabe and coworkers* designed novel tetrahydroisoquinoline derivatives with a fluoroethyl group and evaluated their effectiveness for positron emission tomography (PET) imaging of  $OX_1R$  [18]. To quantify the affinity for  $OX_1R$  and  $OX_2R$ , the *in vitro* competitive inhibition assays using  $OX_1R$  or  $OX_2R$  cells were carried out. The assay used Orexin A as the competitive ligand because of its affinity to  $OX_1R$  and  $OX_2R$ . The compounds synthesized showed higher binding affinities for  $OX_1R$  than  $OX_2R$  *in vitro*. Compounds **3** and **4** displayed superior binding affinities for  $OX_1R$  (at 30 and 31 nM, respectively) than  $OX_2R$  (160 and 332 nM, respectively). The selectivity for  $OX_1R$  (**3**) and  $OX_2R$  (**4**) were 5.3 and 10.6, indicating that THIQ derivatives selectively bind to  $OX_1R$ . A biodistribution study in normal mice was evaluated to determine the brain uptake of compounds **3** and **4**. The results showed that brain uptake of **3** was higher compared to **4**, and the radioactivity of compound **3** remained in the brain for 60 min. Thus, the brain-to-blood ratios of THIQ derivatives increased with time, but the maximum uptake (**3**: 0.99% ID  $g^{-1}$ , and **4**: 0.57% ID  $g^{-1}$ ) and blood-to-brain ratio (**3**: 0.44, and **4**: 0.34) were not satisfactory for *in vivo* brain imaging. Although the compounds synthesized are potentially imaging probes for PET targeting the  $OX_1R$ , optimization or structural changes are needed to improve their brain uptake (Figure 3).

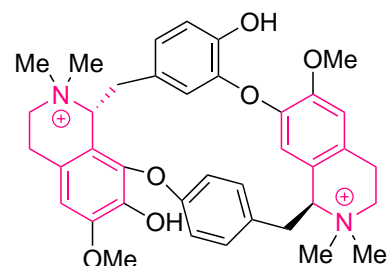
The importance of substitution in positions 6 and 7 of the THIQ moiety and the effect of removing one of the methoxy groups as a selective antagonist of  $OX_1R$  has been reported [19]. The activity of the targeted compounds **5–7** at



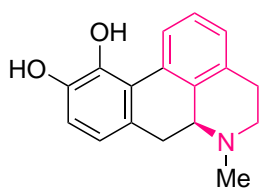
**Quinapril**  
angiotensin-converting enzyme  
(ACE) inhibitor



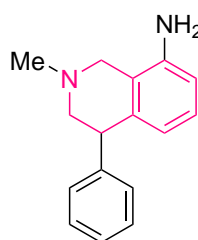
**Noscapine**  
antitumor



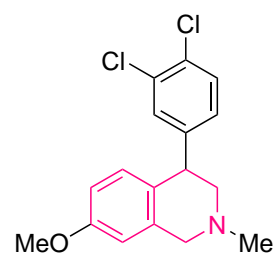
**Tubocurarine**  
neuromuscular blocking agent



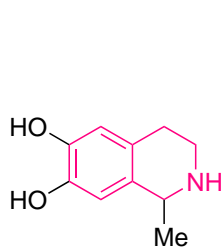
**Apomorphine**  
non-selective dopamine agonist



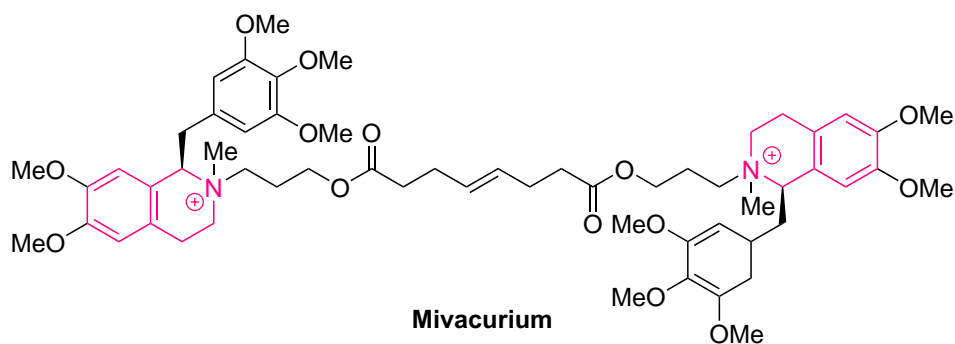
**Nomifensine**  
norepinephrine-dopamine  
reuptake inhibitor



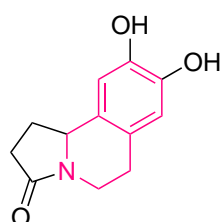
**Diclofensine**  
triple monoamine  
reuptake inhibitor



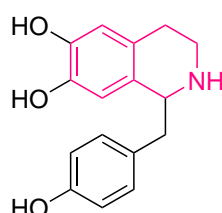
**Salsolinol**



**Mivacurium**  
neuromuscular-blocking drug or skeletal muscle relaxant



**Oleracin E**  
antioxidant and  
antidepressant agent



**Higenamine**  
agonist for beta-2-adrenergic receptor,  
antimycobacterial, and anti-inflammatory drug

**Figure 1.** Some naturally occurring and clinically available THIQ-based compounds

the  $OX_1$  and  $OX_2$  receptors was evaluated using calcium mobilization-based functional curve shift assays. The *n*-propyl derivative **5a** was the most potent compound of the series, with a  $K_e$  value of 23.7 nM, and was 108-fold greater selective for  $OX_1$  over  $OX_2$ . The ethyl and isopropyl substituents showed slight potency compared to **5a**, ( $K_e = 37.3$  nM and 49.7 nM, respectively), but had a superior  $OX_1$  selectivity (268- and 201-fold, respectively). The position 7 is essential for the

$OX_1$  antagonism. Meanwhile, several 6-amino compounds (**7**) containing ester groups showed a moderate potency (**7a**,  $K_e = 427$  nM) (Figure 4).

Perrey *et al.* reported THIQ based compounds **8** and **9** with an excellent  $OX_1$  potency and selectivity [20] (Figure 5). Most of the compounds synthesized demonstrated suitable activities. The introduction of a nitrogen atom into the structure did not significantly change the potency, but reduced the lipophilicity of these

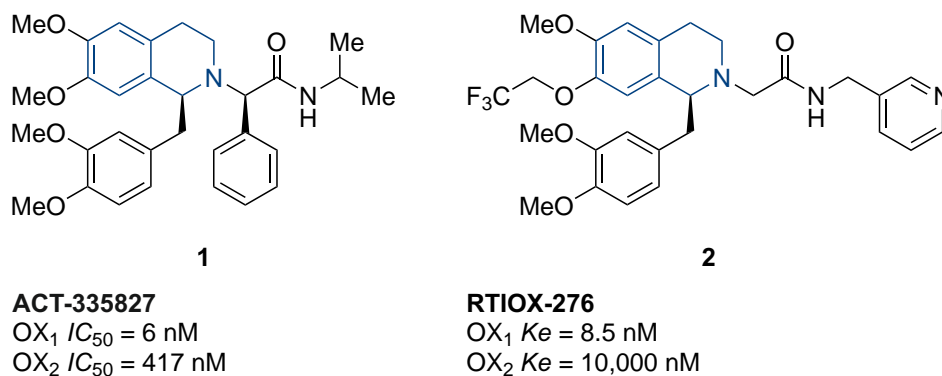


Figure 2. Chemical structures of THIQ derivatives, ACT-335827 and RTIOX-276

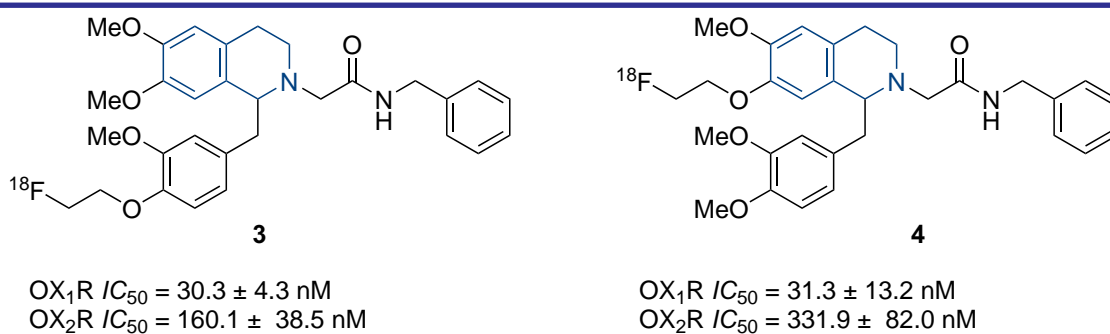


Figure 3. Chemical structures of THIQ derivatives acting as  $OX_{1R}$  antagonists

compounds. The 3-dimethylamino analog was the most potent in the first series, with a  $Ke$  value of 21 nM. When a pyridinylmethyl group was introduced in position 4, the potency was moderate ( $Ke = 96.4 \text{ nM}$ ), and the selectivity of > 100-fold. The substitution at the 1-benzyl position results in compounds with a good selectivity for the  $OX_1$  receptor over the  $OX_2$  receptor. Meanwhile, the replacement of benzylacetamide with the 3-pyridyl group displayed  $OX_1$  antagonists (compound **9a**,  $Ke = 5.7 \text{ nM}$ ). The calculated clogP and PSA value of compound **9a** were 3.07 and 70, respectively, suggesting the solubility of compounds. Further study showed that **9a** displayed a good kinetic solubility (> 200  $\mu\text{M}$ ) and BBB permeability. Besides, compound **9a** possessed the low Pgp activity with an efflux ratio of 3.3.

### PDE4 inhibitors

Phosphodiesterase is an enzyme with unique functions, hydrolyzing the cyclic nucleotides, such as cyclic adenosine-3,5-monophosphate (cAMP) and cyclic guanosine-3,5-monophosphate (cGMP), to their inactive 5'-nucleotide monophosphate, 5'-AMP and 5'-GMP, respectively [21, 22]. Phosphodiesterase 4 (PDE4) is a cAMP specific hydrolase and is identified as one of the 11 members of the PDE super-family. In addition, it predominates in many cells, such as keratinocytes, endothelial cells, hematopoietic cells, and nerve cells. PDE4 is encoded by four genes PDE4A, PDE4B,

PDE4C, and PDE4D, with separate, distinct cellular distributions and functions. PDE4 plays a central role by regulating pro-inflammatory and anti-inflammatory cytokines and cell proliferation via the degradation of cAMP [23]. This has made PDE4 a leading target for the treatment of inflammatory diseases, such as psoriasis, arthritis, and atopic dermatitis. Three PDE4 inhibitors have been clinically evaluated and approved for treating inflammatory disease: roflumilast, apremilast, and crisaborole. To discover potent and effective PDE4B inhibitors, a 3-substituted carboxylic ester was incorporated into the THIQ scaffold **10–13** (Figure 6). All the targeted compounds were evaluated for their inhibitory activity *in vitro* against PDE4B, using rolipram as a positive control [24]. The  $IC_{50}$  values of the compounds being assessed displayed moderate to good inhibition against PDE4B between  $IC_{50}$  values of 0.95–23.25  $\mu\text{M}$ . Compound **13a** showed the most potent inhibitory activity against PDE4B with an  $IC_{50}$  of 0.88  $\mu\text{M}$ , which was 21-fold superior and with more potent selectivity toward PDE4B than PDE4D compared to rolipram. The structure-activity relationship study showed that the presence of either the electron-donating groups, such as the hydroxyl or methoxy group, or the electron-withdrawing group  $OCF_3$  to the phenyl ring in the *para*-position improved the inhibitory activity against PDE4B.



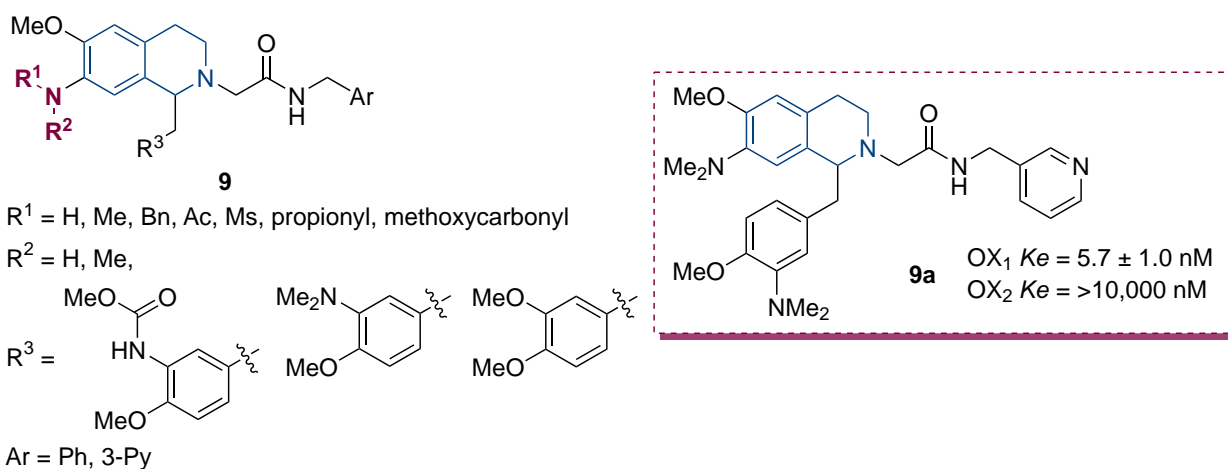
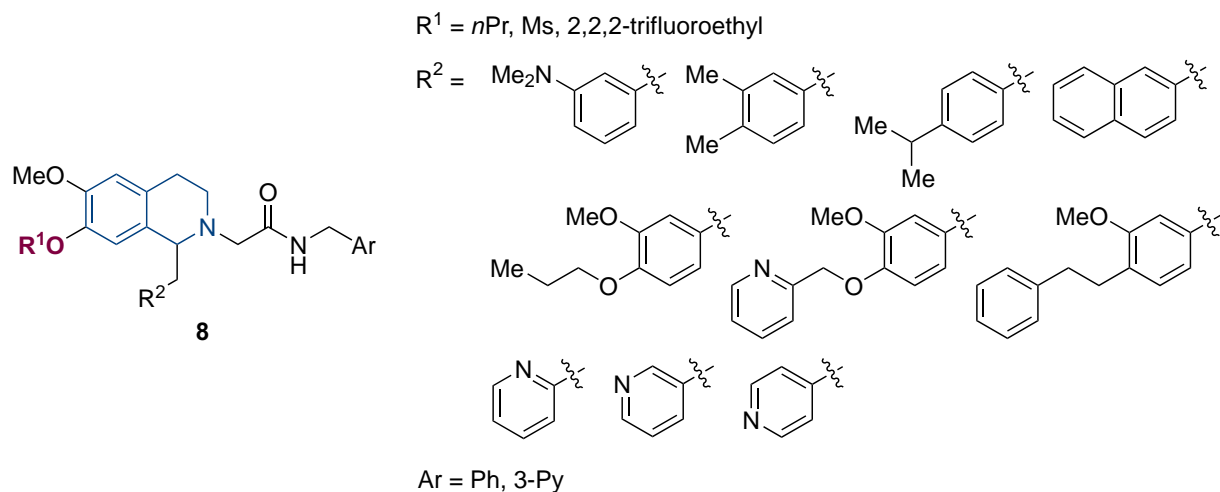


Figure 5. The chemical structure of a THIQ based compound that displayed promising orexin receptor antagonists

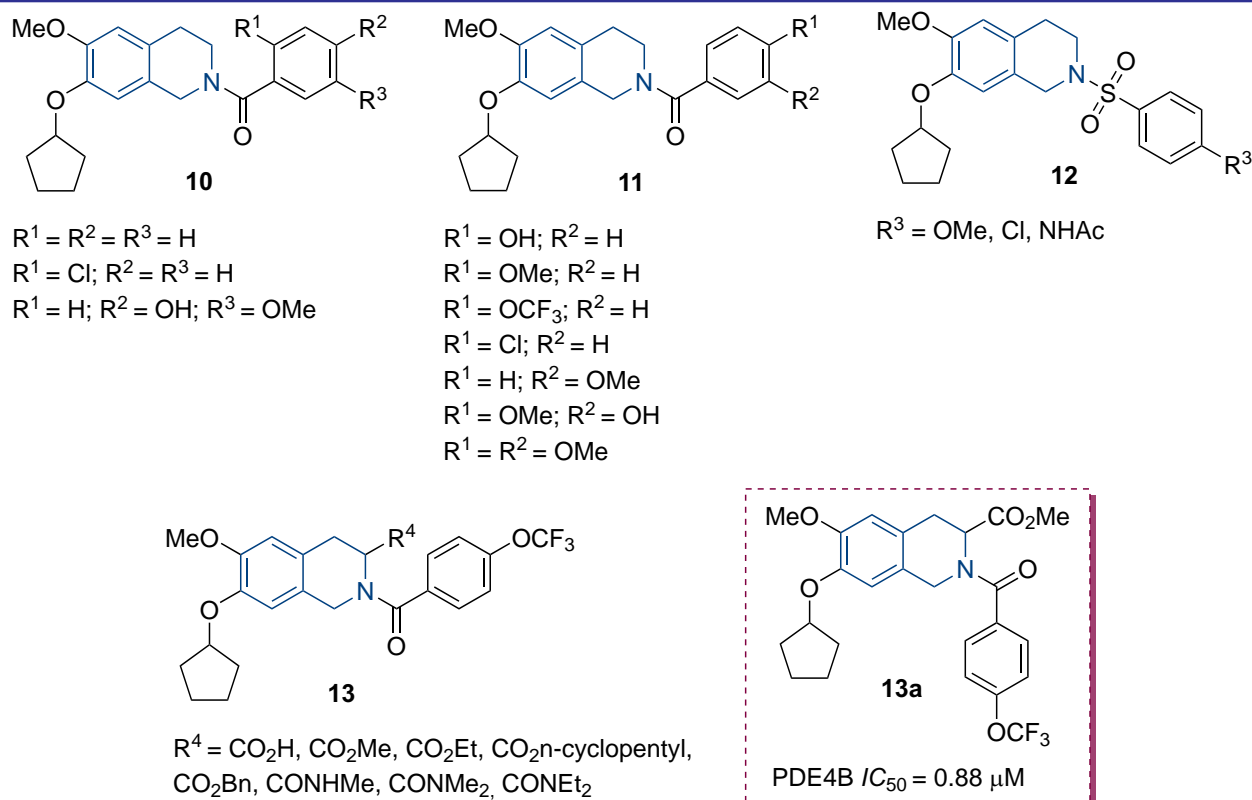


Figure 6. Chemical structures of compounds showing a promising inhibitory activity *in vitro* against PDE4B

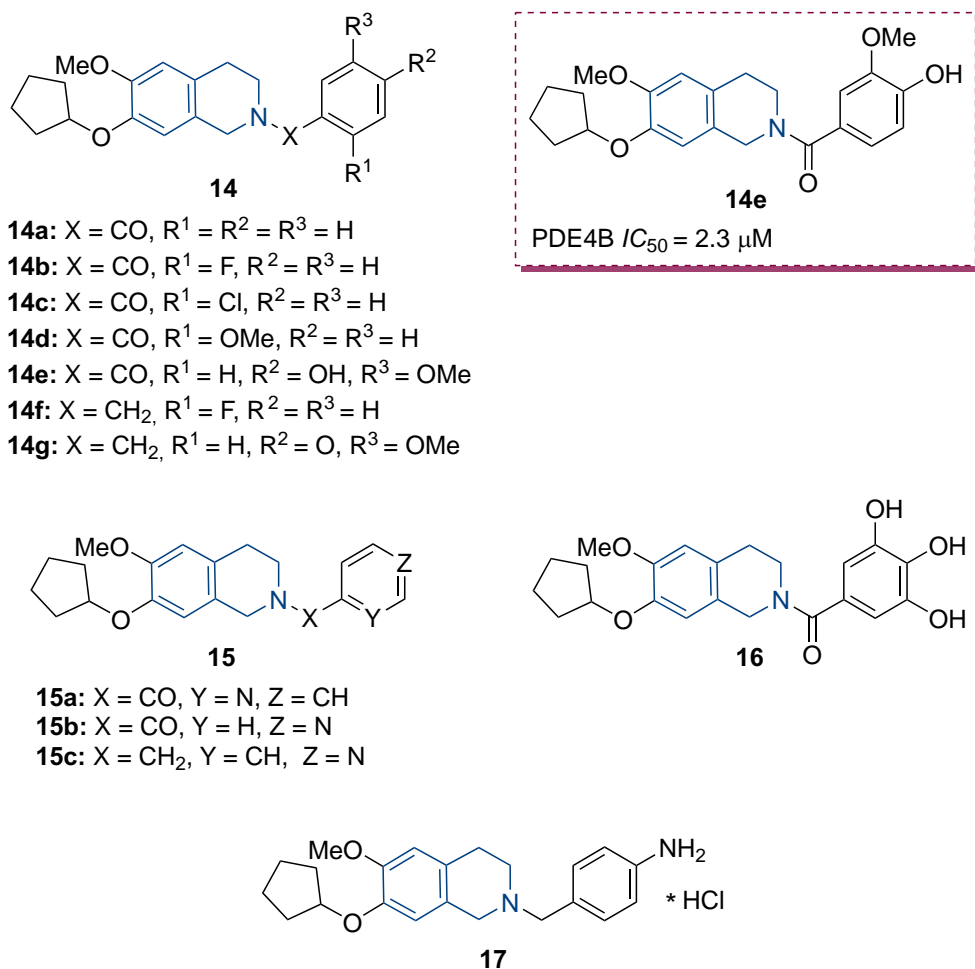


Figure 7. The chemical structure of compounds showing a promising inhibitory activity *in vitro* against PDE4B

### SGLT2 inhibitors

Sodium-dependent glucose cotransporters (or sodium-glucose-linked transporter, SGLT) are a glucose transporter family. SGLT2 is responsible for more than 90% of the renal glucose reabsorption, whereas SGLT1 is for the remaining 10%. This indicated that renal glucose reabsorption is referred mainly by SGLT2 and to a reduced amount by SGLT1. Hence, selective SGLT2 inhibitors would be suitable for antidiabetic agents, and many SGLT2 inhibitors as antidiabetic agents have been approved [26, 27]. *Pan and coworkers* synthesized and evaluated a series of novel THIQ-based C-aryl glucosides to inhibit human SGLT2 [28] (Figure 8). The SGLT2 inhibitors were studied by substituting the proximal phenyl ring of dapagliflozin (**18**) with the conformation restricted THIQ ring (compounds **19** and **20**). All the compounds synthesized were evaluated in a cell-based SGLT2 functional assay in a concentration of 10 mM, and dapagliflozin was used as the reference compound. Compound **19a** containing a naphthalene ring exhibited great potency in the SGLT2 inhibitory activity (81.7%) compared to dapagliflozin (85.4%). The SAR studies

showed that the introduction of thiophene resulted in the unfavored inhibitory activity against SGLT2, indicating that an electron-rich ring was not tolerant in this position. The introduction of the weakly electron-donating C<sub>2</sub>H<sub>5</sub> group increased the inhibitory activity compared to the strong electron-donating (C<sub>2</sub>H<sub>5</sub>O group). The replacement of C<sub>2</sub>H<sub>5</sub> with phenyl significantly increased the inhibitory activity. Since dapagliflozin and compound **19a** exhibited a comparable inhibitory activity *in vitro* against SGLT2, this might be a promising hit for treating type 2 diabetes.

### P-glycoprotein inhibitors

P-glycoprotein (P-GP) can reduce absorption; it also has poor oral bioavailability, and can decrease the retention time of several drugs in coordination with the intestinal wall metabolism [29, 30]. It is noteworthy that P-GP is one of the leading barriers to cancer treatment with chemotherapy. A series of new P-GP inhibitors **21** (Figure 9) were designed and synthesized. The compounds were combined with doxorubicin in MCF-7/ADR cells to evaluate their reversal activity against multidrug resistance (MDR) [31].

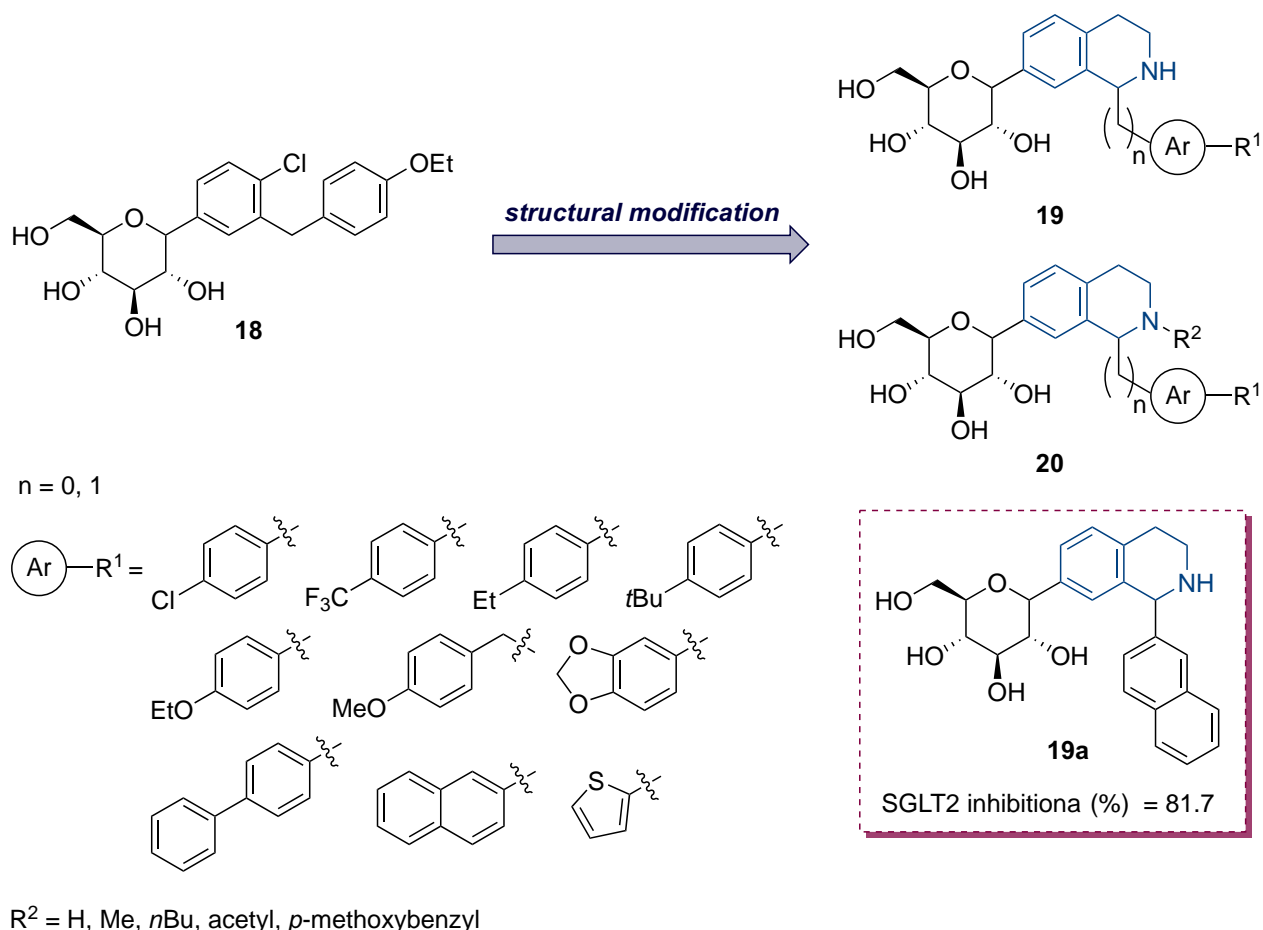


**Figure 8.** Compound **19a** containing a naphthalene ring exhibited great potency in the SGLT2 inhibitory activity

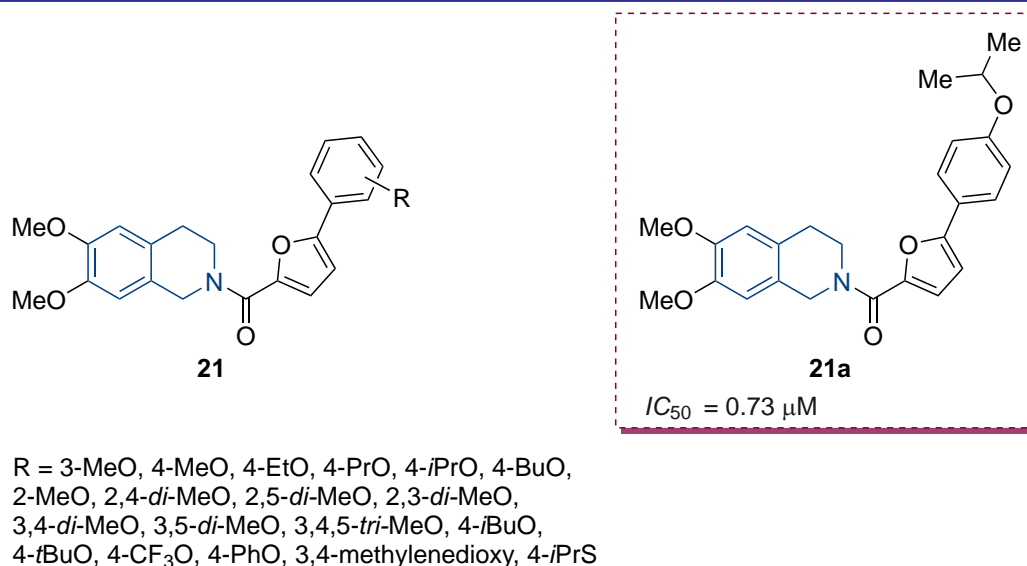
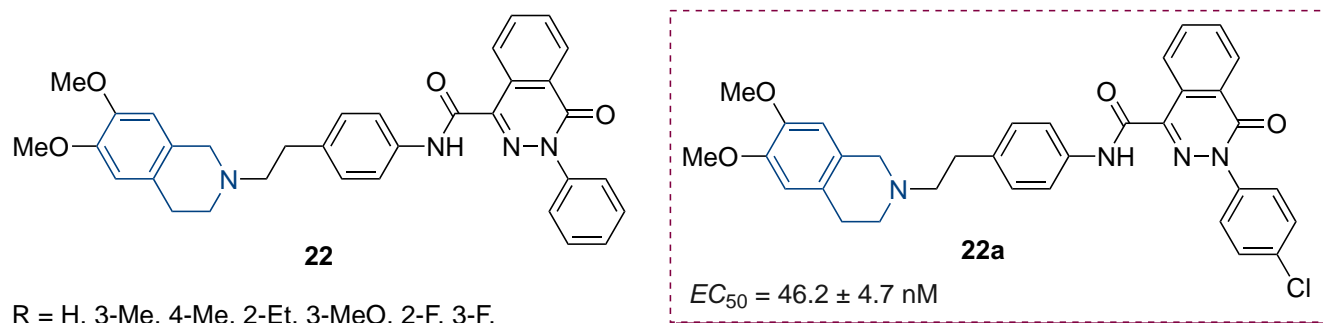


**Figure 9.** Compound **21a** containing isopropoxy displayed higher potency against P-GP

Compound **21a** containing the isopropoxy group displayed higher potency against P-GP mediated MDR in MCF-7/ADR ( $IC_{50}$  (doxorubicin) = 0.73  $\mu\text{M}$ , RF = 69.6 with 5  $\mu\text{M}$  **21a** treated). Further studies showed that **21a** efficiently inhibited the P-GP efflux function but not its expression. The reversal activity of compound **21a** at 5  $\mu\text{M}$  against

doxorubicin in MCF-7/ADR exceeded that of all compounds tested, including the positive controls – cyclosporin A ( $IC_{50}$  (DOX) = 0.86  $\mu\text{M}$ , RF = 59.1) and verapamil ( $IC_{50}$  (DOX) = 4.25  $\mu\text{M}$ , RF = 11.9). The SAR studies showed that the moderate activity was observed in the compound containing more than one methoxy group in the



R = H, 3-Me, 4-Me, 2-Et, 3-MeO, 2-F, 3-F, 2-Br, 3-Br, 4-Cl, 4-NO<sub>2</sub>, 4-CN, 3,4-*di*-Me, 2,5-*di*-F, 3,4-*di*-Cl, 3,5-CF<sub>3</sub>, 2-Py

**Figure 10.** Compound **22a** displayed a high promising inhibitory activity against doxorubicin resistant K562/A02 cells

benzene ring. Meanwhile, the length of the saturated aliphatic chain and the appropriate steric substituents, such as the isopropyl group, are essential to achieve the best activity. The molecular docking analysis demonstrated that compound **21a** formed a crucial hydrogen bonding interaction between the oxygen atom of the furan ring and the NH of Gln721. Besides, there was a lack of amino acid residues around the isopropoxy group that could generate intermolecular actions.

A series of novel P-GP-mediated MDR modulators containing phthalazinone and THIQ scaffolds were designed and synthesized by Qiu *et al.* [32]. Most of the targeted compounds **22** are superior to the standard (verapamil) (Figure 10). Among the targeted compounds, **22a** displayed a high promising inhibitory activity against doxorubicin-resistant K562/A02 cells with a low  $EC_{50}$  ( $46.2 \pm 4.7 \text{ nM}$ ) and the lack of cytotoxicity towards normal cells ( $IC_{50} > 100 \mu\text{M}$ ). The number and position of substituents on the ring significantly influence the reversal activity. Substitution in position 3 of the phenyl ring led to a steady or reduced activity, while substitution in position 4 gave a strong activity. In addition, an increase in the number of substituents reduces the activity. The molecular docking studies described in detail the interaction between the residues and compound **22a** in the hydrophobic pocket of the P-GP. Compound **22a** formed the H-bond interaction with the residue Gln 721 and the  $\pi$ - $\pi$  stacking interaction with Tyr 303. The tertiary amine N atom of compound **22a** captures a hydrogen ion, developing a positive charge center to interact with the residue Phe728; this interaction helps to maintain the activity.

A new MDR reversal agent was designed and synthesized by selecting tariquidar as the lead compound and triazole as the bioisoster to replace benzene. The amido bond was modified

by the secondary amine [33]. Thus, the click chemistry method linked the various chemical structures to the aromatic amides yielding compounds **23** and **24** (Figure 11). Among the compounds tested, compound **23a** containing the 3,4-dimethoxy group in the benzene ring demonstrated a potent effect compared to the positive control and the lack of cytotoxicity towards K562 and K562/ A02 cells. The MDR reversal effect of compound **23a** ( $IC_{50}/\text{DOX} (\mu\text{M}) = 1.30 \pm 0.35$ , RF = 18.7) could last over a certain period, longer than that of VRP. Further research suggested that compound **23a** displayed a significant potency in an increased doxorubicin accumulation in K562/A02 cells and further decreased the P-GP-mediated efflux of Rh123. The compound possessing three substituted dimethoxy groups showed a good potency, while derivatives of compound **24** demonstrated an insignificant activity.

To identify ideal P-GP inhibitors reversing MDR in non-toxic concentrations, THIQ based compounds were designed [34] (Figure 12). The MTT (3-(4,5-dimethylthiazolyl)-2,5-diphenyltetrazolium bromide) assay was used to evaluate the cytotoxicity of the compounds synthesized against the human erythroleukemia K562 cells and the adriamycin (ADM)-resistant K562/A02 cells. The well-known classical P-GP inhibitor (verapamil) was used as the reference compound. Most target compounds displayed a low cytotoxicity and exhibited more active MDR reversal activity than verapamil. Compound **25a** demonstrated the strongest reversal activity with  $IC_{50}$  of  $1.76 \pm 0.3 \mu\text{M}$ . Further studies suggested that the most active compound effectively impeded the ADM efflux function of P-GP and augmented the accumulation of ADM in K562/A02 cells. Thus, **25a** is a promising candidate for developing P-GP-mediated MDR reversal modulator in cancer chemotherapy.

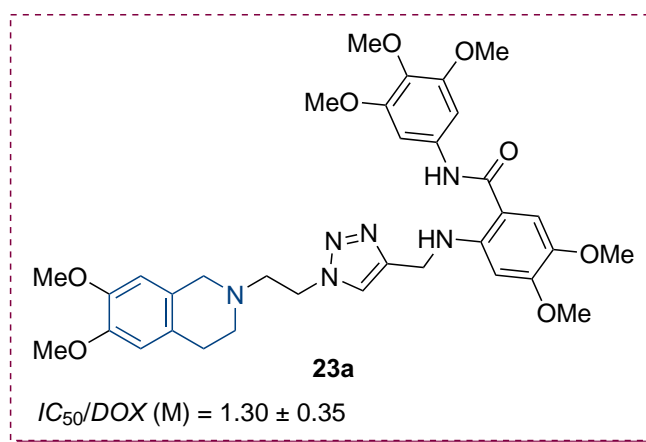
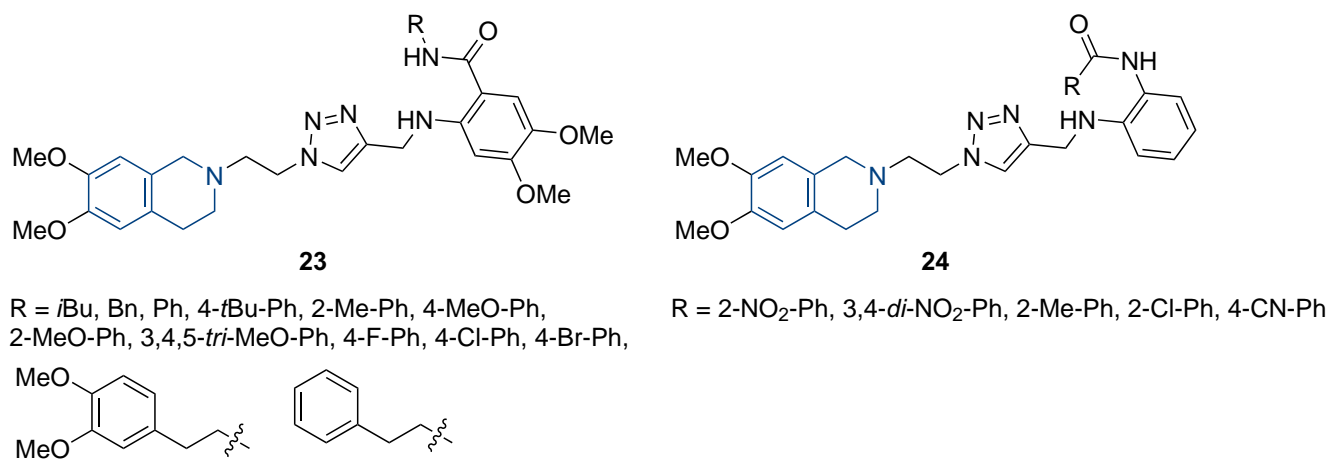


**Figure 11.** The chemical structure of compound **23a** that displayed a significant potency in an increased accumulation of doxorubicin in K562/A02 cells

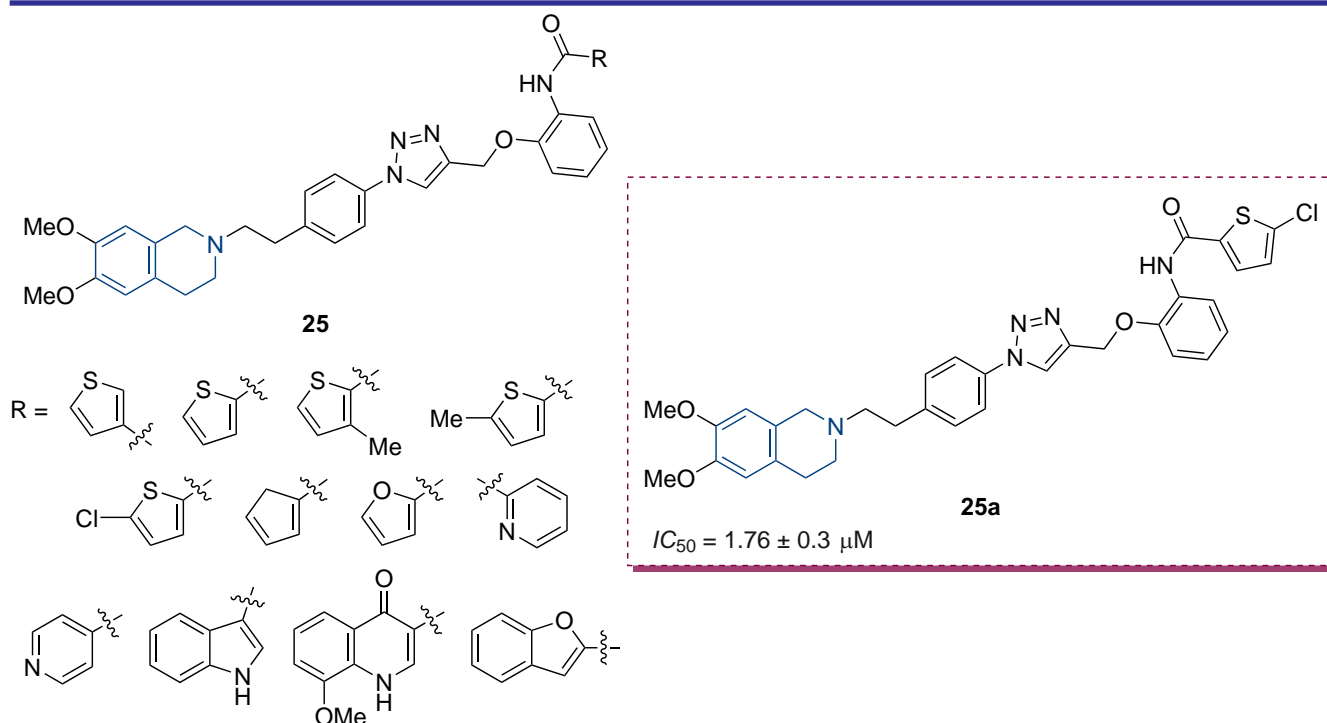


**Figure 12.** The chemical structure of compound **25a** that demonstrated the strongest reversal activity

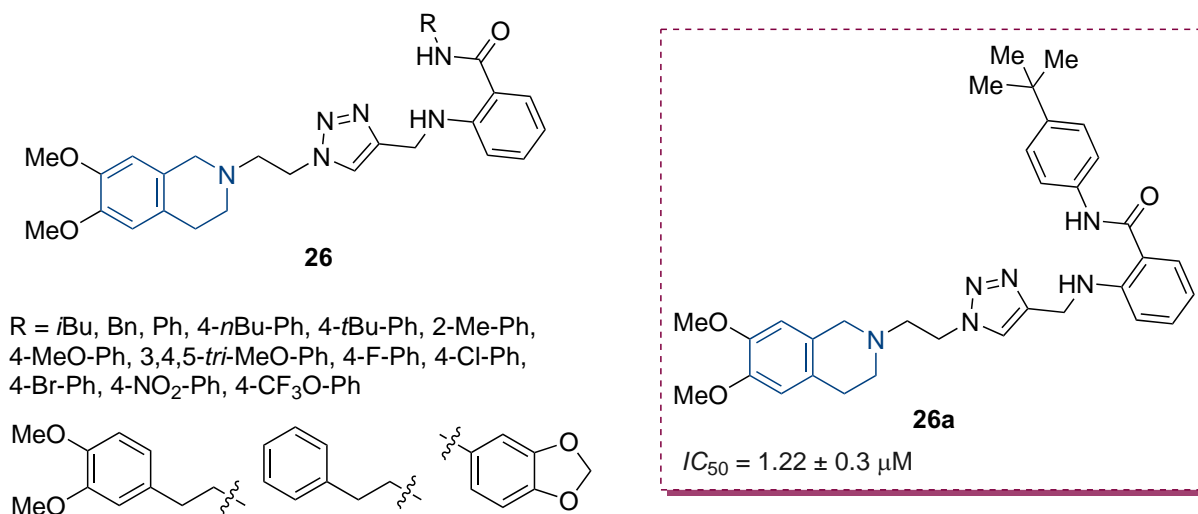


**Figure 13.** The chemical structure of a potent compound against P-GP

A total of 17 novel THIQ P-GP inhibitors were designed and synthesized by structure simplification and bioisosterism [35]. The results of *in vitro* cytotoxicity and reversed MDR activity showed that all the targeted compounds demonstrated no significant cytotoxicity with  $IC_{50} > 30 \mu\text{M}$  on both K562 and K562/A02 cells (P-GP overexpressed). Compound **26a** had the reversal activity, which was superior to the control (verapamil), significantly increased ADM accumulation in K562/A02 cells, and obstruct the efflux of Rh123 concurrently (Figure 13). The SAR studies showed that the compound with 4-*tert*-butylphenyl substituent displayed the highest activity ( $IC_{50} = 1.22 \pm 0.3 \mu\text{M}$ ), while the compound with 3,4-dimethoxyphenethyl substituent was somewhat inactive with  $IC_{50}$  of  $41.48 \pm 1.7 \mu\text{M}$ . In addition, the compounds containing substituents in position 4 of the benzene ring had a significant activity compared to those containing substituents in positions 3, 4. Compound **26a** interacted with the P-GP receptor *via* the  $\pi$ - $\pi$  interaction of the aromatic ring and the hydrophobic interaction. The superimposition with tariquidar indicated that the target compound **26a** might have a similar binding site with the tariquidar in the active pocket of the P-GP receptor.

A library of P-GP inhibitors **28** was designed using alkyl as a linker between the phenolic group of the biphenyl moiety of compound **27** and various furazan derivatives containing substituents with different stereoelectronic and lipophilic properties [36] (Figure 14). Among the compounds tested, **28a–d** displayed the highest activity with  $EC_{50}$ , of 0.97 nM, 1.3 nM, 0.60 nM, and 0.90 nM, respectively, making them potential candidates for reverting MDR by co-administration of chemotherapeutic drugs and P-GP modulating agents.

All the target compounds were inactive against MRP1 and BCRP transported. In addition, the high-affinity substrate profile of the active compounds (**28a–d**) is attractive because of their possible employment *in vivo* imaging of the function of P-GP through non-invasive imaging techniques, such as PET and SPECT.

A series of THIQ derivatives **29–31** containing the 5-phenyl-2-furan moiety were synthesized, and their P-GP potency and selectivity were evaluated [37] (Figure 15). Cyclosporin A and verapamil were adopted as the positive controls. Compound **31a** containing 6,7-dimethoxy and methoxyl groups in the *para*-position of the benzene ring showed the best bioactivity against P-GP ( $EC_{50} = 0.89 \mu\text{M}$ ) among all the title compounds, which displayed better activity than both cyclosporin A and verapamil with an  $EC_{50}$  value of  $83.68 \mu\text{M}$  and  $20.54 \mu\text{M}$  against P-GP, respectively, compared to MC113 [38, 39]. Comparing the inhibitory activity of these three series, compound **29** containing the 6,7-dimethoxy group demonstrated a superior bioactivity than compounds **30** and **31**. Meanwhile, the presence of substituents in the *para*-position of the benzene ring suggested that the position was crucial for bioactivity. Compound **31a** with the highest inhibitory activity increased doxorubicin accumulation 9.2-fold at  $20 \mu\text{M}$  in overexpressing P-GP MCF-7/ADR cells. **31a** was well fitted in the P-GP active site. The hydrogen bond interaction was observed between the O atom of the furan ring and the H at amine of Gln721 (distance: 2.59 Å). The hydrophobic effect was observed with three methoxy groups (-OMe) at the benzene ring and THIQ, which enhanced the binding affinity with the enzyme.

*Wu and coworkers* synthesized and biologically evaluated new series of THIQ as P-GP-mediated

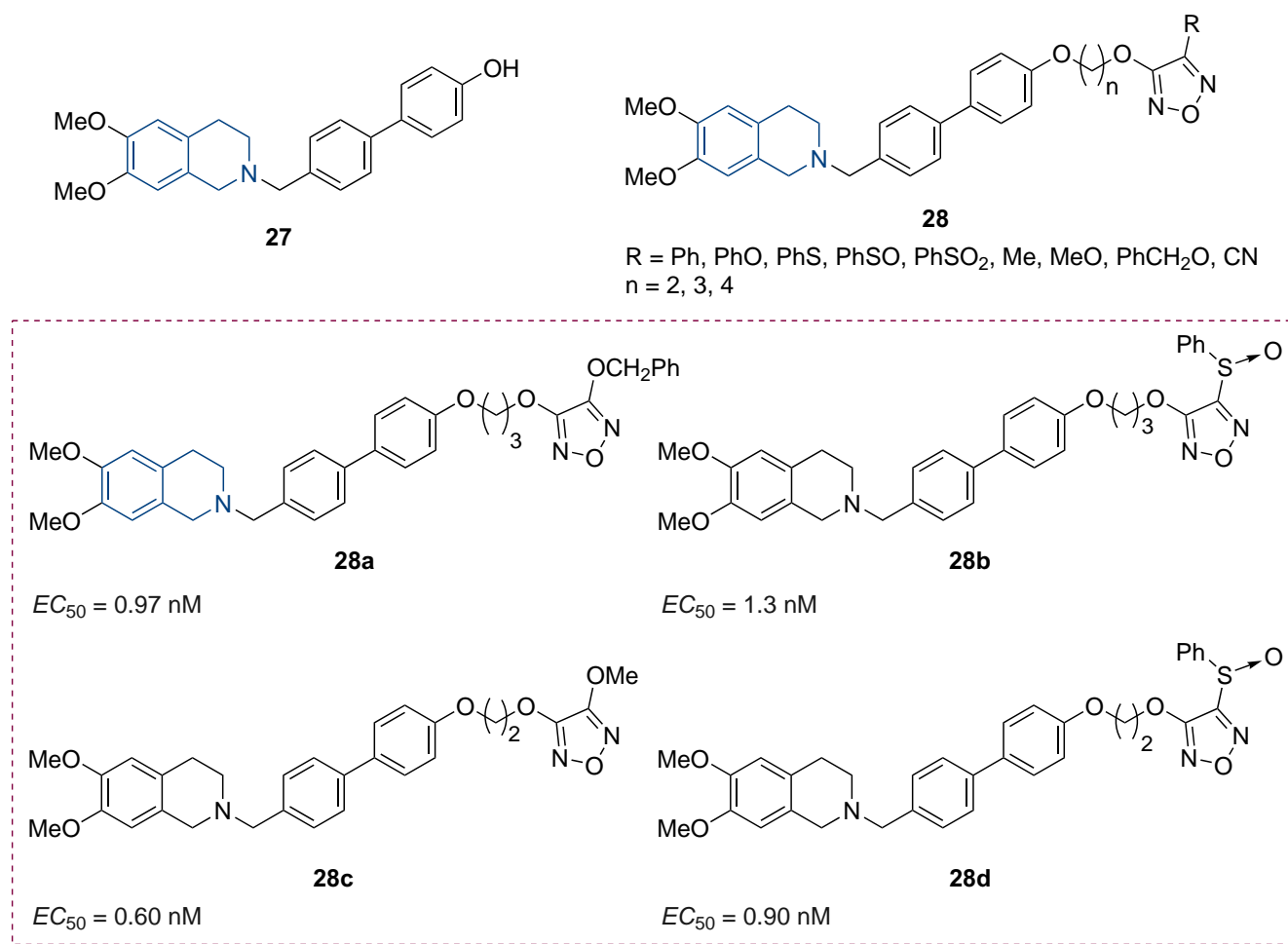


**Figure 14.** Chemical structures of potential candidates for reverting MDR

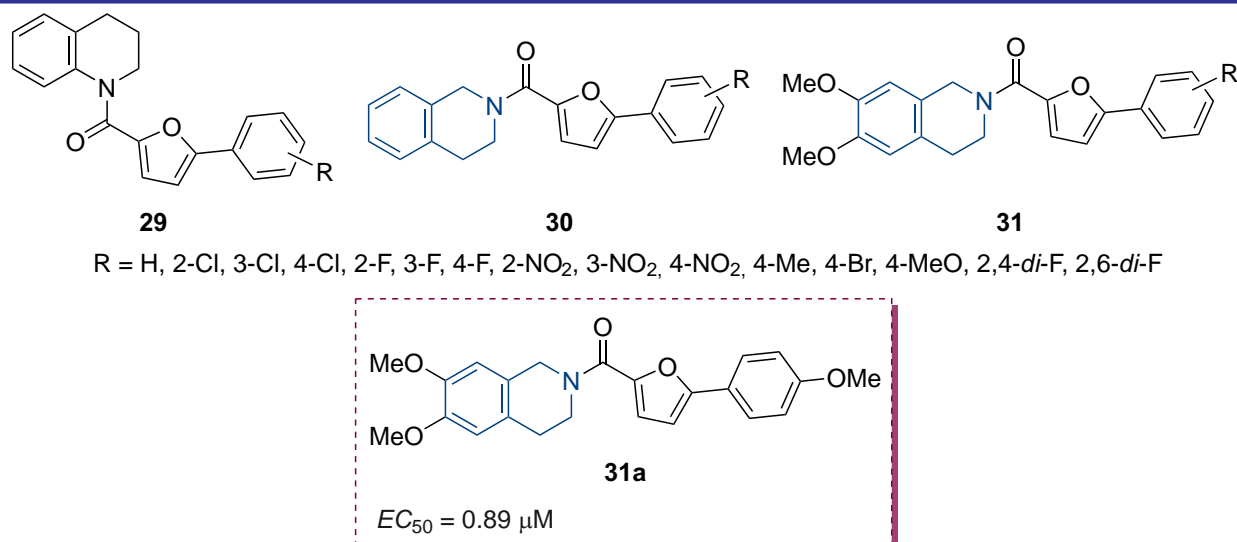


**Figure 15.** The chemical structure of a potent compound against P-GP

MDR inhibitors [40] (Figure 16). The effects of the target compounds on the reversing adriamycin (ADM) resistance toward K-562/A02 cells (P-GP-overexpression) were carried out using the MTT assay. The well-known classical P-GP inhibitor VRP, WK-X-34, and LBM-A5 were used as the positive control. Compounds with triazol-

*N*-phenethyl-tetrahydroisoquinoline **32** were generally more potent than compounds with triazol-*N*-ethyl-tetrahydroisoquinoline **33**. Among them, compound **32a** with a pointedly decreased  $IC_{50}$  of ADM ( $1.21 \pm 0.18$  μM) showed the strongest reversal activity, and its reversal fold (RF) was 31.4 compared to WK-X-34 (RF = 30.4)

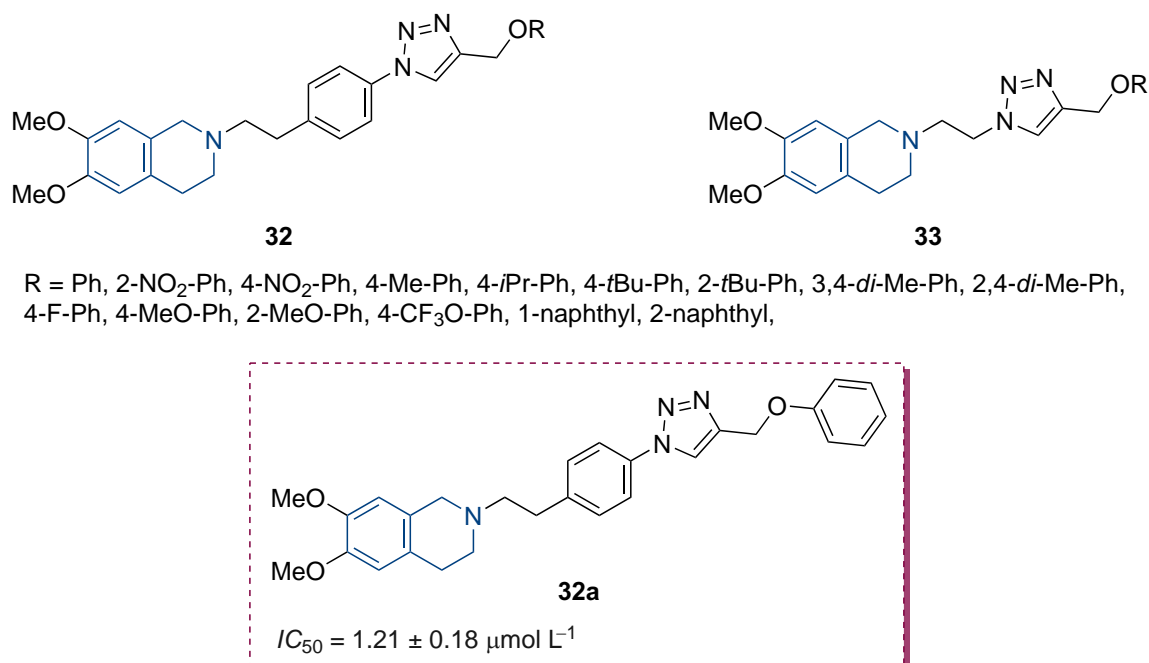


**Figure 16.** The chemical structure of a promising compound that showed the best MDR reversal activity among twenty-five targeted compounds

and slightly higher than LBM-A5 (RF = 23.0). However, most of the targeted compounds exhibited more active MDR reversal activity than VRP when co-administered with ADM under the same condition. Electron-donating groups, such as CH(CH<sub>3</sub>)<sub>2</sub> and C(CH<sub>3</sub>)<sub>3</sub>, showed higher MDR reversal activity than VRP, while OCH<sub>3</sub> showed lower MDR reversal activity than VRP. In addition, electron-withdrawing groups demonstrated a poor MDR reversal activity. The size of the substituent affects the MDR reversal activity. The compound containing 4-*tert*-butyl was more potent and showed more ADM accumulation in K562/A02 cells than the compound substituted by other alkyls. Compound **32a** and the compound with 4-*tert*-butyl substituent showed the best MDR reversal activity among the twenty-five target compounds, with  $IC_{50}$  of  $1.21 \pm 0.18 \mu\text{mol L}^{-1}$  and  $1.86 \pm 0.15 \mu\text{mol L}^{-1}$  compared to the lead compound LBM-A5 ( $IC_{50} = 1.65 \pm 0.22 \mu\text{mol L}^{-1}$ ).

#### Antibacterial

The synthesis of THIQ-triazole derivatives **34** and **35** was strategically designed by using the nitrogen atom of THIQ as an attachment to the terminal alkyne [41] (Figure 17). The alkyne allowed the incorporation of different substituted aromatic rings *via* the formation of the triazole ring using the Cu-catalyzed azide-alkyne cycloaddition. The compounds synthesized were evaluated against Gram-positive bacteria, namely *S. aureus* ATCC25923, *B. subtilis* 168, and *E. coli* MG1655. *S. aureus* ATCC25923 and methicillin. *B. subtilis* 168. Besides, non-pathogenic *E. coli*

MG1655 was used as the model for Gram-negative organisms. All the compounds synthesized were initially screened for the growth inhibition activity against *S. aureus*. Most of the compounds gave a *MIC* value from 4 to 32  $\mu\text{g mL}^{-1}$ , and compounds **34a–c** with *MIC* values of 4  $\mu\text{g mL}^{-1}$  were observed as the promising candidates. Further research showed that all sixteen compounds were not active against Gram-negative *E. coli* in the concentration of 128  $\mu\text{g mL}^{-1}$ . Compound **34a** with an unsubstituted aromatic ring showed no activity, indicating an increase in polarity or even the compound length/size may negatively impact the inhibitory properties. The introduction of the *tert*-butyl group increased the activity against *S. aureus* and *B. subtilis*. The introduction of hydrophobic groups, such as naphthalene and 4-biaryl, maintained the activity. The presence of hydrophilic and electron-withdrawing groups, namely 4-chloro, 4-cyano, 4-nitro, and 4-dimethyl carbamoyl groups, displayed no significant activity when tested against *S. aureus*. The presence of the CF<sub>3</sub> substituent, an electron-withdrawing group with hydrophobic properties, enhanced the action at the *MIC* of 32  $\mu\text{g mL}^{-1}$  and 8  $\mu\text{g mL}^{-1}$ , respectively. The introduction of a nucleophilic N-atom in 3,5-dichloropyridyl drastically reduced the inhibitory activity. It is noteworthy that the presence of electron-donating and electron-withdrawing effects merged with the hydrophobicity of either *tert*-butyl or OBn increased the activity of **34a–c**. In addition, compound **34a**, which effectively



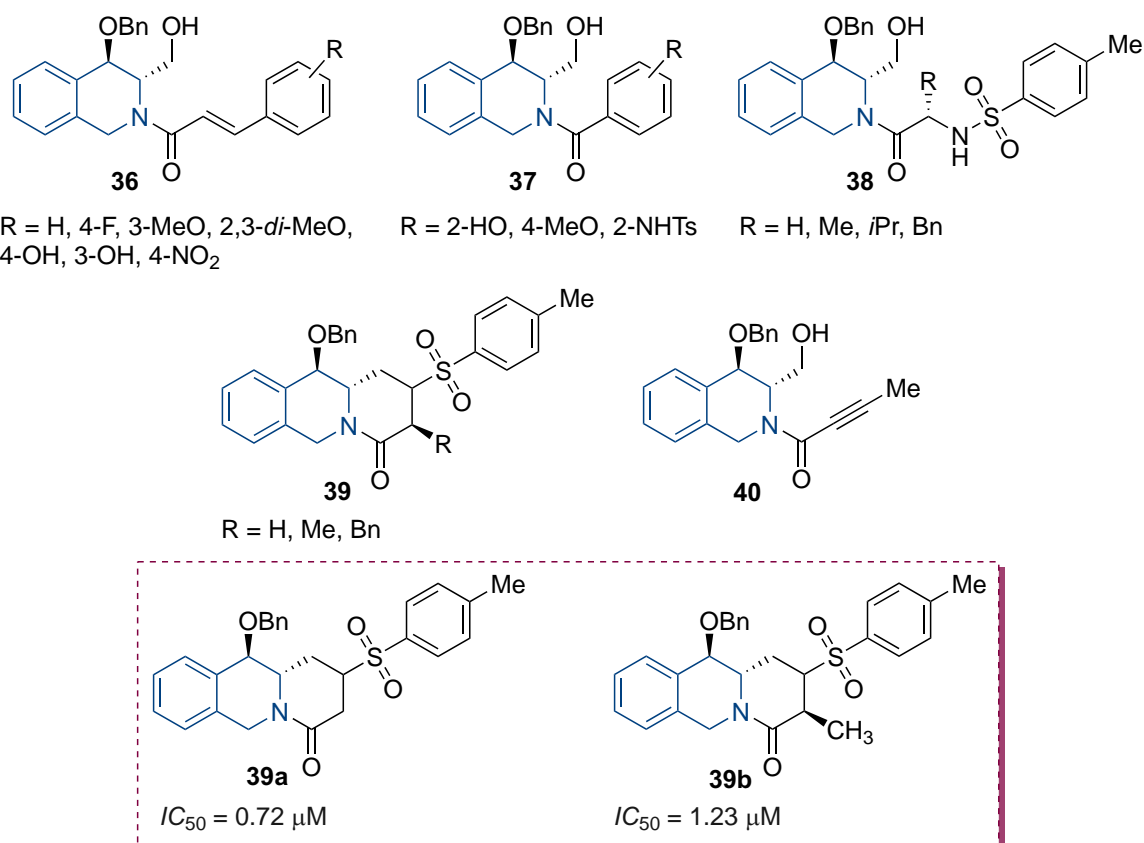


**Figure 18.** Chemical structures of compounds that exhibited a significant activity against the prostate cancer cell line

Colo 320 KRasSL, and SNU-C1 KRasSL) using three different concentrations (0.2  $\mu\text{M}$ , 2  $\mu\text{M}$  and 20  $\mu\text{M}$ ). The results showed that all the compounds studied had a higher overall KRas inhibition. Surprisingly, alcohol **42a** displayed a lower KRas inhibition than other analogs. The amine-containing compound **42c** demonstrated the highest KRas activity profile on RKO KRasSL, revealing that a terminal ionic interaction led to an increased KRas inhibition. The N-aryl-containing compounds (**42d** and **42e**) had the highest KRas inhibition on the colon 320 KRas SL cell line, suggesting that a low electron density aromatic side chain structure resulted in higher KRas activity. Compound **42e** displayed a significant KRas activity in the concentration of 0.2  $\mu\text{M}$  (RKO KRasSL 95.8% inhibition, HCT KRasSL 35.9% inhibition). In addition, amine **42c** and the alcohol **42a** derivatives exhibited a promising antileukemic activity ( $IC_{50} = 2.0$  and 2.6  $\mu\text{M}$ , respectively), and the study of cytotoxic mechanisms suggested the involvement of KRas inhibition in both without additional antiangiogenic effects in the case of compound **42a**. The antiangiogenic evaluation was carried out for **42a–e**. The results showed that **42b** and **42c** possessed an interesting antiangiogenic activity, while **42d** and **42e** exhibited an insignificant

activity, and **42a** was inactive. Compound **42b** containing the nitrile group was the most potent antiangiogenic agent. It displayed the highest antiangiogenic ( $IC_{50} = 2.9 \mu\text{M}$ ) and anti-osteoporotic activity, indicating that the dipolar lipophilic terminal group, such as the nitrile group, enhanced the antiangiogenic and anti-osteoporotic activity.

To identify promising anticancer agents, a new series of THIQ derivatives **45** and **46** were designed and synthesized [44] (Figure 20). The targeted compounds were tested against different human cancer cells. Compounds **45**, incorporating either hydroxyl or trifluoromethyl groups in the R<sup>3</sup> position of the phenyl ring displayed a moderate antiproliferative activity with the  $GI_{50}$  value of 4.365 and 4.224  $\mu\text{M}$ , respectively, whereas the incorporation of the methoxy group in the same position led to the loss of activity. For the THIQ scaffold containing a 4-chlorobenzoyl group, the derivatives with methoxy groups exhibited a significant activity on gastric cancer cells, whereas all three compounds with hydroxyl substituents had an inferior activity. Compound **46a** with an *ortho*-methoxy group led to a 2-fold higher activity ( $GI_{50}$  value = 1.591  $\mu\text{M}$ ) than the compound containing a *para*-methoxy group ( $GI_{50} = 3.627 \mu\text{M}$ ).

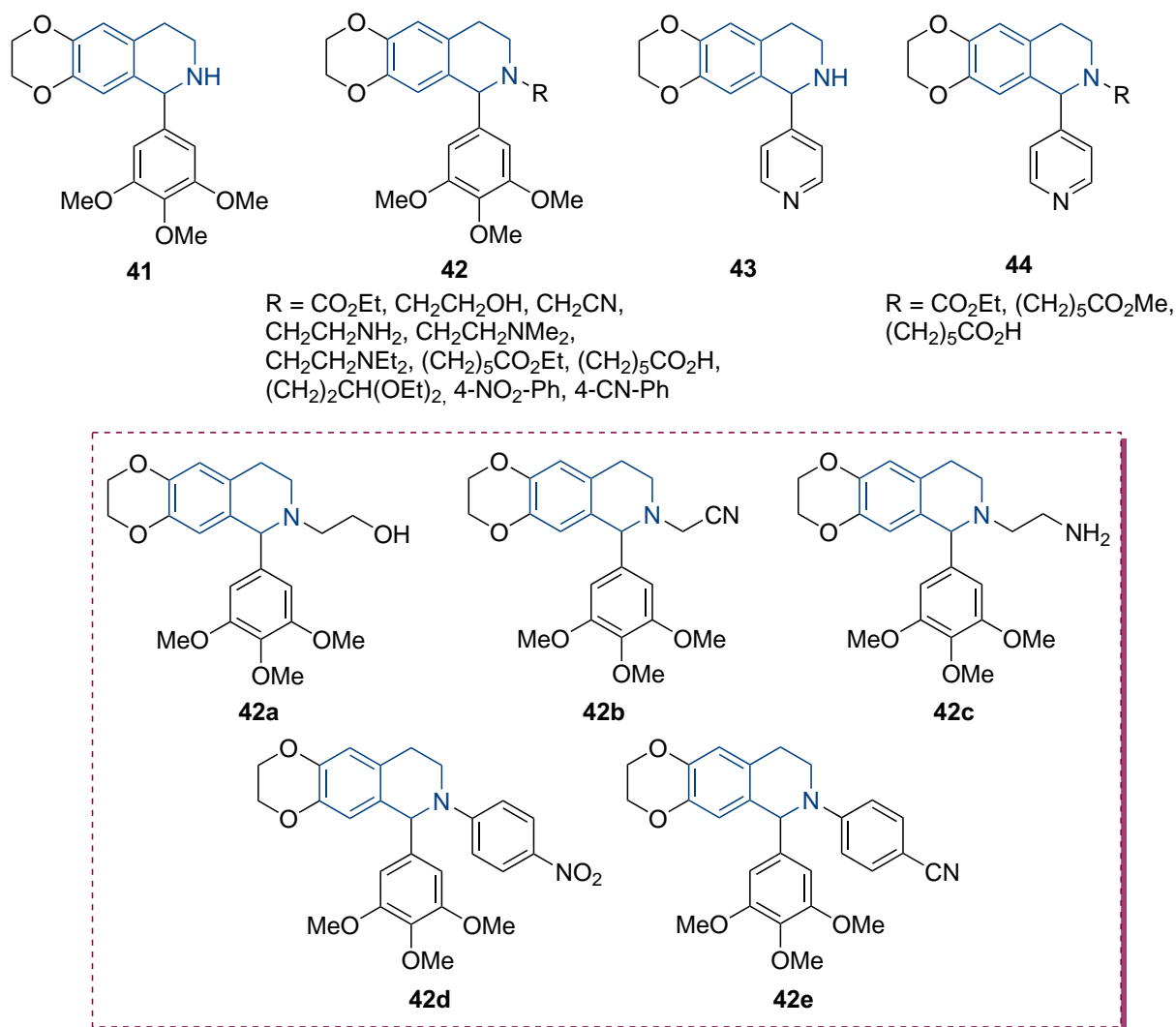


Figure 19. Chemical structures of promising anticancer agents containing the THIQ moiety

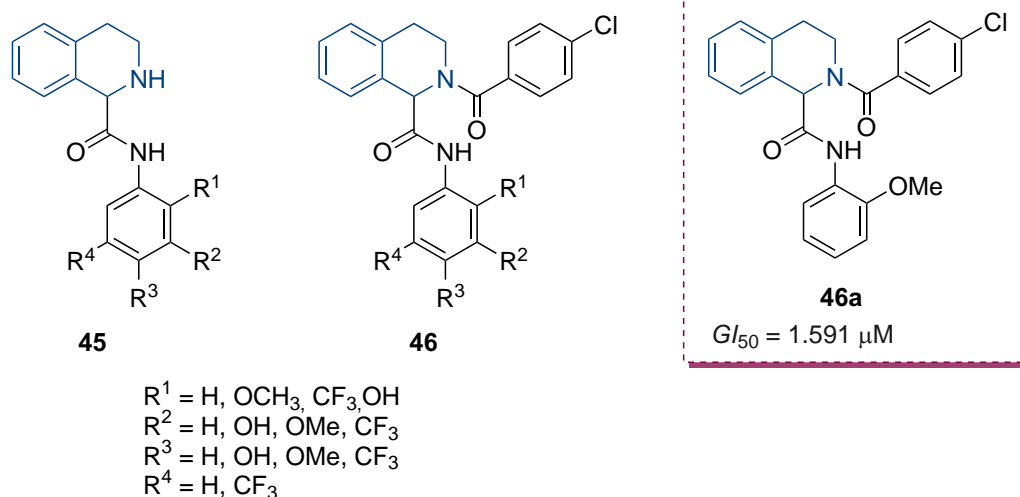
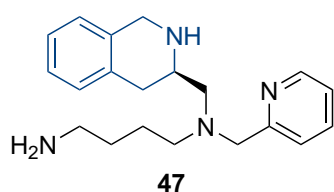


Figure 20. 1-Carbamoyl THIQ derivatives with a promising inhibitory activity against gastric cancer cells

### CXCR4 antagonists

CXCR4 antagonists **47** with an increased liver microsomal stability in human and mouse models compared to the parent molecule TIQ-15

were reported [45] (Figure 21). Compounds **47a,b** containing chloro substituent on the pyridylmethyl moiety are the most promising candidates.



R = H, 2-quin, 1-isoquin, 2-isoquin, 6-Me, 5-Me, 4-Me, 3-Me, 5-Cl, 4-Cl, 3-Cl, 5-F, 3-F, 5-MeO, 3-MeO, 5-MeO, 5-CF<sub>3</sub>, 3-CF<sub>3</sub>, 3-cPr, 3-vinyl, 3,5-*di*-Me, 3-Me-5-F, 5-Me-3-F

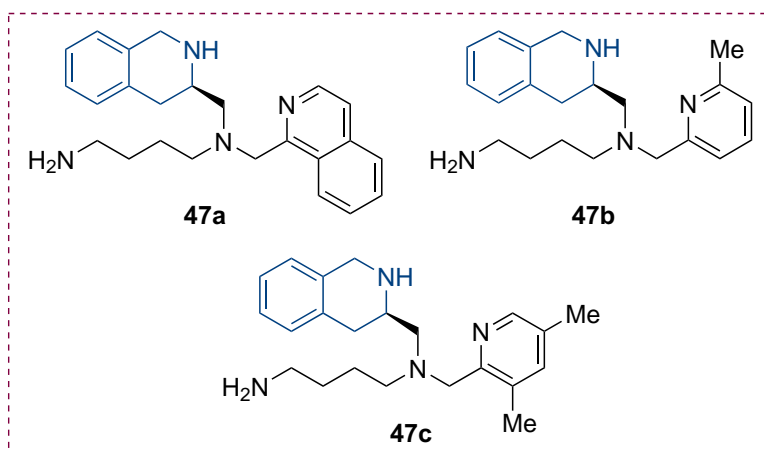


**Figure 21.** Promising CXCR4 antagonists with a THIQ backbone

## Conclusions

This review presents a broad range of biological activities of THIQ, it will give the reader an idea of the therapeutic use of THIQ in various diseases. Due to the promising effect of THIQ in many biological activities, much attention has been paid to its therapeutic role. The SAR studies of the above-mentioned compounds show a

better perception of the choice of an appropriate substitution model comprising electron-donating, electron-withdrawing and some heterocyclic functional groups on the backbone plays a vital role in modulating the biological potential of the compounds synthesized. This review will help pharmaceutical researchers to synthesize novel and potent compounds containing THIQ scaffold.

## References

- Wen, J.; Tan, R.; Liu, S.; Zhao, Q.; Zhang, X. Strong Brønsted acid promoted asymmetric hydrogenation of isoquinolines and quinolines catalyzed by a Rh-thiourea chiral phosphine complex via anion binding. *Chem. Sci.* **2016**, *7* (5), 3047–3051. <https://doi.org/10.1039/c5sc04712a>.
- Bringmann, G.; Brun, R.; Kaiser, M.; Neumann, S. Synthesis and antiprotozoal activities of simplified analogs of naphthylisoquinoline alkaloids. *Eur. J. Med. Chem.* **2008**, *43* (1), 32–42. <https://doi.org/10.1016/j.ejmech.2007.03.003>.
- Fayez, S.; Feineis, D.; Ake Assi, L.; Kaiser, M.; Brun, R.; Awale, S.; Bringmann, G. Ancistrobrevines E-J and related naphthylisoquinoline alkaloids from the West African liana *Ancistrocladus abbreviatus* with inhibitory activities against *Plasmodium falciparum* and PANC-1 human pancreatic cancer cells. *Fitoterapia* **2018**, *131*, 245–259. <https://doi.org/10.1016/j.fitote.2018.11.006>.
- Kumar, A.; Katiyar, S. B.; Gupta, S.; Chauhan, P. M. Syntheses of new substituted triazino tetrahydroisoquinolines and beta-carbolines as novel antileishmanial agents. *Eur. J. Med. Chem.* **2006**, *41* (1), 106–113. <https://doi.org/10.1016/j.ejmech.2005.09.007>.
- Lu, G. L.; Tong, A. S. T.; Conole, D.; Sutherland, H. S.; Choi, P. J.; Franzblau, S. G.; Upton, A. M.; Lotlikar, M. U.; Cooper, C. B.; Denny, W. A.; Palmer, B. D. Synthesis and structure-activity relationships for tetrahydroisoquinoline-based inhibitors of *Mycobacterium tuberculosis*. *Bioorg. Med. Chem.* **2020**, *28* (22), 115784. <https://doi.org/10.1016/j.bmc.2020.115784>.
- Gabet, B.; Kuo, P. C.; Fuentes, S.; Patel, Y.; Adow, A.; Alsakka, M.; Avila, P.; Beam, T.; Yen, J. H.; Brown, D. A. Identification of N-benzyltetrahydroisoquinolines as novel anti-neuroinflammatory agents. *Bioorg. Med. Chem.* **2018**, *26* (21), 5711–5717. <https://doi.org/10.1016/j.bmc.2018.10.020>.
- George, A.; Gopi Krishna Reddy, A.; Satyanarayana, G.; Raghavendra, N. K. 1,2,3,4-Tetrahydroisoquinolines as inhibitors of HIV-1 integrase and human LEDGF/p75 interaction. *Chem. Biol. Drug. Des.* **2018**, *91* (6), 1133–1140. <https://doi.org/10.1111/cbdd.13175>.
- Chander, S.; Ashok, P.; Singh, A.; Murugesan, S. De-novo design, synthesis and evaluation of novel 6,7-dimethoxy-1,2,3,4-tetrahydroisoquinoline derivatives as HIV-1 reverse transcriptase inhibitors. *Chem. Cent. J.* **2015**, *9*, 33. <https://doi.org/10.1186/s13065-015-0111-6>.
- Gitto, R.; Francica, E.; De Sarro, G.; Scicchitano, F.; Chimirri, A. Solution-phase parallel synthesis of novel 1,2,3,4-tetrahydroisoquinoline-1-ones as anticonvulsant agents. *Chem. Pharm. Bull. (Tokyo)* **2008**, *56* (2), 181–184. <https://doi.org/10.1248/cpb.56.181>.
- Singh, K.; Pal, R.; Khan, S. A.; Kumar, B.; Akhtar, M. J. Insights into the structure activity relationship of nitrogen-containing heterocyclics for the development of antidepressant compounds: An updated review. *Journal of Molecular Structure* **2021**, *1237*, 130369. <https://doi.org/10.1016/j.molstruc.2021.130369>.
- Kang, S. H.; Bak, D. H.; Yeoup Chung, B.; Bai, H. W. Transformation of nomifensine using ionizing radiation and exploration of its anti-cancer effects in MCF-7 cells. *Exp. Ther. Med.* **2022**, *23* (4), 306. <https://doi.org/10.3892/etm.2022.11235>.
- Luethi, D.; Hoener, M. C.; Liechti, M. E. Effects of the new psychoactive substances diclofenine, diphenidine, and methoxphenidine on monoaminergic systems. *Eur. J. Pharmacol.* **2018**, *819*, 242–247. <https://doi.org/10.1016/j.ejphar.2017.12.012>.
- Inutsuka, A.; Yamanaka, A. The physiological role of orexin/hypocretin neurons in the regulation of sleep/wakefulness and neuroendocrine functions. *Front. Endocrinol. (Lausanne)* **2013**, *4*, 18. <https://doi.org/10.3389/fendo.2013.00018>.
- Tsujino, N.; Sakurai, T. Role of orexin in modulating arousal, feeding, and motivation. *Front. Behav. Neurosci.* **2013**, *7*, 28. <https://doi.org/10.3389/fnbeh.2013.00028>.
- Steiner, M. A.; Gatfield, J.; Brisbare-Roch, C.; Dietrich, H.; Treiber, A.; Jenck, F.; Boss, C. Discovery and characterization of ACT-335827, an orally available, brain penetrant orexin receptor type 1 selective antagonist. *ChemMedChem* **2013**, *8* (6), 898–903. <https://doi.org/10.1002/cmdc.201300003>.

16. Perrey, D. A.; German, N. A.; Gilmour, B. P.; Li, J. X.; Harris, D. L.; Thomas, B. F.; Zhang, Y. Substituted tetrahydroisoquinolines as selective antagonists for the orexin 1 receptor. *J. Med. Chem.* **2013**, *56* (17), 6901–6916. <https://doi.org/10.1021/jm400720h>.
17. Perrey, D. A.; German, N. A.; Decker, A. M.; Thorn, D.; Li, J. X.; Gilmour, B. P.; Thomas, B. F.; Harris, D. L.; Runyon, S. P.; Zhang, Y. Effect of 1-substitution on tetrahydroisoquinolines as selective antagonists for the orexin-1 receptor. *ACS Chem. Neurosci.* **2015**, *6* (4), 599–614. <https://doi.org/10.1021/cn500330v>.
18. Watanabe, H.; Fukui, K.; Shimizu, Y.; Idoko, Y.; Nakamoto, Y.; Togashi, K.; Saji, H.; Ono, M. Synthesis and biological evaluation of F-18 labeled tetrahydroisoquinoline derivatives targeting orexin 1 receptor. *Bioorg. Med. Chem. Lett.* **2019**, *29* (13), 1620–1623. <https://doi.org/10.1016/j.bmcl.2019.04.044>.
19. Perrey, D. A.; Decker, A. M.; Li, J. X.; Gilmour, B. P.; Thomas, B. F.; Harris, D. L.; Runyon, S. P.; Zhang, Y. The importance of the 6- and 7-positions of tetrahydroisoquinolines as selective antagonists for the orexin 1 receptor. *Bioorg. Med. Chem.* **2015**, *23* (17), 5709–5724. <https://doi.org/10.1016/j.bmc.2015.07.013>.
20. Perrey, D. A.; Decker, A. M.; Zhang, Y. Synthesis and Evaluation of Orexin-1 Receptor Antagonists with Improved Solubility and CNS Permeability. *ACS Chem. Neurosci.* **2018**, *9* (3), 587–602. <https://doi.org/10.1021/acscchemneuro.7b00402>.
21. Boswell-Smith, V.; Spina, D. PDE4 inhibitors as potential therapeutic agents in the treatment of COPD-focus on roflumilast. *Int. J. Chron. Obstruct. Pulmon. Dis.* **2007**, *2* (2), 121–129.
22. Essayan, D. M. Cyclic nucleotide phosphodiesterases. *J. Allergy Clin. Immunol.* **2001**, *108* (5), 671–680. <https://doi.org/10.1067/mai.2001.119555>.
23. Li, H.; Zuo, J.; Tang, W. Phosphodiesterase-4 Inhibitors for the Treatment of Inflammatory Diseases. *Front. Pharmacol.* **2018**, *9*, 1048. <https://doi.org/10.3389/fphar.2018.01048>.
24. Liao, Y.; Guo, Y.; Li, S.; Wang, L.; Tang, Y.; Li, T.; Chen, W.; Zhong, G.; Song, G. Structure-based design and structure-activity relationships of 1,2,3,4-tetrahydroisoquinoline derivatives as potential PDE4 inhibitors. *Bioorg. Med. Chem. Lett.* **2018**, *28* (7), 1188–1193. <https://doi.org/10.1016/j.bmcl.2018.02.056>.
25. Song, G.; Zhao, D.; Hu, D.; Li, Y.; Jin, H.; Cui, Z. Design, synthesis and biological evaluation of novel tetrahydroisoquinoline derivatives as potential PDE4 inhibitors. *Bioorg. Med. Chem. Lett.* **2015**, *25* (20), 4610–4614. <https://doi.org/10.1016/j.bmcl.2015.08.043>.
26. Nomura, S.; Sakamaki, S.; Hongu, M.; Kawanishi, E.; Koga, Y.; Sakamoto, T.; Yamamoto, Y.; Ueta, K.; Kimata, H.; Nakayama, K.; Tsuda-Tsukimoto, M. Discovery of canagliflozin, a novel C-glucoside with thiophene ring, as sodium-dependent glucose cotransporter 2 inhibitor for the treatment of type 2 diabetes mellitus. *J. Med. Chem.* **2010**, *53* (17), 6355–6360. <https://doi.org/10.1021/jm100332n>.
27. Nauck, M. A. Update on developments with SGLT2 inhibitors in the management of type 2 diabetes. *Drug Des. Devel. Ther.* **2014**, *8*, 1335–1380. <https://doi.org/10.2147/DDDT.S50773>.
28. Pan, X.; Huan, Y.; Shen, Z.; Liu, Z. Synthesis and biological evaluation of novel tetrahydroisoquinoline-C-aryl glucosides as SGLT2 inhibitors for the treatment of type 2 diabetes. *Eur. J. Med. Chem.* **2016**, *114*, 89–100. <https://doi.org/10.1016/j.ejmech.2016.02.053>.
29. Amin, M. L. P-glycoprotein Inhibition for Optimal Drug Delivery. *Drug Target Insights* **2013**, *7*, 27–34. <https://doi.org/10.4137/DTI.S12519>.
30. Varma, M. V.; Ashokraj, Y.; Dey, C. S.; Panchagnula, R. P-glycoprotein inhibitors and their screening: a perspective from bioavailability enhancement. *Pharmacol. Res.* **2003**, *48* (4), 347–359. [https://doi.org/10.1016/s1043-6618\(03\)00158-0](https://doi.org/10.1016/s1043-6618(03)00158-0).
31. Li, Y. S.; Yang, X.; Zhao, D. S.; Cai, Y.; Huang, Z.; Wu, R.; Wang, S. J.; Liu, G. J.; Wang, J.; Bao, X. Z.; Ye, X. Y.; Wei, B.; Cui, Z. N.; Wang, H. Design, synthesis and bioactivity study on 5-phenylfuran derivatives as potent reversal agents against P-glycoprotein-mediated multidrug resistance in MCF-7/ADR cell. *Eur. J. Med. Chem.* **2021**, *216*, 113336. <https://doi.org/10.1016/j.ejmech.2021.113336>.
32. Qiu, Q.; Zhou, J.; Shi, W.; Kairuki, M.; Huang, W.; Qian, H. Design, synthesis and biological evaluation of N-(4-(2-(6,7-dimethoxy-3,4-dihydroisoquinolin-2(1H)-yl)ethyl)phenyl)-4-oxo-3,4-dihydrophthalazine-1-carboxamide derivatives as novel P-glycoprotein inhibitors reversing multidrug resistance. *Bioorg. Chem.* **2019**, *86*, 166–175. <https://doi.org/10.1016/j.bioorg.2019.01.039>.
33. Qiu, Q.; Shi, W.; Zhao, S.; Zhu, Y.; Ding, Z.; Zhou, S.; Kairuki, M.; Huang, W.; Qian, H. Discovery to solve multidrug resistance: Design, synthesis, and biological evaluation of novel agents. *Arch. Pharm. (Weinheim)* **2019**, *352* (10), e1900127. <https://doi.org/10.1002/ardp.201900127>.
34. Zhang, B.; Zhao, T.; Zhou, J.; Qiu, Q.; Dai, Y.; Pan, M.; Huang, W.; Qian, H. Design, synthesis and biological evaluation of novel triazole-core reversal agents against P-glycoprotein-mediated multidrug resistance. *RSC advances* **2016**, *6* (31), 25819–25828. <https://doi.org/10.1039/C6RA02405J>.
35. Gao, Y.; Shi, W.; Cui, J.; Liu, C.; Bi, X.; Li, Z.; Huang, W.; Wang, G.; Qian, H. Design, synthesis and biological evaluation of novel tetrahydroisoquinoline derivatives as P-glycoprotein-mediated multidrug resistance inhibitors. *Bioorg. Med. Chem.* **2018**, *26* (9), 2420–2427. <https://doi.org/10.1016/j.bmc.2018.03.045>.
36. Guglielmo, S.; Lazzarato, L.; Contino, M.; Perrone, M. G.; Chegaev, K.; Carrieri, A.; Fruttero, R.; Colabufo, N. A.; Gasco, A. Structure-Activity Relationship Studies on Tetrahydroisoquinoline Derivatives: [4'-(6,7-Dimethoxy-3,4-dihydro-1H-isoquinolin-2-ylmethyl)biphenyl-4-ol](MC70) Conjugated through Flexible Alkyl Chains with Furazan Moieties Gives Rise to Potent and Selective Ligands of P-glycoprotein. *J. Med. Chem.* **2016**, *59* (14), 6729–6738. <https://doi.org/10.1021/acs.jmedchem.6b00252>.
37. Li, Y. S.; Zhao, D. S.; Liu, X. Y.; Liao, Y. X.; Jin, H. W.; Song, G. P.; Cui, Z. N. Synthesis and biological evaluation of 2,5-disubstituted furan derivatives as P-glycoprotein inhibitors for Doxorubicin resistance in MCF-7/ADR cell. *Eur. J. Med. Chem.* **2018**, *151*, 546–556. <https://doi.org/10.1016/j.ejmech.2018.04.012>.
38. Mairinger, S.; Wanek, T.; Kuntner, C.; Doenmez, Y.; Strommer, S.; Stanek, J.; Capparelli, E.; Chiba, P.; Müller, M.; Colabufo, N. A.; Langer, O. Synthesis and preclinical evaluation of the radiolabeled P-glycoprotein inhibitor [(11)C]MC113. *Nucl. Med. Biol.* **2012**, *39* (8), 1219–25. <https://doi.org/10.1016/j.nucmedbio.2012.08.005>.
39. Colabufo, N. A.; Berardi, F.; Cantore, M.; Perrone, M. G.; Contino, M.; Inglese, C.; Niso, M.; Perrone, R.; Azzariti, A.; Simone, G. M.; Paradiso, A. 4-Biphenyl and 2-naphthyl substituted 6,7-dimethoxytetrahydroisoquinoline derivatives as potent P-gp modulators. *Bioorg. Med. Chem.* **2008**, *16* (7), 3732–43. <https://doi.org/10.1016/j.bmc.2008.01.055>.
40. Wu, Y.; Pan, M.; Dai, Y.; Liu, B.; Cui, J.; Shi, W.; Qiu, Q.; Huang, W.; Qian, H. Design, synthesis and biological evaluation of LBM-A5 derivatives as potent P-glycoprotein-mediated multidrug resistance inhibitors. *Bioorg. Med. Chem.* **2016**, *24* (10), 2287–97. <https://doi.org/10.1016/j.bmc.2016.03.065>.
41. Payne, M.; Bottomley, A. L.; Och, A.; Hiscocks, H. G.; Asmara, A. P.; Harry, E. J.; Ung, A. T. Synthesis and biological evaluation of tetrahydroisoquinoline-derived antibacterial compounds. *Bioorg. Med. Chem.* **2022**, *57*, 116648. <https://doi.org/10.1016/j.bmc.2022.116648>.

42. Ramanivas, T.; Sushma, B.; Nayak, V. L.; Chandra Shekar, K.; Srivastava, A. K. Design, synthesis and biological evaluations of chirally pure 1,2,3,4-tetrahydroisoquinoline analogs as anti-cancer agents. *Eur. J. Med. Chem.* **2015**, *92*, 608–618. <https://doi.org/10.1016/j.ejmech.2015.01.030>.
43. Capilla, A. S.; Soucek, R.; Grau, L.; Romero, M.; Rubio-Martínez, J.; Caignard, D. H.; Pujol, M. D. Substituted tetrahydroisoquinolines: synthesis, characterization, antitumor activity and other biological properties. *Eur. J. Med. Chem.* **2018**, *145*, 51–63. <https://doi.org/10.1016/j.ejmech.2017.12.098>.
44. Sim, S.; Lee, S.; Ko, S.; Phuong Bui, B.; Linh Nguyen, P.; Cho, J.; Lee, K.; Kang, J. S.; Jung, J. K.; Lee, H. Design, synthesis, and biological evaluation of potent 1,2,3,4-tetrahydroisoquinoline derivatives as anticancer agents targeting NF- $\kappa$ B signaling pathway. *Bioorg. Med. Chem.* **2021**, *46*, 116371. <https://doi.org/10.1016/j.bmc.2021.116371>.
45. Wilson, R. J.; Jecs, E.; Miller, E. J.; Nguyen, H. H.; Tahirovic, Y. A.; Truax, V. M.; Kim, M. B.; Kuo, K. M.; Wang, T.; Sum, C. S.; Cvijic, M. E.; Paiva, A. A.; Schroeder, G. M.; Wilson, L. J.; Liotta, D. C. Synthesis and SAR of 1,2,3,4-Tetrahydroisoquinoline-Based CXCR4 Antagonists. *ACS Med. Chem. Lett.* **2018**, *9* (1), 17–22. <https://doi.org/10.1021/acsmedchemlett.7b00381>.

---

*Information about the authors:*

**Maryam Amra Jordaán**, Doctor of Philosophy, Research Directorate, Mangosuthu University of Technology;  
<https://orcid.org/0000-0002-3057-123X>.

**Oluwakemi Ebenezer** (*corresponding author*), Research Fellow, Department of Chemistry, Faculty of Natural Science, Mangosuthu University of Technology; <https://orcid.org/0000-0003-1054-9665>; e-mails for correspondence: re.korede@gmail.com, ebenezer.oluwakemi@mut.ac.za.

UDC 633.81: 665.52:543.544.122

S. M. Kovtun-Vodyanytska<sup>1</sup>, I. V. Levchuk<sup>2</sup>, D. B. Rakhmetov<sup>1</sup>, O. V. Golubets<sup>2</sup><sup>1</sup> M. M. Gryshko National Botanical Garden of the National Academy of Sciences of Ukraine,  
1 Sadovo-Botanichna str., 01014 Kyiv, Ukraine<sup>2</sup> Scientific and Research Center for Products Testing, State Enterprise "UkrMetrTestStandart",  
4 Metrology str., 03143 Kyiv, Ukraine

## Chemical Components of Essential Oils from Aerial Parts of *Pycnanthemum virginianum* and *P. californicum* (Lamiaceae) Plants

### Abstract

**Aim.** The research is aimed at determining the qualitative and quantitative content of essential oils in the aerial part of two species of the genus *Pycnanthemum* Michx. (Lamiaceae) – *P. virginianum* (L.) T. Durand & B.D. Jacks. ex B.L. Rob & Fernald and *P. californicum* Norr. ex Durand. The plants were introduced in the M. M. Gryshko National Botanical Garden of National Academy of Sciences of Ukraine (Forest-Steppe zone). These are representatives of the flora of North America, and they are little known in Ukraine. Plants have useful medicinal and nutritional properties, but the biochemical composition of their essential oils has not been sufficiently studied in the world.

**Materials and methods.** In the experiment, the aerial herbal part of plants collected during the flowering phase was used. The quantitative content of the essential oil was determined by the hydrodistillation method, and its qualitative characteristics were found by the GC-MS analysis. The chromatographic profile was obtained on an Agilent Technologies 7890. The component composition of the essential oil was determined on a gas chromatograph with a HP 6890 mass spectrometric detector with a mass spectrometric detector 5973. We used a mass spectrometric detector 1.6 – 800 a.o.m., EI ionization, SIM & Scan mode, "Hewlett Packard", USA. Identification of essential oil components was performed using the NIST mass spectrum library in combination with AMDIS content-time identification programs.

**Results and discussion.** *P. virginianum* was found to produce 1.96 ± 0.17% of essential oil, in which 12 compounds out of 13 were identified; *P. californicum* had 2.66 ± 0.13% of essential oil, 13 compounds out of 15 were identified. The essential oil samples obtained have pulegone as the dominant component: *P. virginianum* – 44.65%, *P. californicum* – 86.07%. In addition to it, they also contain thymol, myrcene, 1.8-cineole, menthone, limonene and other compounds.

**Conclusions.** For the first time, the qualitative and quantitative composition of the essential oils of plants of *P. virginianum* and *P. californicum* species introduced in Ukraine has been determined. The results obtained indicate that when introduced plants have a high biosynthesizing ability to produce essential oil. Pulegone has been found to be the dominant component; therefore, the essential oil can be classified as a pulegone-type essential oil. We believe that the raw material of *P. virginianum* and *P. californicum* are potentially suitable for use in perfumery, cosmetics, aromatherapy, personal care products, dentistry, and in the pharmaceutical and food industries.

**Keywords:** introduced plants; *Pycnanthemum*; components of essential oils; GC-MS

**С. М. Ковтун-Водяницька<sup>1</sup>, І. В. Левчук<sup>2</sup>, Д. Б. Рахметов<sup>1</sup>, О. В. Голубець<sup>2</sup>**

<sup>1</sup> Національний ботанічний сад імені М. М. Гришка НАН України,  
вул. Садово-Ботанічна, 1, м. Київ, 01014, Україна

<sup>2</sup> Науково-дослідний центр випробувань продукції: ДП «УкрМетрТестСтандарт»,  
вул. Метрологічна, 4, м. Київ, 03143, Україна

**Хімічні компоненти ефірних олій із надземних частин рослин *Pycnanthemum virginianum* і *P. californicum* (Lamiaceae)**

### Анотація

**Мета.** Визначити якісний склад та кількісний вміст ефірних олій у надземній частині двох видів роду *Pycnanthemum* Michx. (Lamiaceae) – *P. virginianum* (L.) T. Durand & B.D. Jacks. ex B.L. Rob & Fernald та *P. californicum* Norr. ex Durand. Рослини інтродуковано в Національному ботанічному саду імені М. М. Гришка НАН України (лісостепова зона). Це представники флори Північної Америки, а в Україні вони маловідомі. Рослини мають корисні лікувальні та харчові властивості, але біохімічний склад їхніх ефірних олій у світі вивчено недостатньо.

**Матеріали та методи.** В експерименті використано надземну трав'яну частину рослин, зібрану у фазу квітання. Кількісний вміст ефірної олії визначали методом гідродистиляції, а її якісні характеристики – методом ГХ-МС. Хроматографічний профіль отримували на хроматографі Agilent Technologies 7890. Компонентний склад ефірної олії визначали на газовому хроматографі HP 6890 з мас-спектрометричним детектором 5973. Мас-спектрометричний детектор 1,6 – 800 а.о.м., EI іонізація, SIM & Scan mode, «Hewlett Packard», США. Ідентифікацію компонентів ефірної олії виконували за допомогою бібліотеки мас-спектрів NIST у поєднанні з програмами ідентифікації вмісту AMDIS.

**Результати та їх обговорення.** Виявлено, що *P. virginianum* продукує  $1,96 \pm 0,17\%$  ефірної олії, у якій ідентифіковано 12 сполук із 13 виявлених; *P. californicum* –  $2,66 \pm 0,13\%$ , ідентифіковано 13 сполук із 15. Отримані зразки ефірної олії за домінуючим компонентом мають пулегон: *P. virginianum* – 44,65%, *P. californicum* – 86,07%. Окрім нього, зразки також містять тимол, мірцен, 1,8-цинеол, ментон, лімонен та інші сполуки.

**Висновки.** Уперше визначено якісний та кількісний склад ефірних олій рослин видів *P. virginianum* та *P. californicum*, інтродукованих в умови України. Отримані результати свідчать, що за інтродукції рослини мають високу біосинтезувальну здатність продукувати ефірну олію. Виявлено, що домінуючим компонентом є пулегон, тому ефірну олію можна кваліфікувати як ефірну олію пулегоного типу. Вважаємо, що сировина *P. virginianum* та *P. californicum* потенційно придатна для використання в парфумерії, косметичці, ароматерапії, засобах особистої гігієни, стоматології, у фармацевтичній та харчовій промисловості.

**Ключові слова:** інтродуковані рослини; *Pycnanthemum*; компоненти ефірної олії; ГХ-МС

**Citation:** Kovtun-Vodyanytska, S. M.; Levchuk, I. V.; Rakhmetov, D. B.; Golubets, O. V. Chemical components of essential oils from aerial parts of *Pycnanthemum virginianum* and *P. californicum* (Lamiaceae) plants. *Journal of Organic and Pharmaceutical Chemistry* 2023, 21 (1), 39–45.

<https://doi.org/10.24959/ophcj.23.273810>

**Received:** 3 February 2023; **Revised:** 15 March 2023; **Accepted:** 25 March 2023

**Copyright** © 2023, S. M. Kovtun-Vodyanytska, I. V. Levchuk, D. B. Rakhmetov, O. V. Golubets. This is an open access article under the CC BY license (<http://creativecommons.org/licenses/by/4.0>).

**Funding:** The authors received no specific funding for this work.

**Conflict of interests:** The authors have no conflict of interests to declare.

## ■ Introduction

There was a need for a wider study of the chemical composition of the essential oils of plants of the genus *Pycnanthemum* (Lamiaceae), as evidenced by the analysis of literary sources. In general, a comprehensive assessment of the essential oils of plants of the genus *Pycnanthemum* has not yet been carried out. However, to fully understand the application and benefits of *Pycnanthemum* sp. a deeper understanding of the chemical composition of plants is needed [1].

To date, it is known that the quantitative content of essential oil and especially its qualitative composition in different types of *Pycnanthemum* is different, but the main components are pulegone (medicinal mint), menthone (fresh mint), isomenthone (cereal mint), limonene (citrus), piperitone (mint and camphor). The essential oil of *Pycnanthemum floridanum* E. Grant & Epling has been most fully evaluated and it contains 40 volatile components [2–5].

The consequence of the different composition of the essential oil is the difference in aroma. Differences in aromas are observed not only at the species level. There are reports of different plant aromas among populations of *P. virginianum* – some have a distinct citrus scent similar to *Melissa officinalis* L. or *Monarda citriodora*

*Cerv ex Lag.* Similar information regarding variability in essential oil composition and aroma is available for *Pycnanthemum loomisii* Nutt. Thus, different chemotypes may exist within one species [1, 6].

Considering a wide spectrum of the biological activity of related genera due to the essential oil content, it can be assumed that *Pycnanthemum* sp. has similar properties, in particular, antioxidant, antitumor, antiviral, antifungal and antibacterial properties. Due to their high content of terpenes, *Pycnanthemum* plants have a wide potential for application in pharmaceuticals, cosmetics, culinary and food flavoring [1, 7].

According to the latest taxonomy, the genus *Pycnanthemum* includes 22 taxa, 20 species and 2 varieties [8]. The natural range covers certain areas of North America, administratively subordinate to the United States (mainly the states of the eastern part of the country) and Canada (2 southern provinces). The mountains of North Carolina (USA) are considered to be the center of species diversity [9].

Plants of the genus *Pycnanthemum* are herbaceous perennials up to 80 cm high. The aerial part of the plants contains secondary metabolites – essential oils. On the American continent there is a long tradition of using *Pycnanthemum* sp. by the aboriginal population for medicinal purposes

(in indigestion, colitis, dyspepsia, colds, headaches), in cooking and in ritual ceremonies [10, 11]. An interesting historical reference about the use of *Pycnanthemum* is a book of the 19<sup>th</sup> century. The 1898 edition of the “Royal American Dispensary” mentions the genus *Pycnanthemum* and its medicinal properties: “*Pycnanthemum* is diaphoretic, stimulant, antispasmodic, carminative and tonic. A warm infusion is very useful for postpartum, remitting and other forms of fever, cough, cold, catarrh, etc., and it is very useful for spasmodic diseases, especially colic, stomach spasms, spasms in babies.” [12].

*Pycnanthemum* sp. are also used as good honey plants and ornamental plants [13].

In Ukraine, the *Pycnanthemum* genus is practically not found either in scientific or private collections and is little known. However, taking into account the useful properties of plants of this genus and the possibility of their complex use, they are promising for research. In particular, insufficient study of the biochemical composition prompted us to conduct a series of experimental studies. The results of one of them are presented in this work.

## ■ Materials and methods

### Plant source

The studies used plants of two species, *P. virginianum* and *P. californicum*. These plants were introduced into the Department of Cultural Flora of M. M. Gryshko National Botanical Garden of the National Academy of Sciences of Ukraine (NBG) in 2014 and 2017, respectively.

The plants were grown from seed material obtained from scientific botanical institutions in

the Czech Republic within the framework of the “Index Seminum” exchange system. The growth conditions were as follows: open soil, Forest-Steppe zone of Ukraine. Generatively adult plants are shown in Figure 1 (a, b).

In 2021, the raw material was harvested and analyzed. Harvesting of the raw material was carried out during the phase of mass flowering of plants. Under the raw material of these species, we mean the above-ground herbal leafy part – a mixture of leaves, inflorescences and stems.

### Isolation of the essential oils

The fresh above-ground part of plants was collected on a sunny day, during lunch hours. Then they were crushed into fragments of 1–1.5 cm and left to wither for 24 hours. Next, the raw material was dried to an air-dry state using an Eridri ULTRA FD1000 dryer. Weighing samples of the raw material was carried out on the VLKT–500 g–M scales. The essential oil was obtained by hydrodistillation using an apparatus with a Clevenger-type nozzle. The sample weight was 35 g. The multiplicity of the experiment was 3-fold. The exposure time was 1.5 hours (from the moment the water boils).

### The Gas chromatography – Mass spectrometry analysis (GC-MS)

The chromatographic profile was obtained on an Agilent Technologies 7890 gas chromatograph using a vf-5ms (5%-phenyl)-methylpolysiloxane) capillary column, 25 m long, with an internal diameter of 0.25 mm and a stationary phase thickness of 0.33  $\mu\text{m}$  under the following conditions: gas velocity – carrier – 1.0 mL min<sup>-1</sup>; flow split ratio – 1:20; evaporator temperature – 250 °C; detector temperature (DEP) – 280 °C; column temperature regime – gradual heating from 60 °C to 185 °C.



a



b

**Figure 1.** *Pycnanthemum virginianum* (a) and *P. californicum* (b) introduced in the M. M. Gryshko National Botanical Garden of the NAS of Ukraine (Kyiv, Ukraine)

The component composition of the essential oil was determined on a gas chromatograph with a HP 6890 mass spectrometric detector with a mass spectrometric detector 5973. We used a mass spectrometric detector 1.6 – 800 a.o.m., EI ionization, SIM & Scan mode, “Hewlett Packard”, USA. The chromatographic conditions were as follows: chromatographic column – capillary HP–5ms (5%-phenyl)-methylpolysiloxane), outer diameter – 0.25 mm, length – 30 m; carrier gas – helium; carrier gas velocity – 1.2 mL min<sup>-1</sup>; sample injection heater temperature – 180 °C.

The oven temperature was programmable from 62 to 165 °C at a rate of 5 deg min<sup>-1</sup>. The sample injection (1 µL) was without flow split. For the identification of essential oil components, the NIST mass spectrum library was used in combination with AMDIS content-time identification programs.

## ■ Results and discussions

Under the conditions of the NBG, the introduced species *P. virginianum* and *P. californicum* have a high content of essential oil in the raw material. It has been experimentally determined that in the aerial part of *P. virginianum* the content of essential oil is 1.96 ± 0.17%, in *P. californicum* – 2.66 ± 0.13%. They differ in color – in *P. virginianum*, the essential oil is transparent with a barely noticeable yellowish

tinge, and it is colorless transparent in *P. californicum*. There were 13 components found in the essential oil of *P. virginianum*, 12 of them were identified. As can be seen from Table 1, the main odorants include pulegone (44.65%), thymol (20.16%), menthone (6.61%), isomenthone (5.75%), limonene (2.73%), caryophyllene (2.72%), *p*-cymene (2.36%), myrcene (1.91%). The chromatogram of the *P. virginianum* essential oil is shown in Figure 2.

The presence of the chemical characteristics of *P. virginianum* essential oil in the literature made it possible to compare it with our sample shown in Table 2.

The publication covering the results of studying the essential oil of 4 varieties of *P. virginianum* (Alabama A&M University Research Station, North Alabama, USA) was used [7]. In the samples from North Alabama, the chemical profiles of 4 samples were taken into account, which harvesting was in October 2020 on the 155<sup>th</sup> day after planting the plants from the greenhouse into the open ground. We analyzed the entire flowering aerial herbal part, and colleagues presented the results of screening the essential oil extracted from leaves of the plants. Despite the differences in the experimental material and the lack of other information, we nevertheless used this material and made a comparison.

Obviously, according to the concentration of pulegone, thymol, and caryophyllene in the essential

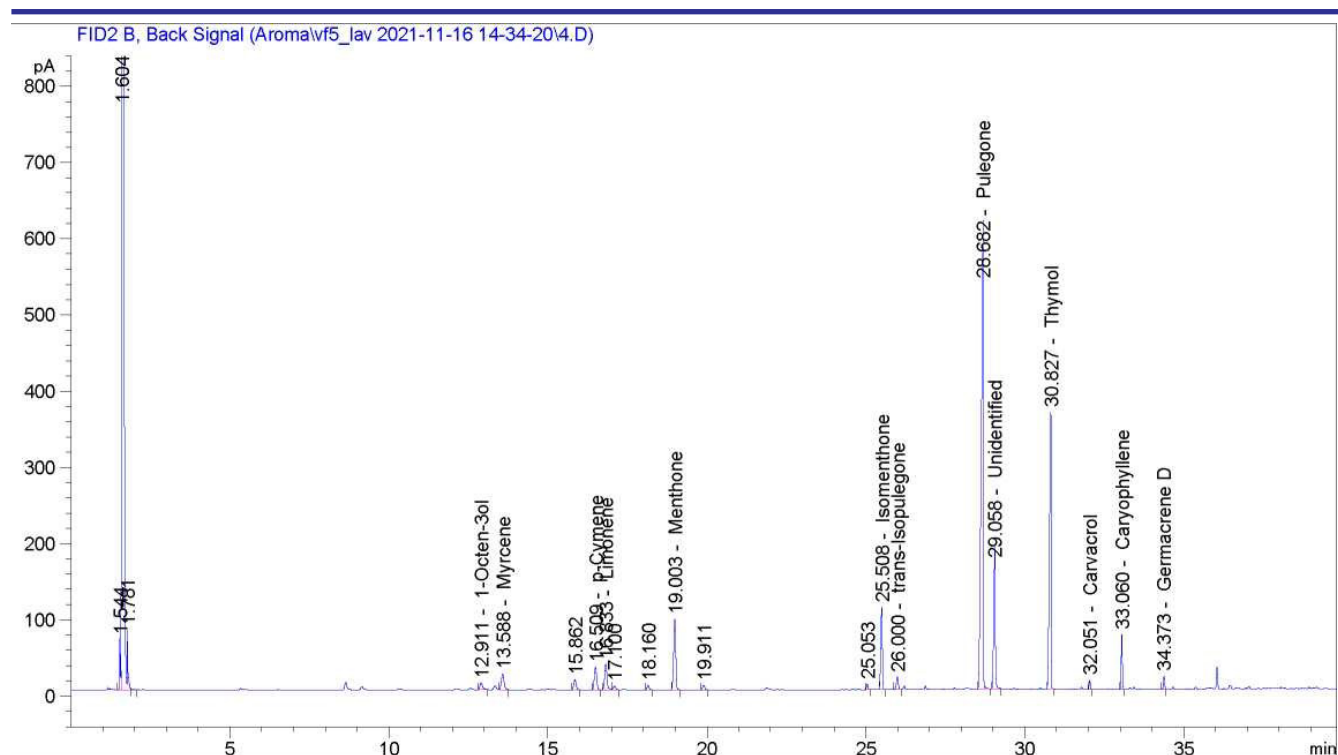


Figure 2. Chromatogram of the *Pycnanthemum virginianum* essential oil

**Table 1.** Chemical constituents of the essential oil of *Pycnanthemum virginianum*

No	Compounds	RetTime, min	Content index, %
1	1-Octen-3-ol	12.911	0.88
2	Myrcene	13.588	1.91
3	<i>p</i> -Cymene	16.509	2.36
4	Limonene	16.833	2.73
5	Menthone	19.003	6.61
6	Isomenthone	25.508	5.75
7	<i>trans</i> -Isopulegone	26.000	1.09
8	Pulegone	28.682	44.65
9	Unidentified	29.058	9.93
10	Thymol	30.827	20.16
11	Carvacrol	32.051	0.48
12	Caryophyllene	33.060	2.72
13	Germacrene D	34.373	0.71
Total			99.98

oil, the *P. virginianum* sample from NBG occupies a leading position. This is despite the fact that the whole herbaceous aboveground part of the plants was subject to analysis, i.e., the sample included not only leaves and inflorescences as organs of the highest encountering frequency of essential oil glands, but also stems, which had a low indicator them.

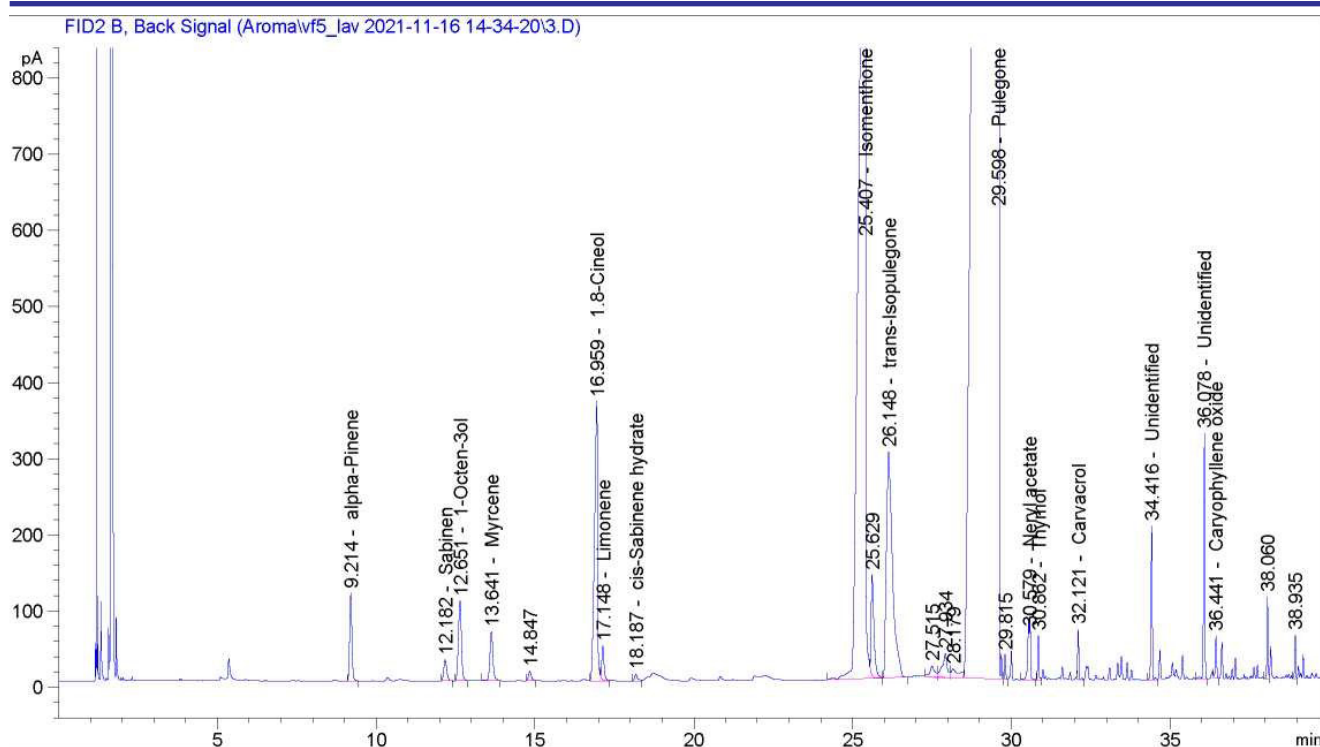
15 components were found in the essential oil of *P. californicum*, 13 of them were identified. The key odorants were pulegone (86.07%), isomenthone (8.77%), *trans*-isopulegone (1.85%),

**Table 2.** The content of major components in the essential oil of *Pycnanthemum virginianum*, in the samples of NBG (our own analysis) and North Alabama (Setzer et al., 2021)

Compounds	Content of dominant compounds, %	
	NBG	North Alabama
1-Octen-3-ol	0.88	1.8–2.0
Myrcene	1.91	0.4–2.6
<i>p</i> -Cymene	2.36	7.1–8.7
Limonene	2.73	1.3–5.5
Menthone	6.61	3.8–9.9
Isomenthone	5.75	0.4–54.7
<i>trans</i> -Isopulegone	1.09	1.1–4.1
Pulegone	44.65	10.8–29.8
Thymol	20.16	0.2–22.1
Carvacrol	0.48	1.4
Caryophyllene	2.72	0.2–1.0
Germacrene D	0.71	0.7–1.5

1,8-cineole (1.14%), 1-octen-3-ol (0.33%), myrcene (0.2%), neryl acetate (0.21%) and limonene (0.11%) as evidenced by the data in Table 3. The chromatogram of *P. californicum* essential oil is shown in Figure 3.

In both species, the dominant component of the essential oil is pulegone (*P. californicum* – 86%, *P. virginianum* – 45%) although the qualitative set of components that form the aroma and pharmacological properties of the essential oil by the quantitative content differ in these two introduced species.

**Figure 3.** Chromatogram of the *Pycnanthemum californicum* essential oil

**Table 3.** Chemical constituents of the essential oil of *Pycnanthemum californicum*

No.	Compounds	RetTime, min	Content index, %
1	Sabinen	12.182	0.09
2	1-Octen-3-ol	12.651	0.33
3	Myrcene	13.641	0.20
4	1.8-Cineol	16.959	1.14
5	Limonene	17.148	0.11
6	<i>cis</i> -Sabinene hydrate	18.187	0.03
7	Isomenthone	25.407	8.77
8	<i>trans</i> -Isopulegone	26.148	1.85
9	Pulegone	29.598	86.07
10	Neryl acetate	30.579	0.21
11	Thymol	30.862	0.07
12	Carvacrol	32.121	0.09
13	Unidentified	34.416	0.27
14	Unidentified	36.078	0.44
15	Caryophyllene oxide	36.441	0.08
Total			99.74

Pulegone belongs to the group of monoterpene ketones, has a sweetish pleasant aftertaste and a refreshing aroma reminiscent of mint. In this, it is similar to other “minty” terpenes – camphor and isopulegon, which also have a cool minty aroma.

Six genera of *Lamiaceae* (*Acinos*, *Calamintha*, *Cyclotrichium*, *Mentha*, *Micromeria* and *Ziziphora*) have been found to contain pulegone as the main component of their oils. Pulegone was first obtained from *Mentha pulegium* L., hence the name. Taking into account the dominant role of pulegone in the composition of *P. virginianum* and *P. californicum* essential oils, the raw material of these species is promising for practical use, for example, as a substitute for *M. pulegium*, in particular the well-known spice “ombalo” – a mixture of dry leaves and inflorescences from *M. pulegium* [14]. According to published data, the content of pulegone in the essential oil of *M. pulegium* varies within 40–45% depending on the origin of the raw material – 43.5% (Egypt) [15], 40.98% (Morocco) [16], 48.7% (Iran) [17], 65.0–83.1% (India) [18], 28.9% (Turkey) [19]. At the same time, it is known that the commercial essential oil of *M. pulegium* contains about 84% pulegone (Center for Aromatic Plant Research, Lehi, Utah, USA) [7].

Pulegone is used in perfumery, cosmetics, aromatherapy, personal care products, dentistry,

and as a source of menthol. In medicine, it is applied as a remedy for colds and coughs, and in the food industry – as a flavoring of foods and alcoholic beverages. Taking into account all the positive characteristics, you should still adhere to certain rules for using pulegone. To date, there are no toxicokinetic studies in humans regarding the effects of pulegone, but there are some studies done in other mammals. When pulegone is ingested, it is broken down in the liver and reacts to form numerous toxic metabolites that can cause harm to the body, in particular a necrotic effect on the liver. Some metabolites identified are mentofuran, piperitenon, piperitone and menthone. If there are no restrictions on the use of pulegone in perfumery and cosmetics, they do exist in the food industry. In particular, for food products, the rate of use of pure pulegone is 25 mg kg<sup>-1</sup>, soft drinks, sweets – 100–350 mg kg<sup>-1</sup> [20]. Due to the high concentration of pulegone in the essential oil of *P. californicum* and *P. virginianum* introduced, their raw material can also be offered as an alternative to synthetic pesticides and as a natural repellent.

## ■ Conclusions

In the M. M. Gryshko National Botanical Garden of the NAS of Ukraine (Forest-Steppe zone), plant species of the North American flora – *P. virginianum* and *P. californicum* family *Lamiaceae*, which are new to Ukraine, have been introduced. According to the results of laboratory studies, it has been found that plants of these species during the flowering period have a high content of essential oil in the aerial part: in *P. virginianum*, the content of essential oil is 1.96 ± 0.17%, *P. californicum* it is 2.66 ± 0.13%. The qualitative and quantitative content of the essential oil in these plant species show that they contain the essential oil of a pulegone type since this substance is the prevailing component in their oil. This fact has an impact on the practical use of essential oils, as well as the aerial herbal part of plants of these species. We believe that the raw material of *P. virginianum* and *P. californicum* are potentially suitable for use in perfumery, cosmetics, aromatherapy, personal care products, dentistry, and in the pharmaceutical and food industries.

## References

- Dein, M. Key Odorants of *Pycnanthemum incanum* and Stereochemistry of Chiral Compounds. Master's Thesis, University of Tennessee, 2019.
- [https://trace.tennessee.edu/utk\\_gradthes/5523](https://trace.tennessee.edu/utk_gradthes/5523).
- Ebadollahi, A.; Ziaee, M.; Palla, F. Essential oils extracted from different species of the Lamiaceae plant family as prospective bioagents against several detrimental pests. *Molecules* **2020**, *25* (7), 1556. <https://doi.org/10.3390/molecules25071556>.
- Karpinski, T. M. Essential oils of Lamiaceae family plants as antifungals. *Biomolecules* **2020**, *10* (1), 103. <https://doi.org/10.3390/biom10010103>.
- Shu, C.-K.; Lawrence, B.M.; Miller, K.L. Chemical Composition of the Essential Oil of *Pycnanthemum floridanum* E. Grant and Epling. *J. Essent. Oil Res.* **1994**, *8* (5), 529–531. <https://doi.org/10.1080/10412905.1994.9698442>.
- Dein, M.; Munafo, J.P. Characterization of key odorants in hoary mountain mint, *Pycnanthemum incanum*. *J. Agric. Food Chem.* **2019**, *67* (9), 2589–2597. <https://doi.org/10.1021/acs.jafc.8b06803>.
- Dein, M.; Munafo, J. P. Characterization of Odorants in Loomis' Mountain Mint, *Pycnanthemum loomisii*. *J. Agric. Food Chem.* **2022**, *70* (45), 14448–14456. <https://doi.org/10.1021/acs.jafc.2c05492>.
- Setzer, W. N.; Duong, L.; Pham, T.; Poudel, A.; Nguyen, C.; Mentreddy, S. R. Essential Oils of Four Virginia Mountain Mint (*Pycnanthemum virginianum*) Varieties Grown in North Alabama. *Plants* **2021**, *10*, 1397. <https://doi.org/10.3390/plants10071397>.
- The Plant List: *Pycnanthemum* Michaux. <http://www.theplantlist.org/tpl1.1/search?q=Pycnanthemum> (accessed Oct 20, 2022).
- Flora of the Carolinas, Virginia, Georgia, northern Florida, and surrounding areas *Pycnanthemum* Michaux (Mountain-mint, Wild-basil). Working Draft of 7 April 2008. [https://ncbg.unc.edu/wp-content/uploads/sites/963/2020/06/WeakleyFlora\\_2008-Apr.pdf](https://ncbg.unc.edu/wp-content/uploads/sites/963/2020/06/WeakleyFlora_2008-Apr.pdf) (accessed Feb 28, 2022).
- Cozzo, D. N. Ethnobotanical classification system and medical ethnobotany of the eastern band of the Cherokee Indians. Athens, Georgia, USA, 2004. [https://getd.libs.uga.edu/pdfs/cozzo\\_david\\_n\\_200405\\_phd.pdf](https://getd.libs.uga.edu/pdfs/cozzo_david_n_200405_phd.pdf) (accessed Sep 09, 2022).
- Small, E. Mountain Mint. *North American Cornucopia: Top 100 Indigenous Food Plants*, 1<sup>st</sup> Ed. CRC Press: 2013, 463–466. <https://doi.org/10.1201/b15818>.
- Felter, H. W.; Lloyd, J. U. King's American Dispensatory. Cincinnati, USA: Ohio Valley Co, 1898. Scan version by H. Kress <https://www.henriettes-herb.com/eclectic/kings/pycnanthemum.html> (accessed 2023-02-02).
- Jenderek, M. M.; Holman, G. E.; Ellis, D. D.; Reed, B. M. Long-term preservation of *Pycnanthemum* genetic resources. In *Book of Abstracts, World Congress on In Vitro Biology Meeting*, Bellevue, WA, United States, June 3–7, 2012.
- Ombalo (m'yata bolotna, bloshyna, bloshnitsa): shcho tse take, chym zaminyty, osoblyvosti vyroshchuvannya, zastosuvannya [Ombalo (swamp mint, flea): what it is, what to replace it with, features of cultivation, application, in Ukrainian]. <https://release.com.ua/?p=37313> (accessed Aug 17, 2022).
- El-Ghorab, A. H. The Chemical Composition of the *Mentha pulegium* L. Essential Oil from Egypt and its Antioxidant Activity. *J. Essent. Oil-Bear. Plants* **2006**, *9* (2), 183–195. <https://doi.org/10.1080/0972060X.2006.10643491>.
- Bouyahya, A.; Et-Touys, A.; Bakri, Y.; Talbaui, A.; Fellah, H.; Abrini, J.; Dakka, N. Chemical composition of *Mentha pulegium* and *Rosmarinus officinalis* essential oils and their antileishmanial, antibacterial and antioxidant activities. *Microb. Pathog.* **2017**, *111*, 41–49. <https://doi.org/10.1016/j.micpath.2017.08.015>.
- Nickavar, B.; Jabbareh, F. Analysis of the Essential Oil from *Mentha pulegium* and Identification of its Antioxidant Constituents. *J. Essent. Oil-Bear. Plants* **2018**, *21* (1), 223–229. <https://doi.org/10.1080/0972060X.2018.1433073>.
- Agnihotri, V. K.; Agarwal, S. G.; Dhar, P. L.; Thappa, R. K.; Baleshwar; Kapahi, B. K.; Saxena, R. K.; Qazi, G. N. Essential oil composition of *Mentha pulegium* L. growing wild in the North-Western Himalayas India. *Flavour Fragr. J.* **2005**, *20* (6), 607–610. <https://doi.org/10.1002/ffj.1497>.
- Yasa, H.; Onar, H. C.; Yusufoglu, A. S. Chemical Composition of the Essential Oil of *Mentha pulegium* L. from Bodrum, Turkey. *J. Essent. Oil-Bear. Plants* **2015**, *15* (6), 1040–1043. <https://doi.org/10.1080/0972060X.2012.10662609>.
- Da Rocha, M. S.; Dodmane, P. R.; Arnold, L. L.; Pennington, K. L.; Anwar, M. M.; Adams, B. R.; Taylor, S. V.; Wermes, C.; Adams, T. B.; Cohen, S. M. Mode of Action of Pulegone on the Urinary Bladder of F<sub>344</sub> Rats. *Toxicol. Sci.* **2012**, *128* (1), 1–8. <https://doi.org/10.1093/toxsci/kfs135>.

### Information about the authors:

**Svitlana M. Kovtun-Vodyanytska** (corresponding author), Ph.D. in Biological Sciences, Senior Researcher, Department of Cultural Flora, M. M. Gryshko National Botanical Garden of the National Academy of Sciences of Ukraine; <https://orcid.org/0000-0002-2367-461X>; e-mail for correspondence: [lcatta777@gmail.com](mailto:lcatta777@gmail.com).

**Iryna V. Levchuk**, Dr.Sci. in Technical Sciences, Senior Researcher, Head of the Scientific and Research Center for Products Testing, State Enterprise "UkrMetrTestStandart"; <https://orcid.org/0000-0002-9337-8816>.

**Dzhamal B. Rakhmetov**, Dr.Sci. in Agricultural Sciences, Professor, Deputy Director for Scientific Work, M. M. Gryshko National Botanical Garden of the National Academy of Sciences of Ukraine; <https://orcid.org/0000-0001-7260-3263>.

**Olga V. Golubets**, Ph.D. in Agricultural Sciences, Senior Researcher, Scientific and Research Center for Products Testing, State Enterprise "UkrMetrTestStandart"; <https://orcid.org/0000-0002-6840-4955>.

UDC 615.322:582.998

A. G. Rustemkulov<sup>2</sup>, T. M. Gontova<sup>1</sup>, B. G. Makhatova<sup>2</sup>, A. E. Rustemkulova<sup>2</sup>,  
U. M. Datkhayev<sup>2</sup>, O. M. Koshovyi<sup>1</sup>

## Standardization Parameters of *Alfredia nivea* KAR.&KIR Herb

<sup>1</sup> National University of Pharmacy of the Ministry of Health of Ukraine,  
53 Pushkinska str., 61002 Kharkiv, Ukraine<sup>2</sup> Asfendiyarov Kazakh National Medical University,  
94 Tole bi str., 050000 Almaty, Kazakhstan

### Abstract

The Kazakhstan flora is rich in promising poorly-studied plants, which are traditionally used in folk medicine, but their introduction into medical practice requires additional in-depth research using modern scientific methods. *Alfredia nivea* KAR.&KIR of the *Asteraceae* family, which is used in folk medicine as a neurotropic agent, is an interesting object for introduction into official medical and pharmaceutical practice.

**Aim.** To create new medicines based on *Alfredia nivea* herb, it is necessary to develop methods for quality control of this raw material, therefore, the aim of the research was to determine the parameters for standardization of the *Alfredia nivea* KAR & KIR. herb.

**Materials and methods.** The study objects were samples of the *A. nivea* herb collected in Kungei Alatau, 4.3 km southeast of the Karabulak village, Eastern Karabulak canyon, Almaty Region, Kazakhstan. The macroscopic and microscopic studies of the *A. nivea* herb were performed according to the methodology of the European pharmacopeia (EuPh) 2.8.23 "Microscopic examination of the medicinal plant raw material". The macroscopic studies were performed using a magnifying glass and a MBS-9 binocular microscope, the microscopic studies were done using MS Microscopes 10 (oculars X5, X10, X15, lenses x10, x40), Micromed XS-4130 (oculars WF15X, lenses x40/0.65, x10/0.25) with a microphotonozzle (China). Identification of the main substances was carried out by the TLC method, testing and the quantitative determination of the flavonoid content were performed according to the EuPh methods.

**Results and discussion.** Morphological and anatomical features of the *A. nivea* herb have been determined; on their basis *Identifications A and B* have been proposed; *TLC Identification C* of the main BAS of the raw material has been developed; indicators of purity tests have been determined. It has been proposed to carry out the quantitative determination by the content of flavonoids.

**Conclusions.** The parameters of the *A. nivea* herb standardization have been determined on the basis of the following indicators: macroscopic and microscopic features, TLC identification of the main BAS of the raw material (hyperoside, rutin, quercetin and chlorogenic acid), related impurities (not more than 2%), stems with a diameter of more than 20 mm (not more than 10%), the loss on drying (not more than 13%), the total ash (not more than 10%) and at least 0.5% flavonoids calculated with reference to rutin.

**Keywords:** *Alfredia nivea*; herb; standardization; quality control methods

**А. Г. Рустемкулов<sup>2</sup>, Т. М. Гонтова<sup>1</sup>, Б. Г. Махатова<sup>2</sup>, А. Є. Рустемкулова<sup>2</sup>, У. М. Датхаєв<sup>2</sup>, О. М. Кошовий<sup>1</sup>**

<sup>1</sup> Національний фармацевтичний університет Міністерства охорони здоров'я України,  
вул. Пушкінська, 53, м. Харків, 61002, Україна

<sup>2</sup> Казахський національний медичний університет імені С. Д. Асфендіярова,  
вул. Толе бі, 94, м. Алмати, 050000, Казахстан

### Параметри стандартизації трави *Alfredia nivea* KAR.&KIR.

#### Анотація

Флора Казахстану багата на перспективні маловивчені рослини, які застосовують у народній медицині, але для їх впровадження в медичну практику потрібні додаткові глибокі дослідження, за допомогою сучасних наукових методів. Цікавим об'єктом для впровадження в офіціальну медичну та фармацевтичну практику є Альфредія снігова (*Alfredia nivea* KAR. & KIR.) родини *Asteraceae*, яку в народній медицині використовують як нейротропний засіб.

**Мета.** Для створення нових лікарських засобів на основі трави Альфредії снігової необхідно розробити методи контролю якості цієї сировини, тому метою досліджень було визначити параметри стандартизації трави *A. nivea* KAR. & KIR.

**Матеріали та методи.** Об'єктами дослідження були зразки трави Альфредії снігової (*A. nivea*), заготовлені в Кунгей Алатау, за 4,3 км південно-східніше від с. Карабулак, ущ. Східний Карабулак, Алматинської області, Казахстан. Макро- і мікроскопічні дослідження трави Альфредії снігової виконували згідно з методикою Європейської фармакопеї (ЄФ) 2.8.23 «Мікроскопічне дослідження лікарської рослинної сировини». Для макроскопічних досліджень використовували лупу та бінокулярний мікроскоп МБС-9, для мікроскопічних – мікроскопи МС 10 (окуляр х5, х10, х15, об'єктиви х10, х40), Micromed XS-4130 (окуляр WF15X, об'єктиви х40/0,65, х10/0,25) з мікрофотонасадкою (КНР). Ідентифікували основні речовини методом ТШХ, випробування та кількісне визначення за вмістом флавоноїдів здійснювали відповідно до методик ЄФ.

**Результати та їх обговорення.** Визначено морфологічні й анатомічні ознаки трави Альфредії снігової, на основі яких запропоновано *Ідентифікації А та В*, розроблено ТШХ *Ідентифікацію С* основних БАР сировини, визначено показники випробувань на чистоту, а також запропоновано проводити кількісне визначення за вмістом флавоноїдів.

**Висновки.** Визначено параметри стандартизації трави Альфредії снігової за такими показниками: макро- та мікроскопічні ознаки, ТШХ ідентифікація основних БАР сировини (гіперозид, рутин, кверцетин та хлорогенова кислота), сторонні домішки (не більше 2%), наявність стебел діаметром понад 20 мм (не більше 10%), втрата в масі під час висушування (не більше 13%), загальна зола (не більше 10%) і не менше 0,5% флавоноїдів у перерахунку на рутин.

**Ключові слова:** Альфредія снігова; *Alfredia nivea*; трава; стандартизація; методи контролю якості

**Citation:** Rustemkulov, A. G.; Gontova, T. M.; Makhatova, B. G.; Rustemkulova, A. E.; Datkhayev, U. M.; Koshovyi, O. M. Standardization parameters of *Alfredia nivea* Kar. & Kir herb. *Journal of Organic and Pharmaceutical Chemistry* 2023, 21 (1), 46–53.

<https://doi.org/10.24959/ophcj.23.276004>

**Received:** 29 December 2022; **Revised:** 30 January 2023; **Accepted:** 10 February 2023

**Copyright** © 2023, A. G. Rustemkulov, T. M. Gontova, B. G. Makhatova, A. E. Rustemkulova, U. M. Datkhayev, O. M. Koshovyi.

This is an open access article under the CC BY license (<http://creativecommons.org/licenses/by/4.0>).

**Funding:** The authors received no specific funding for this work.

**Conflict of interests:** The authors have no conflict of interests to declare.

## ■ Introduction

The Kazakhstan flora is rich in promising poorly-studied plants, which are traditionally used in folk medicine, but their introduction into medical practice requires additional in-depth research using modern scientific methods [1, 2]. *Alfredia nivea* KAR&KIR of the *Asteraceae* family, which is used in folk medicine as a neurotropic agent, is an interesting object for introduction into official medical and pharmaceutical practice in Kazakhstan [3].

*A. nivea* is a perennial plant of 25–70 cm height with leathery, oblong-lanceolate, pinnately lobed leaves. The venation is pinnate, the lateral veins at the ends turn into sharp yellowish spines. The leaf blade is grayish-green on the upper side, whitish-pubescent on the lower side. The inflorescence is a spherical head of pink tubular flowers with a multi-row involucre. The plant blooms in July, fruits ripen in August – September. It grows in the subalpine and alpine belts of the mountains, along the stepped rocky slopes, in spruce-fir forests. It is found in Tarbagatai, Dzungarian, Trans-Ili and Küngöy Ala-Too Range Alatau [4–6]. The plant's raw material reserves are sufficient for the needs of Kazakhstan.

Plants of the *Alfredia* genus are insufficiently studied. Most of the studies are devoted to *A. cernua* L. Thus, extracts of this species have been shown to affect the central nervous system and improve memory [7, 8]. It has also been found

that *A. cernua* extracts have nootropic properties, contribute to the improvement of indicators of orientation-exploratory behavior, the preservation of the passive escape reflex during hypoxic shock, and the increase of physical performance in mice [9, 10]. The most pronounced effect was observed with the use of the *A. cernua* extract obtained with 95% ethanol [10, 11]. It has also been shown that the extract of the *A. nivea* above-ground part in 95% ethanol in the dose of 100 mg kg<sup>-1</sup> restores exploratory behavior and reflex safety after hypoxic trauma [12]. Thus, the *A. nivea* herb is a promising raw material for creating new neurotropic medicines.

Previously, the standardization of the *A. cernua* herb [13], the macroscopic and microscopic study of the *A. nivea* herb were carried out, and its diagnostic signs were determined [14]. These data were taken into account when developing a project of quality control methods for the *A. nivea* herb.

Therefore, the aim of the research was to determine the parameters of the standardization of the *A. nivea* KAR. & KIR. herb.

## ■ Materials and methods

The study objects were samples of the *A. nivea* herb collected in Kungei Alatau, 4.3 km south-east of the Karabulak village, Eastern Karabulak canyon, Almaty Region, Kazakhstan (1762 m above the city, N 43°02'30.2", E 078°34'16.0") July

06, 2021. The identity of the plant was determined by professor Tetiana M. Gontova, D. Sc., National University of Pharmacy (Kharkiv, Ukraine) [4, 15]. Voucher specimens were deposited at the School of Pharmacy, Asfendiyarova Kazakh National Medical University (Almaty, Kazakhstan, No. 432–435). The raw material was dried at room temperature [16, 17] in a well-ventilated area for ten days and stored in paper bags [18, 19].

The macroscopic and microscopic studies of the raw material were performed according to the methodology described in the European Pharmacopoeia (EuPh) 2.8.23 “Microscopic examination of the medicinal plant raw material” [18, 20]. The macroscopic studies were conducted using a magnifying glass and a MBS-9 binocular microscope. The study of the anatomical structure of the *A. nivea* herb was carried out on samples of the whole and cut raw material according to the requirements of the EuPh. The herb was fixed in a mixture of 96% ethanol *R* – glycerin *R* – purified water *R* (1:1:1). The structure of stems and leaves was studied on transverse sections. The epidermal of the organs was considered from the surface according to generally accepted methods [18, 21]. The raw material was crushed according to the requirements of the EuPh monograph 2.9.12 “Sit analysis” and clarified with the help of chloral hydrate *R* [18, 20]. The studies of transverse and longitudinal sections, epidermis and preparations from the surface were carried out using MS Microscopes 10 (oculars X5, X10, X15, lenses x10, x40), Micromed XS-4130 (oculars WF15X, lenses x40/0.65, x10/0.25) with a microphotonozzle (China). The results of the study were recorded using the Canon IXUS 220 HS camera.

To develop the identification method for the main biologically active substances (BAS) in the *A. nivea* herb, the TLC method was used [18, 22]. Merck Silica Gel F254 plates were used for chromatography. Purity of solvents used for the preparation of chromatographic systems were of chemically pure and analytical grades. The ratio of solvents indicated by numbers were taken in volumetric units.

The content of related impurities (2.8.2), the loss on drying (2.2.32), the total ash content (2.4.16) were determined according to the requirements of the EuPh [18, 23, 24].

*Assay of flavonoids.* The assay of flavonoids was determined in accordance with the methodology of the EuPh by the spectrophotometric method calculated with reference to rutin [18, 25].

About 5.0 g of *Alfredia* herb (accurate weight) crushed to the size of particles passing through a sieve with a diameter of 2 mm was placed in a 200 mL ground joint flask, 50 mL of 70% ethanol solution was added. The flask was connected to a condenser and heated on a water bath for 30 min, periodically shaken to wash off particles of the raw material from the walls. The mixture was cooled and filtered through cotton wool, so that the particles of the raw material did not get on the filter. The cotton wool was transferred to the ground joint flask for extraction, and the new portion of the extractant was added. The extraction was repeated twice under the conditions described above, and the extract was filtered in the same flask. The combined extract was evaporated up to  $\frac{1}{4}$  of the initial volume. The evaporated extract was quantitatively transferred to a 50.0 mL measuring flask, cooled and was diluted with 70% ethanol solution to the volume (Solution A).

2.0 mL of Solution A was placed into a measuring 25 mL flask, 2.0 mL of 3% aluminum chloride solution in 96% ethanol *R* was added, the volume was diluted with 70% ethanol solution and mixed.

In 30 min, the solution was filtered through the paper filter, throwing away the first portions of the filtrate, and the optical density was measured on a Specol 1500 spectrophotometer (Switzerland) at a wavelength of 410 nm in a 10 mm cuvette. *Reference solution* contained 2.0 mL of Solution A, diluted with 70% ethanol to the volume in a 25 mL flask.

In parallel, experiment with a *Standard solution* of rutin (pharmacopoeial standard) was carried out in the same conditions. 1.0 mL of 3% aluminum chloride solution was added to 1.0 mL of the *Standard solution* of rutin, and the volume was diluted to 25.0 mL with 70% ethanol. As a reference, 1.0 mL of the *Standard solution* of rutin diluted with 70% ethanol to the volume of 25 mL was used.

The content of flavonoids in the raw material was calculated with reference to rutin (%) by the following equation [28, 29]:

$$X, \% = \frac{A_1 \times a_0 \times 50 \times 1 \times 25 \times 100 \times 100}{A_0 \times a_1 \times 25 \times 2 \times 50 \times (100 - w)} ,$$

where  $A_1$  – is the optical density of the *Test solution*;

$A_0$  – is the optical density of the *Standard solution* of rutin;

$a_1$  – is the accurate weight of raw material, g;

$a_0$  – is the accurate weight of rutin, g;

$w$  – is the loss on drying, %.

*Preparation of the standard solution of rutin.* About 0.01 g (accurate weight) of rutin (pharmacopoeial standard FS 42-2508-87) dried at 135 °C to the constant mass, was placed into a 25.0 mL measuring flask, dissolved in 96% ethanol, diluted with the same solvent to the volume and mixed.

*Preparation of a 3% aluminum chloride solution in 96% ethanol.* According to the State standard 3759-85, 3.0 g of aluminum chloride (chemically pure) was dissolved in 96% ethanol in a 100.0 mL measuring flask, diluted with the same solvent to the volume and mixed.

## ■ Results and discussion

**Source.** The raw material is a dried herb, which includes whole or cut leaves, flowers and stems of *A. nivea* KAR. & KIR. (*Asteraceae*). The herb was collected in summer, the below ground parts were removed, and then the soil was dried to obtain the intact form. Alternatively, the herb was sliced while fresh, and dried immediately to obtain the sliced form of the *A. nivea* herb.

Based on the results of the macroscopic analysis of the *A. nivea* herb [14], such macroscopic signs, which served as the basis for the development of *Identification A*, were determined.

The stem is usually unbranched in the lower part, slightly branched in the upper part, rough, slightly ribbed, 20–60 cm long, 5 mm in diameter. It is externally grayish-green, tomentose-pubescent. The texture is hard. Rosette leaves are 15–35 cm long and 2.5–6.0 cm wide; stem leaves are short-petiolate or sessile, 5.0–7.0 cm long and 1.5–2.5 cm wide, leathery, linear-lanceolate and lanceolate, pinnatipartite, with a pinnate venation with prominent lignified veins and long sharp ends; non-tomentose and green on the adaxial surface and grayish green, abundant tomentose-pubescent on the abaxial surface. The petiole of the rosette leaf is elongated-triangular in outline with elongated “wings” directed upwards at an angle of 45 degrees, narrow at the ends.

The inflorescence is a spherical drooping flower head up to 6.0 cm in diameter with a 3–5-row, tiled involucre made of hard lanceolate, pointed leaflets with filmy fringed-outgrowths on the sides. The tubular pink flowers are 5-tooth, thin, up to 3.0 cm in length; numerous sepals are modified to thin long hairs; stamens and the pistil protrude from the corolla tube; the cypselum is up to 6.0 mm, pale yellowish with variegated brown spots and stripes on the surface.

Based on the results of the microscopic analysis of the *A. nivea* herb [14], such microscopic signs, which served as the basis for the development of *Identification B*, were determined.

The stem and leaves are tomentose-pubescent with covering and rarely glandular trichomes; covering trichomes are of three types – long filamentous hairs with a 2-cell base, large multicellular wide lumen hairs with collapsed cells; and multicellular narrow lumen hairs with collapsed cells; glandular hairs are of 2 types – 1-headed with a 1-celled stalk, and headed with a multicellular stalk and a multicellular head with collapsed cells. The stem is rounded with slightly protruding ribs. The cells of the epidermis are covered with a layer of a folded cuticle; prosenchymatous cells are straight-walled with slightly thickened walls and simple straight pores. The central cylinder is of transitional type. The collenchyma is angular and lacunar; parenchyma cells are collenchymatous; the endoderm is distinct; open collateral bundles are with a well-developed sclerenchyma, xylem vessels are porous and spiral.

Leaf is dorsiventral; the cells of the upper and lower epidermis above the veins are prosenchymatous, straight-walled, with slightly thickened walls and straight pores; between the veins the cells of the upper epidermis are 5–6-angle, isodiametric and on the lower – parenchymal, sinuous-walled, with slightly thickened walls; the stomata are frequent only on the lower epidermis. The stomatal apparatus is anomocytic.

The adaxial surface of the leaf is rarely pubescent with thin long hairs, and abaxial – densely pubescent with filamentous hairs with a 2-cell base and less often multicellular hairs with collapsed cells. The cells of the outer and inner epidermis of the involucre leaflets are elongated, slightly thickened and straight-walled with light brown contents. The inner epidermis is covered with filamentous trichomes. The cells of the petal epidermis are prosenchymatous, thin-walled or heavily thick-walled, straight-walled with colorless, rarely brown contents; the epidermis is covered with a weakly expressed folding cuticle; vessels are thin spiral. The style of the pistil is densely covered with short conical hairs. Pollen grains are rounded, yellow-brown, the structure of ectine is slightly spiny.

**The powdered raw material.** The powder is yellowish-green in color, examined under a microscope using *Chloral hydrate solution R*. The powder shows the following diagnostic signs: fragments of epidermis (Figure 1, A) composed of cells

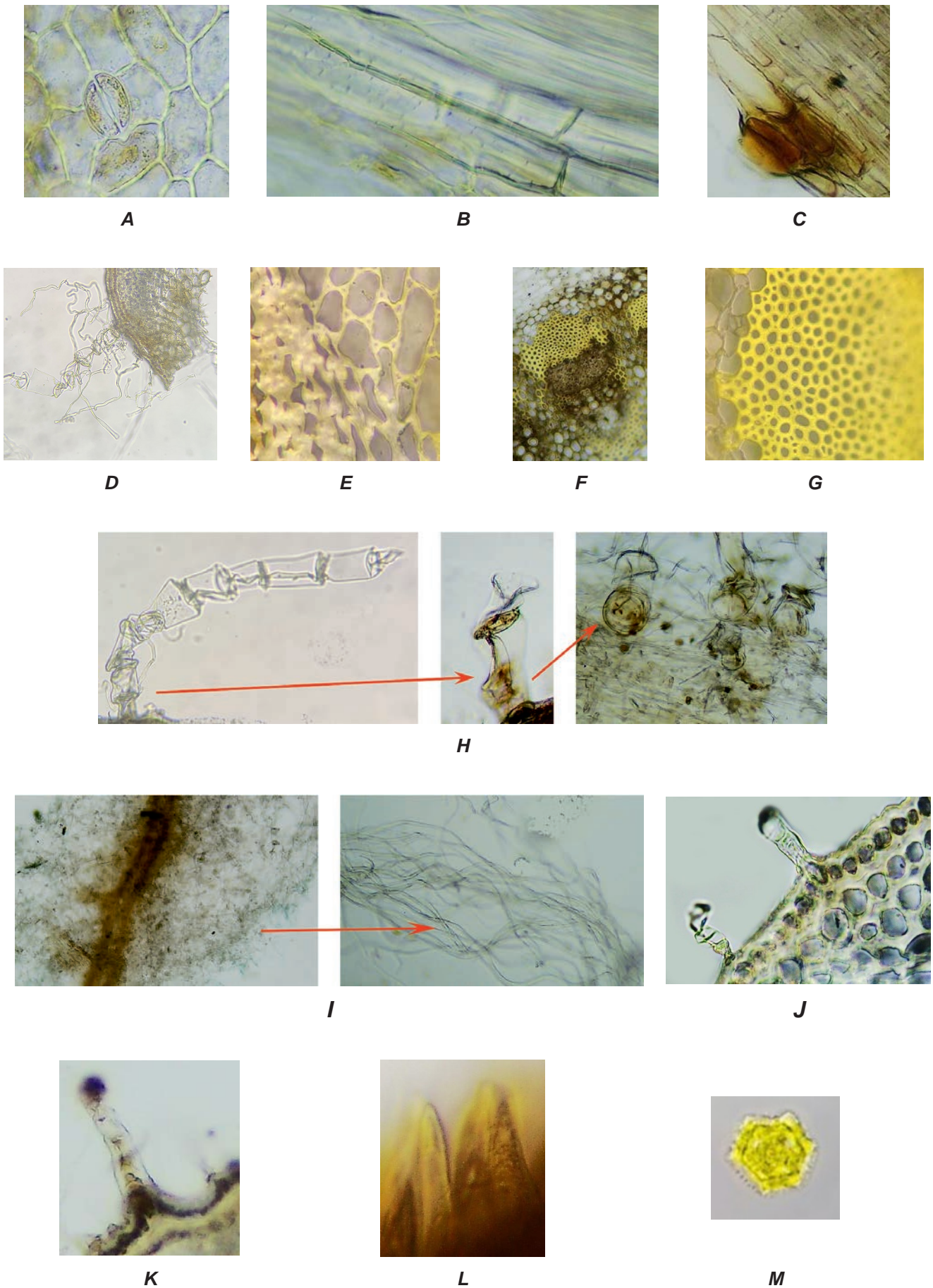


Figure 1. Microscopic features of the powder

with prosenchymatous straight-walled and slightly thick-walled cells with simple straight pores (Figure 1, B); cells with light brown contents (Figure 1, C); stomata of the anomocytic type (Figure 1, A); fragments of the angular and lacunar collenchyma (Figure 1, D); collenchymatous cells of the parenchyma (Figure 1, E); open collateral bundles (Figure 1, F); sclerenchyma (Figure 1, G), porous and spiral vessels; long filamentous hairs with a 2-cell base, large multicellular wide lumen hairs with collapsed cells (Figure 1, H), and multicellular narrow lumen hairs with collapsed cells (Figure 1, I); glandular hairs of 2 types – 1-headed with a 1-celled stalk (Figure 1, J), and headed with a multicellular stalk and a multicellular head with collapsed cells (Figure 1, K); styles with short conical hairs (Figure 1, L); rounded, yellow-brown pollen grains with slightly spiny ectine (Figure 1, M).

**Identification C** of BAS of the *A. nivea* herb was developed using the TLC method with standards of hyperoside, quercetin, rutin and chlorogenic acid in the system: ethylacetate *R* – aqua *R* – formic acid *R* – acetic acid anhydrous *R* (72:14:7:7).

For this analysis, 300 mg of the *Alfredia* herb was extracted with 3 mL of methanol for 30 min at 40 °C on a water bath with ultrasound irradiation. 15 µL of the extract was applied to the chromatogram. The standards were prepared by

dissolving 1 mg of the standards in 10 mL of pure methanol. After spraying the plate with diphenylborinic acid 2-aminoethyl ester *R*, macrogol 400 *R* the zones at the level of quercetin, hyperoside, rutin and chlorogenic acid were detected in UV light [28].

A photo of the sequence of zones on the chromatogram of the *A. nivea* the test extract and the reference solutions are presented in Figure 2. The main substances found in the TLC chromatogram are quercetin, chlorogenic acid, rutin and hyperoside. Other additional fluorescent zones can be found on the chromatogram of the test extract, but they do not play an important role when identifying the raw material. Also, using the chromatogram obtained in the same conditions, after spraying the plate with the Drangendorff reagent [29], it was determined that there were no alkaloids in the raw material.

In the lower part of the chromatogram of the reference solutions, a yellow fluorescent zone corresponding to rutin, as well as the blue fluorescent zone corresponding to chlorogenic acid, and the yellow fluorescent zone corresponding to hyperoside, were found. The yellow fluorescent zone corresponding to quercetin was detected in the upper part of the chromatogram. On the chromatogram of the test extract, the intense fluorescent yellow zone at the level of the reference solution of rutin was detected. At the level of the reference solution of chlorogenic acid the intense blue fluorescent zone was also determined.

Since the zones of rutin and quercetin are most clearly identified and have a significant area during the TLC analysis, it has been noticed that they dominate in the raw material, therefore, the quantitative determination of BAS in the *A. nivea* herb should be carried out by the assay of flavonoids calculated with reference to rutin adapting the methodology of the EuPh [18].

The results of determining related impurities, indicators “loss on drying during drying”, “total ash” and the quantitative content of flavonoids are given in Table.

The tests were proposed to be carried out according to the following indicators: related impurities (2.8.2), namely, stems with a diameter of more than 20 mm – not more than 10%; other impurities – not more than 2%; the loss on drying (2.2.32) – not more than 13.0% (1.000 g of the raw material crushed into a powder at a temperature of 105°C for 2 h); the total ash (2.4.16) – not more than 10%.

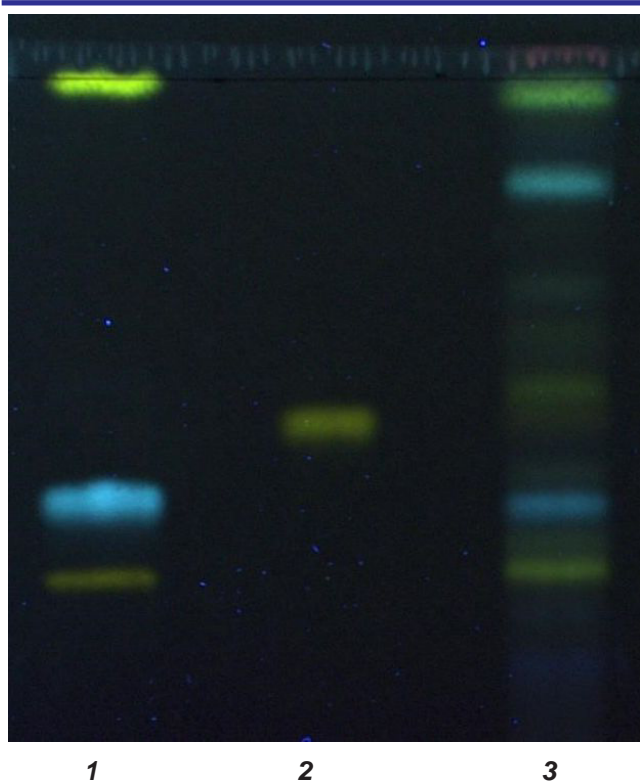


**Figure 2.** The TLC chromatogram of *A. nivea* phenolic compounds: 1. the standards of quercetin, chlorogenic acid, rutin; 2. hyperoside; 3. the *A. nivea* herb extract

**Table.** The results of the analysis of the *A. nivea* herb

Indicators	Standardization	Samples of the raw material					
		1	2	3	4	5	6
Description	According to the parameters developed	+	+	+	+	+	+
Identification A. External signs – macroscopy	According to the parameters developed	+	+	+	+	+	+
Identification B. Anatomical signs – microscopy	According to the parameters developed	+	+	+	+	+	+
Identification C. TLC method	According to the parameters developed	+	+	+	+	+	+
Impurities	Stems with a diameter of more than 20 mm not more than 10%	8.7	6.2	9.6	7.1	8.5	8.0
	Related impurities – not more than 2%	1.5	1.8	1.0	1.5	1.0	0.5
Loss on drying	Not more than 13.0%	8.7	9.3	7.2	9.7	8.5	11.0
Total ash	Not more than 10%	7.2	6.6	8.6	5.3	8.2	8.9
The content of flavonoids calculated with reference to rutin	Not less than 0.5%	0.74	0.69	0.63	0.76	0.60	0.58

Note: «+» – meets the requirements

The assay was proposed to be carried out by the content of flavonoids – at least 0.5% calculated with reference to rutin (C<sub>27</sub>N<sub>30</sub>O<sub>16</sub>; M.M. 610.5) in the dry raw material.

## Conclusions

The parameters of the *A. nivea* herb standardization have been determined on the basis

of the following indicators: macroscopic and microscopic features, TLC identification of the main BAS of the raw material (hyperoside, rutin, quercetin and chlorogenic acid), related impurities (not more than 2%), stems with a diameter of more than 20 mm (not more than 10%), the loss on drying (not more than 13%), the total ash (not more than 10%) and at least 0.5% flavonoids calculated with reference to rutin.

## References

- Zhumashova, G.; Kukula-Koch, W.; Koch, W.; Baj, T.; Sayakova, G.; Shukirbekova, A.; Głowniak, K.; Sakipova, Z. Phytochemical and antioxidant studies on a rare *Rheum cordatum* Losinsk. Species from Kazakhstan. *Oxidative Medicine and Cellular Longevity* **2020**, 2019, Article ID 5465463. <https://doi.org/10.1155/2019/5465463>.
- Sayakova, G.; Boshkayeva, A.; Ibadullayeva, G.; Khamitova, A.; Begimova, G. Actual prospects of using some types of larch growing in Kazakhstan in medicine. *Journal of medicine and life* **2022**, 15 (8), 1038–1046. <https://doi.org/10.25122/jml-2021-0373>.
- Kiyekbayeva, L. N.; Datkhayev, U. M.; Derbisbekova, U. B.; Akhtaeva, N. C.; Litvinenko, Y. A. Phytochemical investigation and technology production of alkaloids in the Kazakh endemic plant *Echinops albicaulis* Kar. Et Kir. (Asteraceae). *International Journal of Green Pharmacy* **2017**, 11 (2, Suppl. issue), S312–S319. <https://doi.org/10.22377/ijgp.v11i02.1041>.
- Catalogue of Life China: 2022 Annual Checklist, Beijing, China. <http://www.gbifchina.org.cn/resource?r=species2000-2022-annual#anchor-citation> (accessed January 17, 2023).
- Novozhilova, E. V.; Boyko, E. V. Morphological and anatomical structure of the cypselas of *Alfredia* (Asteraceae: Cardueae). *Turczaninowia* **2019**, 22 (4), 42–56.
- Korneyev, S. V. Revision of species of the genus *Tephritis* Latreille 1804 (Diptera: Tephritidae) with entire apical spot. *Zootaxa* **2013**, 3620 (1), 067–088. <http://dx.doi.org/10.11646/zootaxa.3620.1.3>.
- Shilova, I. V.; Kuvacheva, N. V.; Kolmakova, A. A.; Losev, V. N.; Minakova, M. Y. Biologically Active Substances in the Aqueous Fraction of *Alfredia cernua* (L.) Cass. Extract Possessing Antiamnesic Properties. *Pharm. Chem. J.* **2021**, 54 (12), 1239–1242. <https://doi.org/10.1007/s11094-021-02349-5>.
- Shilova, I. V.; Baranovskaja, N. V.; Mustafin, R. N.; Suslov, N. I. Features of the composition macro elements and trace elements of the extract of *Alfredia cernua* (L.) Cass., possessing psychotropic effect. *Khimiya Rastitel'nogo Syr'ya* **2019**, 4, 191–198. <https://doi.org/10.14258/jcprm.2019045422>.
- Shilova, I. V.; Kukina, T. P.; Suslov, N. I.; Sal'nikova, O. I.; Mustafin, R. N. Studies of the Lipophilic Components of a Dense Extract of the Herb *Alfredia cernua* and its Nootropic Properties. *Pharm. Chem. J.* **2014**, 48 (3), 181–185. <https://doi.org/10.1007/s11094-014-1074-y>.
- Mustafin, R. N.; Suslov, N. I.; Shilova, I. V.; Kuvacheva, N. V. Influence of *Alfredia cernua* extracts on the behavior, memory, and physical work capacity of experimental animals. *Ekspiermental'naya i klinicheskaya farmakologiya* **2010**, 73 (1), 16–19.
- Mustafin, R. N.; Shilova, I. V.; Suslov, N. I.; Kuvacheva, N. V.; Amelchenko, V. P. Nootropic Activity of Extracts from Wild and Cultivated *Alfredia cernua*. *Bulletin of Experimental Biology and Medicine* **2011**, 150 (3), 333–335. <https://doi.org/10.1007/s10517-011-1135-0>.
- Shilova, I. V.; Suslov, N. I. Nejiroprotektornaya aktivnost biologicheskii aktivnykh veshestv *Alfredia nivea* [Neuroprotective activity of biologically active substances from *Alfredia nivea*, in Russian]. In *The role of metabolomics in the improvement of biotechnological means of production*, Proceedings of the 2<sup>nd</sup> International scientific conference, June 06–07, 2019, 223–227.

13. Kuvacheva, N. V.; Shilova, I. V. Standardizaciya travy alfredii ponikshej [Standardization of the herb *Alfredia cernua*, in Russian]. *Voprosy biologicheskoy, medicinskoj i farmacevticheskoy himii* **2011**, *5*, 9–12.
14. Rustemkulov, A.; Gontova, T.; Makhatova, B.; Rustemkulova, A.; Gemedzhieva, N.; Shormanova, A.; Starchenko, G.; Raal, A.; Datkhaev, U.; Koshovyi, O. Macro and microscopic analysis of *Alfredia nivea* KAR. & KIR herb. *ScienceRise: Pharmaceutical Science* **2023**, *1*, 41–49. <https://doi.org/10.15587/2519-4852.2023.274766>.
15. Baitenov, M. S. *Flora Kazakhstana. Illyustrirovannyj opredelitel rodov i semejstv* (Tom 1) [Kazakhstan flora. Illustrated guide to genera and families (Vol. 1), in Russian]. Almaty, 1999.
16. Shynkovenko, I. L.; Ilyina, T. V.; Kovalyova, A. M.; Goryacha, O. V.; Golembiovskaya, O. I.; Koshovyi, O. M. Saponins of the extracts of *Galium aparine* and *Galium verum*. *News of Pharmacy* **2018**, *4*, 16–23. <https://doi.org/10.24959/nphj.18.2225>.
17. Vlasova, I. K.; Koshovyi, O. M. Standardization of dry extracts from large cranberry leaves. *Journal of organic and pharmaceutical chemistry* **2022**, *20* (3), 40–45. <https://doi.org/10.24959/ophcj.22.265845>.
18. European Pharmacopoeia. 10th Ed. Council of Europe, Strasbourg. **2019**.
19. Shanaida, M.; Hudz, N.; Korzeniowska, K.; Wieczorek, P. Antioxidant activity of essential oils obtained from aerial part of some *Lamiaceae* species. *International Journal of Green Pharmacy* **2018**, *12* (3), 200–204. <https://doi.org/10.22377/ijgp.v12i03.1952>.
20. Vlasova, I.; Gontova, T.; Grytsyk, L. et al. Determination of standardization parameters of *Oxycoccus macrocarpus* (Ait.) Pursh and *Oxycoccus palustris* Pers. Leaves. *ScienceRise: Pharmaceutical Science* **2022**, *3*, 48–57. <http://doi.org/10.15587/2519-4852.2022.260352>.
21. Kiyekbayeva, L. N.; Akhtaeva, N. Z.; Datkhayev, U. M.; Omarkhan, A. B.; Litvinenko, Y. A.; Tynybekov, B. M.; Berkenov, A. K. Pharmacognosy signs of aerial parts medicinal plant *Echinops albicaulis* KAR. & KIR. *Asian Journal of Pharmaceutical and Clinical Research* **2017**, *10* (6), 346–348. <https://doi.org/10.22159/ajpcr.2017.v10i6.18037>.
22. Koshovyi, O.; Romanenko Ye.; Komissarenko A. The study of the phenolic composition of the dry extract of motherwort herb and its psychotropic activity. *American Journal of Science and Technologies* **2016**, *3* (1), 1055–1059.
23. Krivoruchko, E.; Markin, A.; Samoilo, V.; Ilyina, T.; Koshovyi, O. Research in the chemical composition of the bark of *Sorbus aucuparia*. *Ceska a Slovenska farmacie: casopis Ceske farmaceuticke spolocnosti a Slovenske farmaceuticke spolocnosti* **2018**, *67* (3), 113–115.
24. Myha, M.; Koshovyi, O.; Gamulya, O.; Ilyina, T.; Borodina, N.; Vlasova, I. Phytochemical study of *Salvia grandiflora* and *Salvia officinalis* leaves for establishing prospects for use in medical and pharmaceutical practice. *ScienceRise: Pharmaceutical Science* **2020**, *1*, 23–28. <https://doi.org/10.15587/2519-4852.2020.197299>.
25. Koshovyi, O.; Granica, S.; Piwowarski, J.P.; Stremoukhov, O.; Kostenko, Y.; Kravchenko, G.; Krasilnikova, O.; Zagayko, A. Highbush Blueberry (*Vaccinium corymbosum* L.) Leaves Extract and Its Modified Arginine Preparation for the Management of Metabolic Syndrome—Chemical Analysis and Bioactivity in Rat Model. *Nutrients* **2021**, *13*, 2870. <https://doi.org/10.3390/nu13082870>.
26. Chaika, N.; Koshovyi, O.; Ain, R.; Kireyev, I.; Zupanets, A.; Odyntsova, V. Phytochemical profile and pharmacological activity of the dry extract from *Arctostaphylos uva-ursi* leaves modified with phenylalanine. *ScienceRise: Pharmaceutical Science* **2020**, *6*, 74–84. <https://doi.org/10.15587/2519-4852.2020.222511>.
27. Shynkovenko, I. L.; Kashpur, N. V.; Ilyina, T. V.; Kovalyova, A. M.; Goryacha, O. V.; Koshovyi, O. M.; Toryanyk, E. L.; Kryvoruchko, O. V. The immunomodulatory activity of the extracts and complexes of biologically active compounds of *Galium verum* L. herb. *Ceska a Slovenska farmacie: casopis Ceske farmaceuticke spolocnosti a Slovenske farmaceuticke spolocnosti* **2018**, *67* (1), 25–29.
28. Koshovyi, O. M. Fenolnyi sklad deiakykh predstavnykiv pidrodu *Sclarea* rodu *Salvia* [Phenolic composition of some representatives of the subgenus *Sclarea* of the genus *Salvia*, in Ukrainian]. *Current issues in pharmacy and medicine: science and practice* **2012**, *3*, 11–14.
29. Raal, A.; Meos, A.; Hinrikus, T.; Heinämäki, J.; Romäne, E.; Gudienė, V.; Jaktas, V.; Koshovyi, O.; Kovaleva, A.; Fursenco, C.; Chiru, T.; Nguyen, H. T. Dragendorff's reagent: Historical perspectives and current status of a versatile reagent introduced over 150 years ago at the University of Dorpat, Tartu, Estonia. *Die Pharmazie – An International Journal of Pharmaceutical Sciences* **2020**, *75* (7), 299–306. <https://doi.org/10.1691/ph.2020.0438>.

#### Information about the authors:

**Almat G. Rustemkulov**, Postgraduate Student of the “Pharmaceutical Production Technology” Program, Asfendiyarov Kazakh National Medical University; <https://orcid.org/0000-0002-1792-9399>; e-mail: arustemkulov@gmail.com.

**Tetiana M. Gontova**, D.Sc. in Pharmacy, Professor of the Pharmacognosy Department, National University of Pharmacy of the Ministry of Health of Ukraine; <https://orcid.org/0000-0003-3941-9127>; e-mail: tetianaviola@ukr.net.

**Balzhhan G. Makhatova**, Postgraduate Student, Associate Professor of Engineering Disciplines and Good Practices Department, Asfendiyarov Kazakh National Medical University; <https://orcid.org/0000-0002-0206-0416>; e-mail: makhatova.b@kaznmu.kz.

**Aisana E. Rustemkulova**, Postgraduate Student of the “Pharmaceutical Production Technology” Program, Asfendiyarov Kazakh National Medical University; <https://orcid.org/0000-0003-2363-7576>; e-mail: rustemkulova.a@gmail.com.

**Ubaidilla M. Datkhaev**, D.Sc. in Pharmacy, Professor, Vice-Rector for Corporate Development, Asfendiyarov Kazakh National Medical University; <https://orcid.org/0000-0002-2322-220X>.

**Oleh M. Koshovyi** (corresponding author), D.Sc. in Pharmacy, Professor of the Pharmacognosy Department, National University of Pharmacy of the Ministry of Health of Ukraine; <https://orcid.org/0000-0001-9545-8548>; e-mail for correspondence: oled.koshovyi@gmail.com.

UDC 54.057:615

M. M. Suleiman<sup>1</sup>, A. I. Fedosov<sup>1</sup>, R. K. Mohapatra<sup>2</sup>, I. A. Sych<sup>1</sup>, L. O. Grinevich<sup>1</sup>,  
N. P. Kobzar<sup>1</sup>, V. D. Yaremenko<sup>1</sup>, L. O. Perekhoda<sup>1</sup><sup>1</sup> National University of Pharmacy of the Ministry of Health of Ukraine,  
53 Pushkinska str., 61002 Kharkiv, Ukraine<sup>2</sup> Government College of Engineering, Keonjhar, 758002 Orissa, India

## The Search for Potential SARS-CoV-2 Inhibitors Using the *In Silico* Research

### Abstract

**Aim.** Using *in silico* technologies to search for potential SARS-CoV-2 inhibitors among novel tetracyclic ring systems, which are the common core of Crinipellin.

**Materials and methods.** The study object was new compounds previously synthesized *via* oxidative dearomatization of Crinipellin A. The method of the flexible molecular docking was applied in the study.

**Results and discussion.** Using the molecular docking, the affinity of five compounds for the receptor-ACE2 SARS-CoV-2 (PDB ID: 7DF4), a spike protein SARS-CoV-2 (PDB ID: 1WNC), a PL protein SARS-CoV-2 (PDB ID: 7CJD) and a reverse transcriptase enzyme SARS-CoV-2 (PDB ID: 6YYT) was studied. The results of the molecular docking obtained suggest that 8,8-dimethyl-5-(phenylsulfonyl)-3,3a,4,5,8,9-hexahydroindeno[3a,4-b]furan-2(7H)-one may be a potential SARS-CoV-2 inhibitor; it is the basis for its further experimental pharmacological study.

**Conclusions.** The study constitutes one of the stages of searching for SARS-CoV-2 inhibitors. According to the results obtained, a way to search for potential SARS-CoV-2 inhibitors based on Crinipellin A derivatives was proposed. Using the most promising compound with hexahydroindeno[3a,4-b]furan core further studies open up another direction for searching for compounds of SARS-CoV-2 inhibitors and will save time and laboratory animals while conducting targeted experimental research.

**Keywords:** COVID-19 virus; Crinipellin A; flexible molecular docking; SARS-CoV-2 inhibitor

M. M. Сулейман<sup>1</sup>, А. І. Федосов<sup>1</sup>, Р. К. Мохapatра<sup>2</sup>, І. А. Сич<sup>1</sup>, Л. О. Гринеvич<sup>1</sup>,  
Н. П. Кобзар<sup>1</sup>, В. Д. Яременко<sup>1</sup>, Л. О. Перехода<sup>1</sup><sup>1</sup> Національний фармацевтичний університет Міністерства охорони здоров'я України,  
вул. Пушкінська, 53, м. Харків, 61002, Україна<sup>2</sup> Державний інженерний коледж, Кеонджхар, Орісса 758002, Індія

### Пошук потенційних інгібіторів SARS-CoV-2 за допомогою *in silico* методів

#### Анотація

**Мета роботи.** За використання *in silico* технологій здійснити пошук потенційних інгібіторів SARS-CoV-2 серед нових тетрациклічних кільцевих систем, які є загальним ядром криніпеліну.

**Матеріали та методи.** Об'єктом дослідження є п'ять нових сполук, одержаних шляхом деароматизації криніпеліну А і синтезованих у попередніх дослідженнях. В *in silico* дослідженнях використано метод гнучкого молекулярного докінгу.

**Результати та їх обговорення.** Шляхом використання докінгових досліджень вивчено афінитет п'яти сполук до рецептора ACE2 SARS-CoV-2 (PDB ID: 7DF4), spike протеїну SARS-CoV-2 (PDB ID: 1WNC), PL протеїну SARS-CoV-2 (PDB ID: 7CJD) та ферменту зворотної транскриптази SARS-CoV-2 (PDB ID: 6YYT). Одержані результати докінгових досліджень дозволяють стверджувати, що 8,8-диметил-5-(фенілсульфоніл)-3,3a,4,5,8,9-гексагідроіндено[3a,4-b]фуран-2(7H)-он може бути потенційним інгібітором SARS-CoV-2, що є підставою для його подальшого експериментального фармакологічного вивчення.

**Висновки.** Подане дослідження є одним з етапів пошуку інгібіторів SARS-CoV-2. З огляду на одержані результати запропоновано шлях пошуку потенційних інгібіторів SARS-CoV-2 на основі похідних криніпеліну А. Подальші дослідження з використанням найбільш перспективної похідної гексагідроіндено[3a,4-b]фурану відкривають ще один напрям пошуку сполук інгібіторів SARS-CoV-2 та дають можливість заощадити час і лабораторних тварин у межах виконання цілеспрямованих експериментальних досліджень у майбутньому.

**Ключові слова:** COVID-19 вірус; криніпелін А; гнучкий молекулярний докінг; інгібітор SARS-CoV-2

**Citation:** Suleiman, M. M.; Fedosov, A. I.; Mohapatra, R. K.; Sych, I. A.; Grinevich, L. O.; Kobzar, N. P.; Yaremenko, V. D.; Perekhoda, L. O. The Search for Potential SARS-CoV-2 Inhibitors Using the *In Silico* Research. *Journal of Organic and Pharmaceutical Chemistry* 2023, 21 (1), 54–60.

<https://doi.org/10.24959/ophcj.23.276412>

**Received:** 14 January 2023; **Revised:** 5 March 2023; **Accepted:** 9 March 2023

**Copyright** © 2023, M. M. Suleiman, A. I. Fedosov, R. K. Mohapatra, I. A. Sych, L. O. Grinevich, N. P. Kobzar, V. D. Yaremenko, L. O. Perekhoda. This is an open access article under the CC BY license (<http://creativecommons.org/licenses/by/4.0>).

**Funding:** The authors received no specific funding for this work.

**Conflict of interests:** The authors have no conflict of interests to declare.

## ■ Introduction

Currently, there is no drug that is effective in various forms of the new coronavirus, severe acute respiratory syndrome, coronavirus 2 (SARS-CoV-2). Since there is no efficient approved treatment or SARS-CoV-2 inhibitor drugs, the computational strategy is a promising way and plays a significant role in the pharmaceutical industry for the discovery of new drugs [1].

This work is one of the stages of searching for effective SARS-CoV-2 inhibitors. In this study, we examined five compounds previously synthesized and tested their binding affinity for the human receptor SARS-CoV-2 – ACE2 (PDB ID: 7DF4), a spike protein SARS-CoV-2 (PDB ID: 1WNC), a PL protein SARS-CoV-2 (PDB ID: 7CJD), a reverse transcriptase SARS-CoV-2 (PDB ID: 6YYT) using the molecular docking research.

## ■ Materials and methods

Continuing the work in the direction of searching for new antiviral drugs, scientists have synthesized new compounds based on the common core of Crinipellin A *via* oxidative dearomatization [2]. The structures of the test compounds are shown in Figure 1.

The target compounds were designed by chemical modification of the common core of Crinipellin A in such a way that the drug could exhibit the high activity and bioavailability, as well as the low toxicity. The results of predicting their antimicrobial, antiviral, antitumor, antifungal and anti-inflammatory activity and a good pharmacokinetic profile have been confirmed by the data provided by the authors in the article [3].

Ligands were prepared using the MGL Tools 1.5.6 program. The ligand optimization was performed using the Avogadro program.

The analysis of literature data shows that it is the S protein after binding to the ACE2 receptor that determines the penetration of the virus into the cell. This fact indicates that S protein is the main factor in the pathogenesis of COVID-19;

therefore, it is promising for the development *in silico* of specific ligands that can be used as SARS-CoV-2 inhibitors [4–7].

SARS-S engages angiotensin-converting enzyme 2 (ACE2) as the entry receptor and employs the cellular serine protease TMPRSS2 for S protein priming. The SARS-S/ACE2 interface has been elucidated at the atomic level, and it has been found that the efficiency of using ACE2 is a key determining the SARS-CoV transmissibility [8, 9]. The papain-like protease (PLpro) of type 2 coronavirus with a severe acute respiratory syndrome (SARS-CoV-2) plays an essential role in virus replication and immune evasion, representing an attractive drug target. Considering that the PLpro proteases of SARS-CoV-2 and SARS-CoV

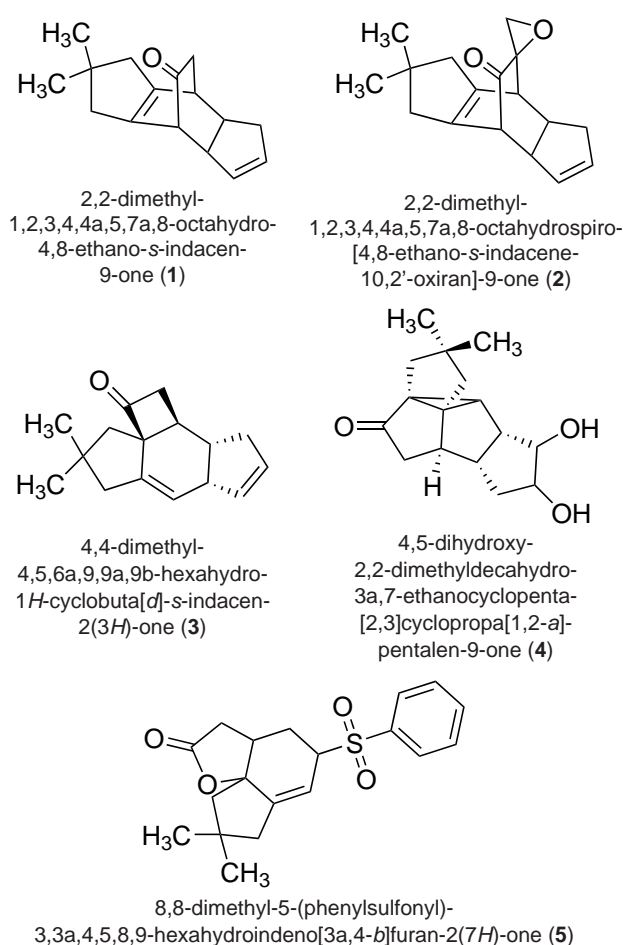


**Figure 1.** The structural formulas of test compounds

have significant homology, the PL<sub>pro</sub> inhibitor developed for SARS-CoV is a promising starting point for therapeutic development [10]. The SARS-CoV-2 uses an RNA-dependent RNA polymerase (RdRp) to replicate its genome and transcribe its genes. Therefore, we use the SARS-CoV-2 reverse transcriptase structure in an active form that mimics a replicating enzyme [11].

In the present study, to carry out the docking studies, active macromolecules centers of the human receptor-ACE2 (PDB ID proteins: 7DF4), a spike protein SARS-CoV-2 (PDB ID: 1WNC), a PL protein SARS-CoV-2 (PDB ID: 7CJD), reverse transcriptase SARS-CoV-2 (PDB ID: 6YYT) domains were chosen as biological targets for the antivirus activity from the Protein Data Bank (PDB) [12]. The receptor maps were made in MGL Tools and AutoGrid programs. Water molecules, ions, and the ligand were removed from the PDB file ID: 7DF4, 1WNC, 7CJD, 6YYT.

For the receptor-oriented flexible docking the Autodock 4.2 software package was used. To perform calculations in the Autodock 4.2 program the output formats of the receptor and ligand data were converted to a special PDBQT format. In our previous studies, a similar software package and docking parameters were used [12].

The following docking parameters were determined: the maximum RMS tolerance for the conformational cluster analysis – 2 Å; the free energy coefficient for torsional degrees of freedom – 0.2983; the cluster tolerance – 2 Å; the external grid energy – 1000; the maximum initial energy – 0; the maximum number of retries – 10000; the number of individuals in the population – 150; the maximum number of energy evaluations – 2500000; the maximum number of generations – 27000; the number of top individuals to survive to the next generation – 1; the rate of gene mutation – 0.02; the rate of crossover – 0.8; the crossover mode – arithmetic;

the  $\alpha$ -parameter of Gauss distribution – 0; the  $\beta$ -parameter of Gauss distribution – 1.

The visual analysis of complexes of substances in the active center of the human receptor-ACE2 (PDB ID: 7DF4), a spike protein SARS-CoV-2 (PDB ID: 1WNC), a PL protein SARS-CoV-2 (PDB ID: 7CJD), a reverse transcriptase SARS-CoV-2 (PDB ID: 6YYT) was performed using the Discovery Studio Visualizer program.

## ■ Results and discussion

Based on the results of the molecular docking we calculated the scoring function indicating the enthalpy contribution to the value of the free binding energy (Affinity DG) for the best conformation positions; the values of the free binding energy and binding constants (Edoc (kcal mol<sup>-1</sup>) and Ki ( $\mu$ M micromolar/ mM millimolar) for a definite conformational position of the ligand. It allowed us to evaluate the stability of complexes formed between ligands and the corresponding targets (Table 1).

The inhibitory activity of the test molecules in relation to the biotargets selected can be exhibited by the formation of complexes between them; their stability is provided mainly due to the energetically favorable geometric arrangement of ligands in the active site, as well as the formation of hydrogen bonds, and intermolecular electrostatic and donor-acceptor interactions between them. As a consequence, the thermodynamic probability of this binding is confirmed by negative values of the Affinity DG scoring function (kcal mol<sup>-1</sup>), the calculated values of the free binding energy Edoc (kcal mol<sup>-1</sup>), and binding constants Ki ( $\mu$ M).

Hence, further experimental studies are required. The formation of intermolecular interactions, negative values of scoring functions, free binding energy and the calculated binding constants

**Table 1.** The values of Affinity DG, free binding energy, and binding coefficients for the best conformational positions of the test compounds combined with biotargets (PDB ID: 7DF4, 1WNC, 7CJD, 6YYT)

Molecule	7DF4			1WNC			7CJD			6YYT		
	Affinity DG, kcal mol <sup>-1</sup>	Edoc kcal mol <sup>-1</sup>	Ki $\mu$ M micromolar / mM millimolar	Affinity DG, kcal mol <sup>-1</sup>	Edoc kcal mol <sup>-1</sup>	Ki $\mu$ M micromolar / mM millimolar	Affinity DG, kcal mol <sup>-1</sup>	Edoc kcal mol <sup>-1</sup>	Ki $\mu$ M micromolar / mM millimolar	Affinity DG, kcal mol <sup>-1</sup>	Edoc kcal mol <sup>-1</sup>	Ki $\mu$ M micromolar / mM millimolar
1	-6.9	-5.37	115.63 $\mu$ M	-5.3	-3.70	1.93 mM	-6.1	-5.74	61.84 $\mu$ M	-7.0	-5.45	100.60 $\mu$ M
2	-6.8	-5.66	70.61 $\mu$ M	-5.1	-3.91	1.36 mM	-7.4	-5.26	139.54 $\mu$ M	-7.1	-5.13	174.21 $\mu$ M
3	-7.2	-6.24	26.82 $\mu$ M	-5.6	-4.78	312.46 $\mu$ M	-7.1	-6.71	12.13 $\mu$ M	-7.5	-6.18	29.61 $\mu$ M
4	-8.3	-6.08	34.89 $\mu$ M	-5.9	-4.64	399.57 $\mu$ M	-6.9	-6.13	31.88 $\mu$ M	-7.5	-5.79	56.83 $\mu$ M
5	-8.2	-7.00	7.37 $\mu$ M	-6.2	-5.08	188.85 $\mu$ M	-7.0	-6.54	16.10 $\mu$ M	-7.8	-6.84	9.61 $\mu$ M

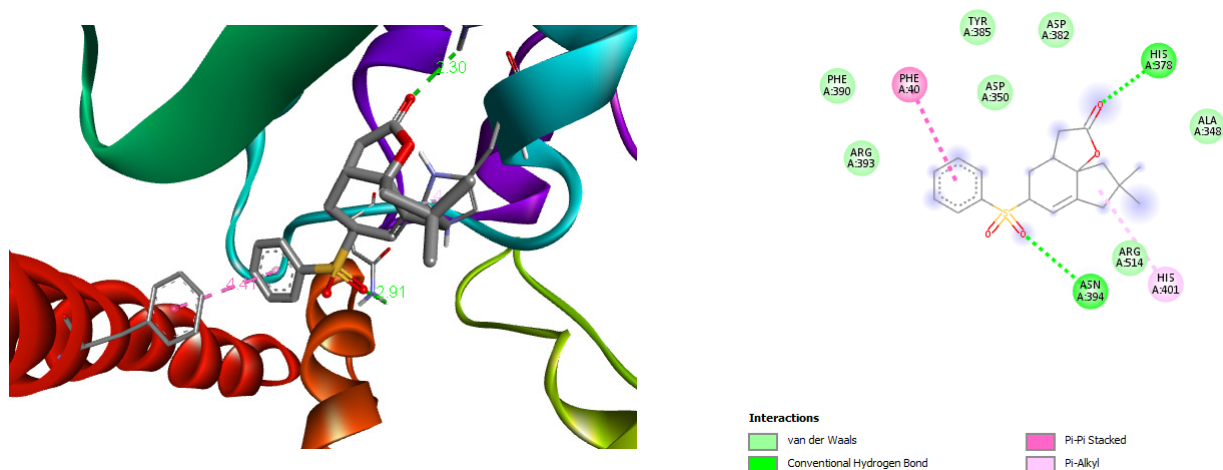


**Figure 2.** The superposition of molecule **5** and a diagram of intermolecular interactions in the complex with the human receptor-ACE2 (PDB ID: 7DF4)

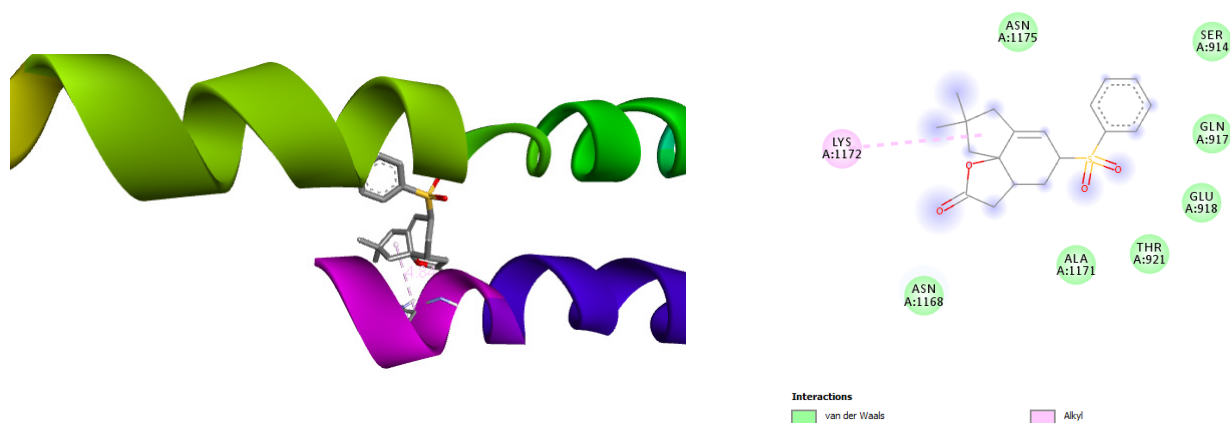


**Figure 3.** The superposition of molecule **5** and a diagram of intermolecular interactions in the complex with a spike protein SARS-CoV-2 (PDB ID: 1WNC)

have confirmed that the compounds studied have a significant affinity for the specified biotargets.

As can be seen from the results, molecule **5**, which has the best indicators in relation to all targets selected, is the leader among the compounds under research (the human receptor – ACE2 PDB ID: 7DF4 (Affinity DG = -8.2 kcal mol<sup>-1</sup>, Edoc = -7.00, Ki = 7.37 μM), a spike protein SARS-CoV-2 PDB ID: 1WNC (Affinity DG = -6.2 kcal mol<sup>-1</sup>, Edoc = -5.08, Ki = 188.85 μM), a PL protein SARS-CoV-2 PDB ID: 7CJD (Affinity DG = -7.0 kcal mol<sup>-1</sup>, Edoc = -6.54, Ki = 16.10 μM), a reverse transcriptase SARS-CoV-2 PDB ID: 6YYT (Affinity DG = -7.8 kcal mol<sup>-1</sup>, Edoc = -6.84, Ki = 9.61 μM)) (Table 1).

For hit compound **5**, a detailed analysis of the geometric location in the active sites of the corresponding targets was performed. This will provide a complete understanding of which fragments of the molecule are involved in binding to biotargets, and will allow giving clear

recommendations for the rational design of future candidates.

Molecule **5** with the human receptor-ACE2 PDB ID: 7DF4 forms a complex due to hydrogen bonds between the oxygen atoms of the sulfonyl group and the carbonyl oxygen of oxolan-2-one with residues of His378 and Asn394 amino acids. Additionally, the complex of the π-π, π-Alk interactions occurring between the phenyl residue and the cyclopentane fragment of the molecule with Phe40 and His401, respectively, is stabilized (Figure 2).

The active molecule complex with a spike protein SARS-CoV-2 PDB ID: 1WNC is formed in the presence of the Alk intermolecular interaction between the cyclopentane fragment of the molecule and the Lys1172, Val1171 lysine residue (Figure 3).

The complex with a PL protein SARS-CoV-2 PDB ID: 7CJD is formed by the participation of a hydrogen bond and the Alk intermolecular

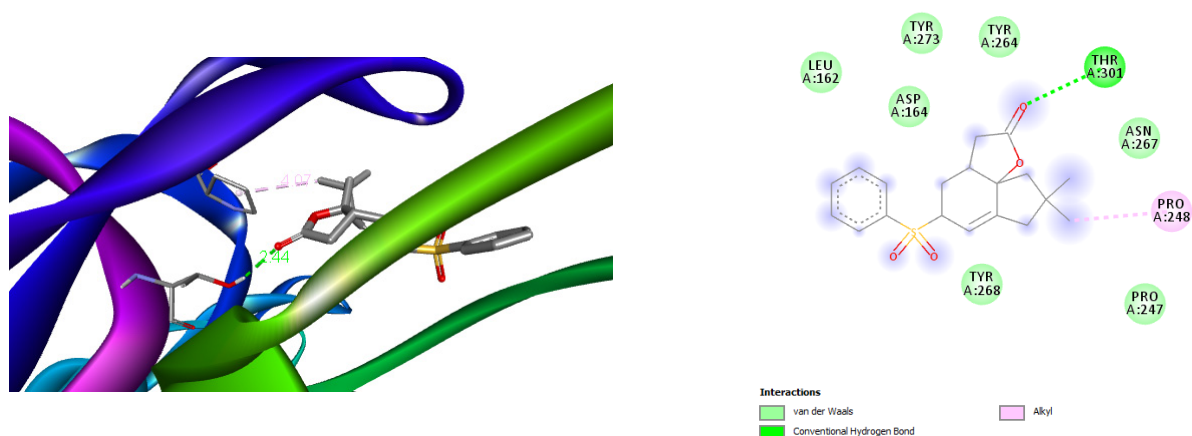


**Figure 4.** The superposition of molecule **5** and a diagram of intermolecular interactions in the complex with a PL protein SARS-CoV-2 PDB ID: 7CJD

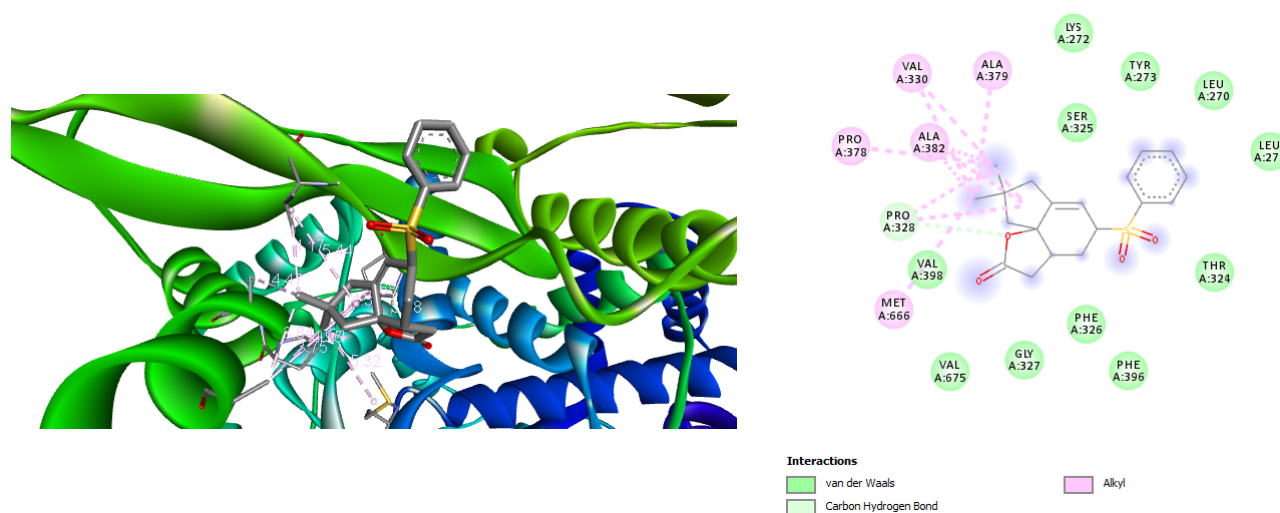


**Figure 5.** The superposition of molecule **5** and a diagram of intermolecular interactions in the complex with a reverse transcriptase SARS-CoV-2 (PDB ID: 6YYT)

interaction between the carbonyl oxygen atom of oxolan-2-one and the metal substitute with the Thr301 and Pro248 threonine residues, respectively (Figure 4).

Molecule **5** forms a hydrogen bond with the Pro328 proline residue due to the oxygen atom of the oxolan-2-one fragment in the active site of a reverse transcriptase SARS-CoV-2 PDB ID: 6YYT. The stabilization of the complex is provided by Alk interactions with the Pro328, Pro378, Met666, Val330, Ala382, Ala379 residues (Figure 5).

The values of interatomic distances in active sites between fragments of molecule **5** and amino acid residues shown in the diagrams (Figures 2–5), categories and types of intermolecular interactions are given in Table 2.

Among all the molecules tested, compound **5** has the best affinity for biotargets (PDB ID: 7DF4, 1WNC, 7CJD, 6YYT). This is evidenced by the formation of a number of intermolecular

interactions between them, the negative values of scoring functions, the free binding energy, and the calculated values of binding constants.

The final stage of molecular docking results is to provide certain recommendations for the rational design of future drug candidates. These recommendations can be provided on the basis of the results of the calculated evaluation functions obtained and a detailed analysis of the geometric location of the tested ligands in the active site of the target. This approach of using docking data provides information on the participation in the creation of appropriate intermolecular contacts of certain atoms, pharmacophore groups, functional groups of the test compounds with amino acid residues of the site. The binding energy of each individual contact is included in the total free energy of binding, which is the main marker for predicting the affinity for a specific target.

**Table 2.** The values of interatomic distances, categories and types of intermolecular interactions of molecule 16 in active biotarget sites (PDB ID: 7DF4, 1WNC, 7CID, 6YYT)

7DF4			1WNC			7CID			6YYT		
Distance, Å	Category	Types	Distance, Å	Category	Types	Distance, Å	Category	Types	Distance, Å	Category	Types
2.30	Hydrogen Bond	Conventional Hydrogen Bond				2.44	Hydrogen Bond	Conventional Hydrogen Bond	3.68	Hydrogen Bond	Carbon Hydrogen Bond
2.91	Hydrogen Bond	Conventional Hydrogen Bond							4.68	Hydrophobic	Alkyl
4.41	Hydrophobic	$\pi$ - $\pi$ Stacked							5.44	Hydrophobic	Alkyl
									4.47	Hydrophobic	Alkyl
									4.95	Hydrophobic	Alkyl
									3.84	Hydrophobic	Alkyl
4.66	Hydrophobic	Pi-Alkyl	4.84	Hydrophobic	Alkyl	4.07	Hydrophobic	Alkyl	3.7484	Hydrophobic	Alkyl
									4.17	Hydrophobic	Alkyl
									4.34	Hydrophobic	Alkyl
									4.54	Hydrophobic	Alkyl
									5.32	Hydrophobic	Alkyl

Using the results of calculation obtained and visualization of molecular docking, it is possible to provide recommendations for the rational designing of future SARS-CoV-2 inhibitors, namely:

- creation of basic rigid systems using the example of tetracyclic ring frameworks;
- saturation of such a system with hydrogen acceptors, in particular oxygen- and sulfur-containing groups in the form of carbonyl fragments, sulfonyl and hydroxyl groups, that enables the formation of intermolecular donor-acceptor interactions with amino acid residues of the active center;

## References

1. Mohapatra, R. K.; Pintilie, L.; Kandi, V.; Sarangi, A. K.; Das, D.; Sahu, R.; Perekhoda, L. The recent challenges of highly contagious COVID-19, causing respiratory infections: Symptoms, diagnosis, transmission, possible vaccines, animal models, and immunotherapy. *Chemical Biology & Drug Design* **2020**, *96* (5), 1187–1208. <https://doi.org/10.1111/cbdd.13761>.
2. Sahu, R.; Mohapatra, R. K.; Al-Resayes, S. I.; Das, D.; Parhi, P. K.; Pintilie, L.; Azam, M. An Efficient Synthesis Towards the Core of Crinipellin and Alliacol-B Along With Their Docking Studies. *Preprints.org* **2020**, 2020120206. <https://doi.org/10.20944/preprints202012.0206.v1>.
3. Mohapatra, R. K.; Perekhoda, L.; Azam, M.; Suleiman, M.; Sarangi, A. K.; Semenets, A.; Pintilie, L.; Al-Resayes, S. I. Computational investigations of three main drugs and their comparison with synthesized compounds as potent inhibitors of SARS-CoV-2 main protease (Mpro): DFT, QSAR, molecular docking, and in silico toxicity analysis. *Journal of King Saud University – Science* **2021**, *33* (2), 101315. <https://doi.org/10.1016/j.jksus.2020.101315>.
4. Xia, S.; Zhu, Y.; Liu, M.; Lan, Q.; Xu, W.; Wu, Y.; Ying, T.; Liu, S.; Shi, Z.; Jiang, S.; Lu, L. Fusion mechanism of 2019-nCoV and fusion inhibitors targeting HR1 domain in spike protein. *Cellular & Molecular Immunology* **2020**, *17* (7), 765–767. <https://doi.org/10.1038/s41423-020-0374-2>.
5. Wrapp, D.; Wang, N.; Corbett, K. S.; Goldsmith, J. A.; Hsieh, C.-L.; Abiona, O.; Graham, B. S.; McLellan, J. S. Cryo-EM structure of the 2019-nCoV spike in the prefusion conformation. *Science* **2020**, *367* (6483), 1260–1263. <https://doi.org/10.1126/science.abb2507>.
6. Walls, A. C.; Park, Y.-J.; Tortorici, M. A.; Wall, A.; McGuire, A. T.; Velesler, D. Structure, Function, and Antigenicity of the SARS-CoV-2 Spike Glycoprotein. *Cell* **2020**, *181* (2), 281–292.e6. <https://doi.org/10.1016/j.cell.2020.02.058>.
7. Xu, Y.; Lou, Z.; Liu, Y.; Pang, H.; Tien, P.; Gao, G. F.; Rao, Z. Crystal Structure of Severe Acute Respiratory Syndrome Coronavirus Spike Protein Fusion Core. *J. Biol. Chem.* **2004**, *279* (47), 49414–49419. <https://doi.org/10.1074/jbc.M408782200>.
8. Hoffmann, M.; Kleine-Weber, H.; Schroeder, S.; Krüger, N.; Herrler, T.; Erichsen, S.; Schiergens, T. S.; Herrler, G.; Wu, N.-H.; Nitsche, A.; Müller, M. A.; Drosten, C.; Pöhlmann, S. SARS-CoV-2 Cell Entry Depends on ACE2 and TMPRSS2 and Is Blocked by a Clinically Proven Protease Inhibitor. *Cell* **2020**, *181* (2), 271–280.e8. <https://doi.org/10.1016/j.cell.2020.02.052>.
9. Xu, C.; Wang, Y.; Liu, C.; Zhang, C.; Han, W.; Hong, X.; Wang, Y.; Hong, Q.; Wang, S.; Zhao, Q.; Wang, Y.; Yang, Y.; Chen, K.; Zheng, W.; Kong, L.; Wang, F.; Zuo, Q.; Huang, Z.; Cong, Y. Conformational dynamics of SARS-CoV-2 trimeric spike glycoprotein in complex with receptor ACE2 revealed by cryo-EM. *Science Advances* **2021**, *7* (1), eabe5575. <https://doi.org/10.1126/sciadv.abe5575>.
10. Gao, X.; Qin, B.; Chen, P.; Zhu, K.; Hou, P.; Wojdyła, J. A.; Wang, M.; Cui, S. Crystal structure of SARS-CoV-2 papain-like protease. *Acta Pharmaceutica Sinica B* **2021**, *11* (1), 237–245. <https://doi.org/10.1016/j.apsb.2020.08.014>.
11. Hillen, H. S.; Kocic, G.; Farnung, L.; Dienemann, C.; Tegunov, D.; Cramer, P. Structure of replicating SARS-CoV-2 polymerase. *Nature* **2020**, *584* (7819), 154–156. <https://doi.org/10.1038/s41586-020-2368-8>.
12. Mohapatra, R. K.; El-ajaily, M. M.; Alassbaly, F. S.; Sarangi, A. K.; Das, D.; Maihub, A. A.; Ben-Gweirif, S. F.; Mahal, A.; Suleiman, M.; Perekhoda, L.; Azam, M.; Al-Noor, T. H. DFT, anticancer, antioxidant and molecular docking investigations of some ternary Ni(II) complexes with 2-[(E)-[4-(dimethylamino)phenyl]methyleneamino]phenol. *Chemical Papers* **2021**, *75* (3), 1005–1019. <https://doi.org/10.1007/s11696-020-01342-8>.

## Information about the authors:

**Marharyta M. Suleiman** (corresponding author), Ph.D. in Pharmacy, Associate Professor of the Medicinal Chemistry Department, National University of Pharmacy of the Ministry of Health of Ukraine; <https://orcid.org/0000-0001-6388-5342>; e-mail for correspondence: [suleiman.nfau@outlook.com](mailto:suleiman.nfau@outlook.com).

**Andrii I. Fedosov**, Dr.Sci. in Pharmacy, Professor, Chief Vice-Rector on Educational Work, National University of Pharmacy of the Ministry of Health of Ukraine; <https://orcid.org/0000-0003-1180-9836>.

**Ranjan K. Mohapatra**, Assistant Professor of the Department of Chemistry, Government College of Engineering; <https://orcid.org/0000-0001-7623-3343>.

**Irina A. Sych**, Ph.D. in Pharmacy, Associate Professor of the Medicinal Chemistry Department, National University of Pharmacy of the Ministry of Health of Ukraine; <https://orcid.org/0000-0001-9540-7038>.

**Lina O. Grinevich**, Ph.D. in Pharmacy, Associate Professor of the Medicinal Chemistry Department, National University of Pharmacy of the Ministry of Health of Ukraine; <https://orcid.org/0000-0003-3762-8670>.

**Nataliia P. Kobzar**, Ph.D. in Pharmacy, Associate Professor of the Medicinal Chemistry Department, National University of Pharmacy of the Ministry of Health of Ukraine; <https://orcid.org/0000-0002-2062-2769>.

**Vitaliy D. Yaremenko**, Ph.D. in Pharmacy, Associate Professor of the Medicinal Chemistry Department, National University of Pharmacy of the Ministry of Health of Ukraine; <https://orcid.org/0000-0002-0850-1489>.

**Lina O. Perekhoda**, Dr.Sci. in Pharmacy, Professor, Head of the Medicinal Chemistry Department, National University of Pharmacy of the Ministry of Health of Ukraine; <https://orcid.org/0000-0002-8498-331X>.

## Conclusions

According to the results obtained, we have proposed a way to search for potential SARS-COV-2 inhibitors based on Crinipellin A derivatives. Using the most promising compound **5** further studies open up another direction for searching for compounds of SARS-COV-2 inhibitors.

## ЗМІСТ / CONTENTS

## Advanced Research

- O. V. Oksiuta, A. E. Pashenko, R. V. Smalii, D. M. Volochnyuk, S. V. Ryabukhin  
HETEROCYCLIZATION VS COUPLING REACTIONS: A DNA-ENCODED LIBRARIES CASE..... 3
- О. В. Оксюта, А. Є. Пашенко, Р. В. Смалій, Д. М. Волочнюк, С. В. Рябухін /  
Гетероциклізація або реакції каплінгу: випадок ДНК-кодованих бібліотек

## Review Article

- M. A. Jordaan, O. Ebenezer  
BIOLOGICAL ACTIVITIES OF TETRAHYDROISOQUINOLINES DERIVATIVES ..... 20
- М. А. Джордаан, О. Ебенезер / Біологічна активність похідних тетрагідроізохіноліну

## Original Research

- S. M. Kovtun-Vodyanytska, I. V. Levchuk, D. B. Rakhmetov, O. V. Golubets  
CHEMICAL COMPONENTS OF ESSENTIAL OILS FROM AERIAL PARTS  
OF *RYCNANTHEMUM VIRGINIANUM* AND *P. CALIFORNICUM* (LAMIACEAE) PLANTS ..... 39
- С. М. Ковтун-Водяницька, І. В. Левчук, Д. Б. Рахметов, О. В. Голубець /  
Хімічні компоненти ефірних олій із надземних частин рослин *Pycnanthemum virginianum*  
і *P. californicum* (Lamiaceae)

## Original Research

- A. G. Rustemkulov, T. M. Gontova, B. G. Makhatova, A. E. Rustemkulova, U. M. Datkhayev,  
O. M. Koshovi  
STANDARDIZATION PARAMETERS OF *ALFREDIA NIVEA* KAR.&KIR HERB ..... 46
- А. Г. Рустемкулов, Т. М. Гонтова, Б. Г. Махатова, А. Є. Рустемкулова, У. М. Датхаєв,  
О. М. Кошовий / Параметри стандартизації трави *Alfredia nivea* KAR.&KIR.

## Original Research

- M. M. Suleiman, A. I. Fedosov, R. K. Mohapatra, I. A. Sych, L. O. Grinevich, N. P. Kobzar,  
V. D. Yaremenko, L. O. Perekhoda  
THE SEARCH FOR POTENTIAL SARS-CoV-2 INHIBITORS USING THE *IN SILICO*  
RESEARCH..... 54
- М. М. Сулейман, А. І. Федосов, Р. К. Мохapatра, І. А. Сич, Л. О. Гріневич, Н. П. Кобзар,  
В. Д. Яременко, Л. О. Перехода / Пошук потенційних інгібіторів SARS-CoV-2 за допомогою  
*in silico* методів